NTNU – Trondheim
Norwegian University of
Science and Technology

Numerical Modelling of Sediment Transport in the Arctic

Syeda Wahida Rafiq

Coastal and Marine Engineering and Management
Submission date: June 2015
Supervisor: Raed Khalil Lubbad, BAT

Norwegian University of Science and Technology
Department of Civil and Transport Engineering

ERASMUS MUNDUS MSC PROGRAMME
COASTAL AND MARINE ENGINEERING AND MANAGEMENT
(COMEM)

NUMERICAL MODELLING OF SEDIMENT TRANSPORT IN THE ARCTIC

Norwegian University of Science and Technology, Trondheim, Norway
29th June 2015

SYEDA WAHIDA RAFIQ
746237

The Erasmus Mundus MSc Coastal and Marine Engineering and Management is an integrated programme organized by five European partner institutions, coordinated by Norwegian University of Science and Technology (NTNU). The joint study programme of 120 ECTS credits (two years full-time) has been obtained at least two of the five CoMEM partner institutions:

- Norwegian University of Science and Technology (NTNU) Trondheim, Norway
- Technische Universiteit (TU) Delft, The Netherlands
- City University London, Great Britain
- Universitat Politècnica de Catalunya (UPC), Barcelona, Spain
- University of Southampton, Southampton, Great Britain

The full range of distinctive skills offered by the five partners is brought together: these can only be accessed by student mobility. Thus CoMEM is divided into five tracks (specialisations): 1: Arctic Marine Coastal Engineering (NTNU); 2: Marine Operations and Management (City, London); 3: Environment and Management (Southampton); 4: Coastal Engineering (TU Delft); 5: Engineering and Environment (UPC, Barcelona). During semester 1, all students attend NTNU for a common foundation suitable for the five different tracks. Courses are taken with a focus on advanced topics in the selected area of specialization.

In the fourth and final semester an MSc project and thesis have to be completed. The two year CoMEM programme leads to two/three officially recognized MSc diploma certificates. These will be issued by the two/three universities which have been attended by the student. The transcripts issued with the MSc Diploma Certificate of each university include grades/marks for each subject. A complete overview of subjects and ECTS credits is included in the Diploma Supplement, as received from the CoMEM coordinating university, the Norwegian University of Science and Technology (NTNU). Information regarding the CoMEM programme can be obtained from the programme coordinator

Professor Øivind A. Arntsen
Department of Civil and Transport Engineering
Norwegian University of Science and Technology (NTNU)
NO-7491 Trondheim, Norway
E-mail: comem@ivt.ntnu.no

NORWEGIAN UNIVERSITY OF SCIENCE AND TECHNOLOGY

DEPARTMENT OF CIVIL AND TRANSPORT ENGINEERING

Report Title: **Numerical Modelling of Sediment Transport in the Arctic**	Date: 29/06/2015 Number of pages (incl. appendices) : 93			
	Master Thesis	√	Project Work	
Name: **Syeda Wahida Rafiq**				
Professor in charge/supervisor: **Prof. Raed Lubbad**				
Other external professional contacts/supervisors:				

Abstract:

The purpose of this research is to model coastal erosion mainly dune or bluff erosion in the Arctic for storm event using numerical analysis. A case study of Varandey, Russia is considered for the analysis. The numerical modelling done can be divided in two parts, i.e., (i) wave modelling and (ii) coastal erosion modelling. Wave modelling is carried out to transform the offshore boundary condition to a near-shore boundary and thereby to down-scale the domain area for erosion analysis. For wave modelling, SWAN has been used as numerical tool. For cliff erosion modelling during storm period, use of X-beach is considered.

The wave boundary conditions derived from SWAN run is used for X-beach run and a model is set up for assessing cliff erosion of the area. The model is calibrated using the data available from a storm event on 24th July 2010 and found to be valid. Sensitivity analysis of some parameters utilized in setting up the model is carried out to observe their effect on cliff erosion. Finally a simulation is run with calibrated parameters with 2D bathymetry to have an idea on the applicability of the numerical tool for larger domain.

Keywords:

1. Numerical modelling
2. SWAN
3. X-beach
4. Cliff erosion
5. Varandey, Russia

_____

NTNU
Faculty of Engineering Science and Technology
Institute of Civil and Transport Engineering

Date: 29/06/2015

MASTER DEGREE THESIS

Spring 2015

for

Student: Syeda Wahida Rafiq

NUMERICAL MODELLING OF SEDIMENT TRANSPORT IN THE ARCTIC

BACKGROUND

Since the ancient times, coastal areas are central for lots of human activities. To ensure the safety of any infrastructure near the coastline, a proper planning is necessary with detailed knowledge of the prevailing coastal processes in the vicinity. Failure to assess this may result in devastative effects on the environment and consequent loss of property. One of the prime risks is coastal erosion which should be predicted before undertaking any project near a coast line. Various empirical formulae and models are already available to estimate this process.

With the growing interest in utilizing the natural resources in the Arctic, it is very important to acquire the knowledge that assures a sustainable development of this valuable and vulnerable region. . The presence of sea-ice cover and permafrost soils together with the considerable variation in temperature across the seasons and the possible effects of climate change make the setting of an Arctic area different from others. Only little is known until now about coastal erosion mechanisms in the Arctic and the way to model them. The objective of the research will be to develop new knowledge, and numerical models to improve the prediction of sediment transport processes and hence the Arctic coastal erosion and the influence of climate changes.

The location for this study is chosen as Varandey, Russia. It is located in the northern part of Russia and at the southern part of Pechora Sea. Emerging hydrocarbon industry in Varandey has made this area more attractive to commercial investors. Various types of industrial activities are coming into existence in the area day-by-day making it more vulnerable to geomorphologic changes. The selection of the site is done based on the data available from field investigations arranged by Sustainable Arctic Marine and Coastal Technology (SAMCoT) in Varandey, Russia.

The objective of this study is to set up a model of the above mentioned coast using a suitable numerical tool for erosion. For this study short term change of cross-shore profile due to extreme events is aimed to model. The approach followed by the current study is more involved in understanding the hydrodynamic and sediment transport process and conduct a sensitivity analysis for parameters governing sediment transport.

TASK DESCRIPTION

The first step towards the task is to obtain data from different source that are required to prepare the model. The model is intended to set up using hindcast data from the storm on 24th July 2010. The records for wind, wave and tide for that specific time will be used to simulate the model. The measured erosion rates obtained from other sources will be useful to validate the model prepared. The amount of erosion found from model run will be compared to measured value for this purpose. The task will be carried out in two parts:

- A wave modelling analysis will be done using SWAN to transform the offshore boundary condition to a near-shore boundary and thereby to down-scale the domain area for erosion analysis. X-beach is going to be used as numerical tool for modelling Varandey coast for erosion due to storm events. The model generated will be calibrated using the data from the storm observed on 24th July 2010.
- A sensitivity analysis for some parameters utilized in setting up the model will be carried out to observe their effect on cliff erosion. Influence of the parameters governing sediment transport and physical processes will also be analysed as a part of this research.

Initial References

Rachold, V., Are, F. E., Atkinson, D. E., Cherkashov, G., & Solomon, S. M., 2005. Arctic coastal dynamics (ACD): An introduction. *Geo-Marine Letters*,*25*(2), 63-68.

Ogorodov, S.A., Kokin, O.V., Sinitsyn A.O. , Guegan E., Rodionov I.V. , Udalov L.E. , Kuznetsov D.E. , Likutov P.E. , Kondratieva S.T. (2013). Research on the Dynamics of the Coastal Area of the Barents and Kara Seas under Conditions of the Climate Change in the Arctic Region.N.N.Zubov State Oceanographic Institute, Moskow.

General about content, work and presentation

The text for the master thesis is meant as a framework for the work of the candidate. Adjustments might be done as the work progresses. Tentative changes must be done in cooperation and agreement with the professor in charge at the Department.

In the evaluation thoroughness in the work will be emphasized, as will be documentation of independence in assessments and conclusions. Furthermore the presentation (report) should be well organized and edited; providing clear, precise and orderly descriptions without being unnecessary voluminous.

The report shall include:

- Standard report front page (from DAIM, http://daim.idi.ntnu.no/)
- Title page with abstract and keywords.(template on: http://www.ntnu.no/bat/skjemabank)
- Preface
- Summary and acknowledgement. The summary shall include the objectives of the work, explain how the work has been conducted, present the main results achieved and give the main conclusions of the work.
- The main text.
- Text of the Thesis (these pages) signed by professor in charge as Attachment 1.

The thesis can as an alternative be made as a scientific article for international publication, when this is agreed upon by the Professor in charge. Such a report will include the same points as given above, but where the main text includes both the scientific article and a process report.

Advice and guidelines for writing of the report is given in “Writing Reports” by Øivind Arntsen, and in the departments “Råd og retningslinjer for rapportskriving ved prosjekt og masteroppgave” (In Norwegian) located at http://www.ntnu.no/bat/studier/oppgaver.

Submission procedure

Procedures relating to the submission of the thesis are described in DAIM (http://daim.idi.ntnu.no/). Printing of the thesis is ordered through DAIM directly to Skipnes Printing delivering the printed paper to the department office 2-4 days later. The department will pay for 3 copies, of which the institute retains two copies. Additional copies must be paid for by the candidate / external partner.

On submission of the thesis the candidate shall submit a CD with the paper in digital form in pdf and Word version, the underlying material (such as data collection) in digital form (e.g. Excel). Students must submit the submission form (from DAIM) where both the Ark-Bibl in SBI and Public Services (Building Safety) of SB II has signed the form. The submission form including the appropriate signatures must be signed by the department office before the form is delivered Faculty Office.
Documentation collected during the work, with support from the Department, shall be handed in to the Department together with the report.

According to the current laws and regulations at NTNU, the report is the property of NTNU. The report and associated results can only be used following approval from NTNU (and external cooperation partner if applicable). The Department has the right to make use of the results from the work as if conducted by a Department employee, as long as other arrangements are not agreed upon beforehand.

Tentative agreement on external supervision, work outside NTNU, economic support etc.
Separate description is to be developed, if and when applicable.
See http://www.ntnu.no/bat/skjemabank for agreement forms.

Health, environment and safety (HSE) http://www.ntnu.edu/hse
NTNU emphasizes the safety for the individual employee and student. The individual safety shall be in the forefront and no one shall take unnecessary chances in carrying out the work. In particular, if the student is to participate in field work, visits, field courses, excursions etc. during the Master Thesis work, he/she shall make himself/herself familiar with “Fieldwork HSE Guidelines”. The document is found on the NTNU HMS-pages at
http://www.ntnu.no/hms/retningslinjer/HMSR07E.pdf

The students do not have a full insurance coverage as a student at NTNU. If you as a student want the same insurance coverage as the employees at the university, you must take out individual travel and personal injury insurance.

Startup and submission deadlines

The work on the Master Thesis starts on 9th February 2015.

The thesis report as described above shall be submitted digitally in DAIM at the latest 6th July 2015 at 3pm.

Professor in charge: Prof. Raed Lubbad

Other supervisors:-

Department of Civil and Transport Engineering, NTNU
Date: 24.06.2015, (Revised: dd.mm.yyyy)

_____
Professor in charge (signature)

Acknowledgements

Foremost, I take this opportunity to express my heartiest gratitude to CoMEM committee for giving me the opportunity to study in this program. I would like to express my sincere gratitude to my thesis supervisor, Dr. Raed Lubbad for his continuous guidance, support, encouragement and patience. I am also grateful to Emilie Guegan, PhD student at NTNU/ SAMCoT for her useful comments and valuable suggestions. I want to thank Norwegian Meteorological Institute for providing the offshore data used in the study. I also place on record, my sense of gratitude to all the professors from both the universities – the Norwegian University of Science and Technology (NTNU) and Delft University of Technology (TUD). I am thankful to Mohammad Saud Afzal, PhD student at NTNU and Mamdouh Abdl H. Eljueidi, research assistant at NTNU for their kind help to learn the software used for this study. Finally I am indebted to all my near and dear ones for their continuous support and love throughout this entire process.

Abstract

Coastal erosion is an alarming topic in the field of coastal and marine engineering which calls for extensive research. The vulnerability of a coast to erosion can draw devastating impact on infrastructures and human lives near the area. A detailed knowledge on physical processes behind erosion mechanisms and assessment of erosion rate can lead to increased level of certainty for design life of coastal structures and thereby increased safety of valuable properties. Numerical modelling is a very useful tool for prior estimation of coastal erosion induced by environmental conditions.

Arctic coasts are no exception from other coasts in terms of erosion. But the mechanisms behind coastal erosion in the Arctic may differ from the mechanisms dominating elsewhere. The excessive temperature variation during winter and summer is responsible for this. The coast undergoes through erosion only in ice-free period when waves can reach the shore to activate the erosion process. Two widely established concepts for coastal erosion in Arctic are Thermo-denudation and Thermo-abrasion. These processes cannot be described based on wave dynamics only since thermal and geotechnical properties of sediments play an important role.

A number of computer programs are available to model with a good accuracy the erosion of a typical sandy coast. However, the situation is different for Arctic coasts and there is an expressed need to develop better numerical tools capable of predicting the erosion there. Since 2011, research is being conducted by Sustainable Arctic Marine and Coastal Technology (SAMCoT) to relate the wave mechanics with thermal factors and geotechnical formulations to develop tools that will be able to successfully estimate erosion in Arctic.

This study is aimed to model an Arctic coast for erosion due to extreme event with main concentration on dune or coastal bluff erosion i.e. for cross-shore sediment transport only. The area for current study is chosen as Varandey, Russia. This is a coast located in the northern part of Russia and at the southern part of Pechora sea. It shows Arctic behaviour in winter. But in summer it is more like a typical coast. The coast was eroded severely during a devastating storm on 24th July 2010. The eastern part of the coast named Medynskiy is observed to show maximum erosion. The data from this event is found very useful for calibrating the model.

As the wave data was obtained far offshore, a wave modelling tool, SWAN is used to get transformed wave conditions in a near-shore area at first. X-beach is used for modelling the coastal erosion. The output from SWAN is applied as input boundary conditions in X-beach. The model is validated using above mentioned data.

Sensitivity analysis is also carried out to have a proper understanding of impacts of some parameters on results. They are wind stress, critical avalanching slope below water level and critical avalanching slope above water level. The sensitivity test shows that the result mainly depends on wind speed and critical avalanching slope below water level while changes in wind direction and critical avalanching slope above water level does not show any drastic

variation in outputs. Finally the model is run with two-dimensional coastal area to comment on if it is suitable for the analysis of larger domain.

In conclusion, limitations of the study and recommendations for further research are narrated.

Content

List of Tables

List of Figures

1 Introduction

1.1 Background and motivation

Coastal erosion has been focus of many scientific studies for long. With the increase of human settlement near coast, significant knowledge on the vulnerability of coastline has become essential. Fatalities near a coastal zone are severe if there is a natural hazard like storms or hurricanes. The design and constructions of various coastal structures also ask for detailed understanding of coast behaviour in changing climate conditions. It is essential to forecast the possible morphological changes induced by coastal erosion or accretion to avoid such hazards. With the growing knowledge on sediment transport, researchers and scientists are able to outline the underlying processes of coastal erosion and provide some formulations. But these processes are highly variable with surrounding circumstances. No unique recipe is available which can fit for all of the coasts in the world. Therefore researches are still in progress to validate the empirical theories already developed by comparing the results from different coasts with different geographic settings.

In an upper beach area swash zone is the most dynamic part which interacts continuously with incoming waves. Breaking of waves in surf zone produces strong and unsteady flow and increases the turbulence in near-shore area. This results in large sediment transport rates eventually leading to relatively large morphological changes. The beach area continues its reshaping process to reach an equilibrium with the existing environment posed by incoming wave conditions.

In an Arctic area, the geodetic setting makes it different from other temperate or tropical coasts. The wave conditions are not the same during summer and winter because of presence of sea ice and the beach materials behave in a different way as thermal properties become important as well. The role of temperature becomes important for sediment transport process which can trigger different transport mechanism depending on current environment. This is why the coasts in the Arctic are considered very sensitive with the rising global temperature due to climate change and now-a-days a lot of attention is paid to the researches related to Arctic.

Numerical modelling is an important tool used to analyse any natural system for understanding the process. It basically approaches to the solution by using a set of formulations derived empirically. Then validation with existing data of this solution is required to justify the accuracy of model. This is considered as a very effective tool for study of coastal erosion.

Sustainable Arctic Marine and Coastal Technology (SAMCoT) is a renowned national and international research-based organization hosted by The Norwegian University of Science and Technology (NTNU). It supports the innovation of technology for Arctic coastal development. This has been a leading organization carrying out a lot of studies that involves the exploration of coastal erosion and the mechanisms behind in Arctic. Different mechanisms are invented to describe the natural processes that influence the erosion. For the

same purpose Varandey coast in Russia has been investigated to understand the geotechnology-based mechanism underlying erosion.

The objective of this study is to set up a model of the above mentioned coast using a suitable numerical tool for erosion. Choice of both time-scale and boundary in space becomes important for any kind of analysis. For this study short term change of cross-shore profile due to extreme events is aimed to model. The long-time variation of coastline affected by other environmental forces or infrastructures is ignored. Two modelling tools are used for the current study- SWAN for wave modelling and X-beach for modelling of coastal erosion. SWAN, developed by Delft University of Technology can model waves propagating towards shallow water in the near-shore area including important phenomena influenced by the depth-induced non-linear behaviour. X-beach is a program developed to estimate the morphological changes during time-varying storm and hurricane conditions including dune or bluff erosion.

The validation of model requires field data which is not currently available. The sediment properties and erosion rates are estimated based on published data and personal communication. The approach followed by the current study is more involved in understanding the hydrodynamic and sediment transport process and conduct a sensitivity analysis for parameters governing sediment transport.

1.2 Structure of the thesis

Chapter 1 outlines the objective of the report and its organization.

Chapter 2 describes some theory of coastal morphodynamics. This chapter is dedicated to provide readers a basic knowledge on natural processes that play role behind reshaping of a coastal profile. This includes wave transformation, sediment transport and subsequent morphological changes.

Chapter 3 explains briefly the erosion mechanisms that dominate in the Arctic.

Chapter 4 gives the readers a general idea about the numerical tools used in this study. The formulations and assumptions in setting up the model are illustrated very concisely.

Chapter 5 describes the area that is going to be modelled for coastal erosion. The geological setting and climate data are presented to depict the general characteristic of the coast to be analysed. This chapter also includes the source and reliability of data that are used for modelling.

Chapter 6 represents the details on model set-up and result from the simulation. The outcomes from simulation run and sensitivity test of some factors governing sediment transport are discussed there.

Chapter 7 contains a summary of the findings, limitations and recommendations for further study.

2 Coastal Morphodynamics

2.1 Introduction

Coastal morphology refers to the geomorphology of a coast. The term coastal morphodynamics is defined as the 'mutual adjustment of topography and fluid dynamics involving sediment transport' (Wright & Thom, 1977) or, alternatively, the ‘dynamic behaviour of alluvial boundaries’ of fluid motions (de Vriend, 1991). The natural processes near coast and their impacts depending on the other factors such as environmental conditions, hydrodynamics, sediment properties, human intervention and their complex interaction are the focus of this particular branch of science.

Many factors e.g. wind, waves, currents, tidal characteristics, sediment properties etc., influence the change in sediment transport rate in different parts of a coastal zone. This results in either erosion or deposition of sediments. The bathymetry keeps updating as the response. The changed morphology again influences the other processes and this process continues until equilibrium is reached.

2.2 Coastal hydrodynamics

Wind, waves, currents and tides characterize coastal hydrodynamic. Wind on sea generates waves and the properties of the generated waves depend on the wind speed, fetch length and water depth. Wind energy is transformed into wave energy in the offshore location and the generated waves propagate to different directions. The waveform approaching to the shore undergoes some other phenomena like wave set-up and set-down, refraction, shoaling, diffraction, wave breaking etc. These phenomena are responsible for wave-induced cross-shore and long-shore currents, which control sediment transport toward offshore or onshore direction. Coastal hydrodynamics refers to the part of the coastal process, which deals with wave propagation, transformation and dissipation, wave induced water level changes and long-shore and cross-shore currents due to wave, wind and tidal actions.

2.2.1 Ocean Waves

Waves play a very important role in coastal hydrodynamics. Therefore in-depth knowledge on wave mechanics is a must for this study. Wind waves are generated by the exchange of momentum between wind and underlying water surface. In deep sea, waves act weakly non-linear and thus can be represented as sum of a large number of independent waves interacting with each other. This produces an irregular wave field which follows Gaussian distribution. As the waves propagate to shallower water, they start to feel the bottom and the bed resistance result in increasing non-linear behaviour. This is responsible for the phenomena like refraction and shoaling.

Any waveform can be analyzed as a combination of sine waves. A simple representation of wave is show in Figure 2.1. But ocean waves cannot be described as a regular surface. Therefore it is not possible to characterize them in a deterministic way.

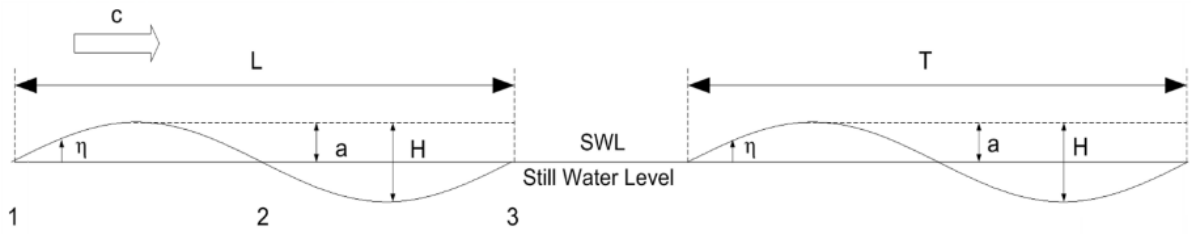

Figure 2.1: Simple representation of a wave. Here a=amplitude, L=wave length, T=wave period, H=wave height, c= wave speed and η= temporal variation of water level. (source: Bosboom J. & Stive M, 2013)

The stochastic behaviour of sea surface produced by ocean waves can be described by spectrum. The spectrum represents the sea state by providing the distribution of waves in frequency domain.

2.2.2 Spectral analysis

Spectral analysis is a statistical representation of the sea state using sine waves to represent the irregularity of the surface with different frequencies of which, the amplitudes and phases can be determined using Fourier analysis. A spectrum is plotted with the frequencies of a stationary random process and the mean square spectral density of the system on *x* and *y* axes respectively.

The wave spectrum is proportional to the wave energy distribution as a function of the wave number as shown in the following equation

$$E = \rho g Var(\eta) = \rho g \int_k \Psi(\mathrm{k}) \mathrm{d}^2\mathrm{k} \qquad (2.1)$$

Where E is wave energy, ρ is the density of fluid, η is the surface elevation, k is the wave number ($2\pi/L$) and function $\Psi(k)$ signifies the density of waves around the wave number. A regular wave field is represented by a narrow spectrum. A spectrum contains more energy if it shifts towards lower frequency and consists of larger and longer waves. If a spectrum contains both sea and swell waves, two significant peaks are observed, i.e., one represents swell and the other represents sea waves. A typical bimodal spectrum with both swell and sea waves is shown in Figure 2.2.

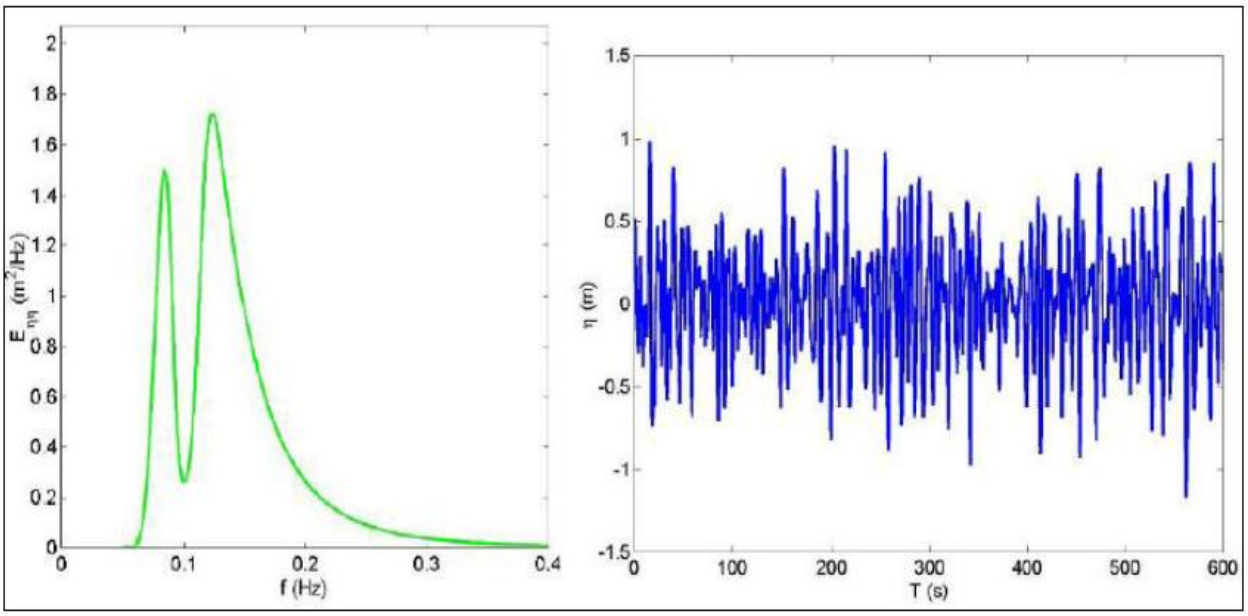

Figure 2.2: Bimodal spectrum of sea and swell (source: Bosboom J. &Stive M, 2013)

The individual waves in a spectrum vary in frequency. As the group of waves propagates through deep water, frequency dispersion is observed which means that waves with different wavelengths travel with different phase speeds. The group of waves forms a wave train and travels as a unit. This is known as wave envelope. In a wave envelope, new waves seem to emerge at the back of a wave group, grow in amplitude until they are at the center of the group, and vanish at the wave group front. A wave envelope travels with group velocity instead of individual phase velocity of carrier waves. The phase velocity is two times faster than group velocity in deep water. Figure 2.3 is presented to illustrate the concept of wave envelope. . The blue curve shows the fast varying the carrier wave, which is being modulated and the red curve indicates the slowly varying wave envelope.

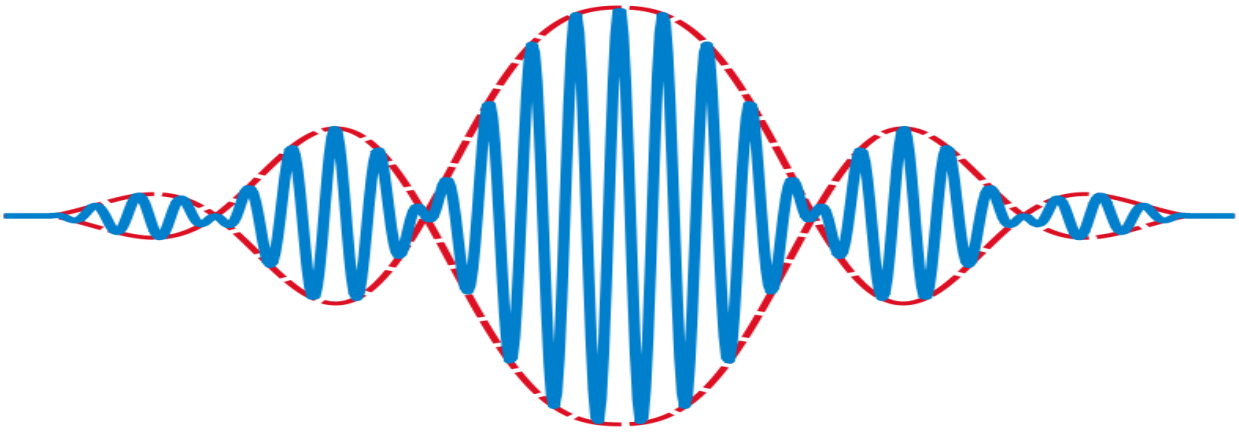

Figure 2.3: Illustration of the envelope of an amplitude-modulated wave (source: Wikipedia)

2.2.3 Wave Transformation

As described above, waves are typically generated offshore and then they propagate to coast. During travelling near-shore they start to experience non-linear effects and various phenomena comes into action like refraction, shoaling, wave set-up, set-down, wave breaking

etc. These phenomena are known as wave transformation. There are many theories available to estimate this non-linear effect like Stokes, Cnoidal, Boussinesq etc.

2.2.3.1 Wave refraction and shoaling

As waves enter the shallow zone, the conservation of energy in the wave system and the reduction of wave group velocity together lead to refraction and shoaling. Refraction is described as the distortion of the wave front due to reduced velocity because of the friction with the sea bed as wave propagates towards the shore. Shoaling can be defined as the increase in wave height that results from conservation of energy and reduced wave group velocity for waves entering shallower water. Figure 2.4 represents a line diagram to show wave refraction and Figure 2.5 shows wave shoaling.

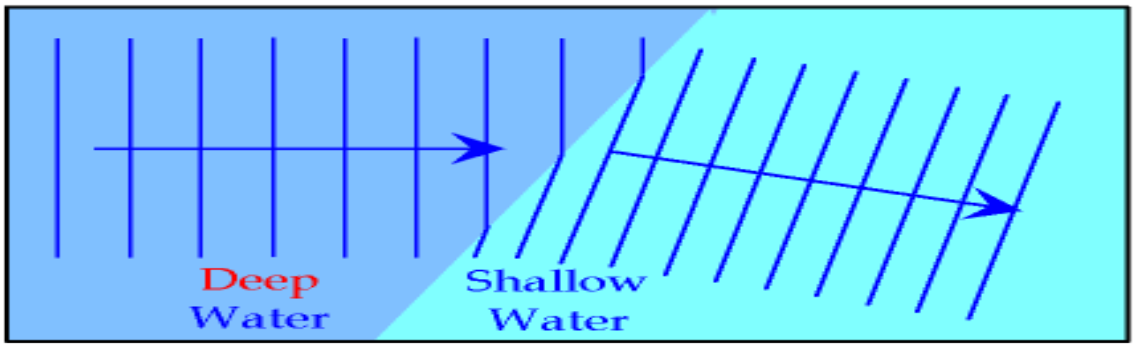

Figure 2.4: Wave refraction (source: the website of physicsforums)

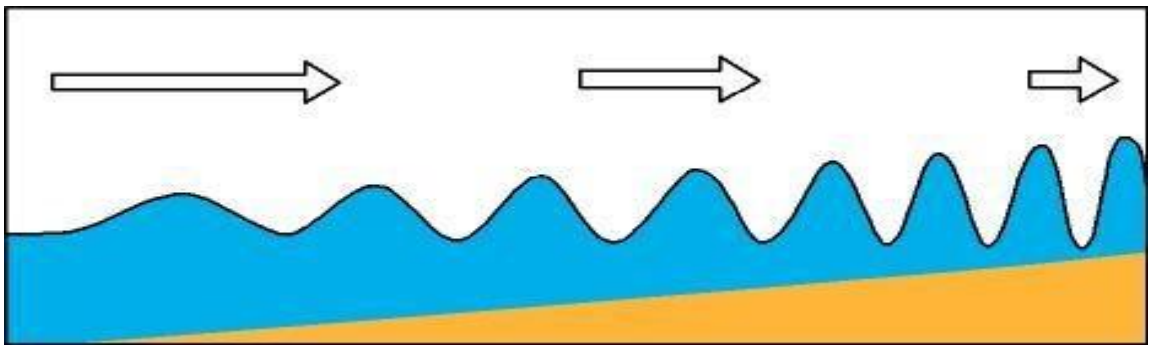

Figure 2.5: Wave shoaling (source: the website of magicsweed)

2.2.3.2 Wave breaking

Wave breaking is observed when the particle velocity of the wave front exceeds the phase velocity. Depth induced wave breaking in shallow water is a very important process regarding dissipation of energy producing a lot of turbulence. In deep water wave breaks due to wave steepness. The limiting steepness is expressed by Miche (1994) based on stokes wave theory as following:

$$\left[\frac{H}{L}\right]_{max} = 0.142\tanh(kd) = 0.142(fordeepwaters) \approx \frac{1}{7} \qquad (2.2)$$

where *Hmax* and *Lmax* are limiting wave height and wave length respectively, and d is the water depth. A limit for depth induced breaking can be derived based on linear wave theory. The breaker index for depth induced breaking is expressed by Battjes and Janssen (1978) as

approximately $\frac{H_b}{h_b} = 0.78$ where H_b is the breaking wave height and h_b is the breaking water depth. Figure 2.6 represents wave breaking phenomena.

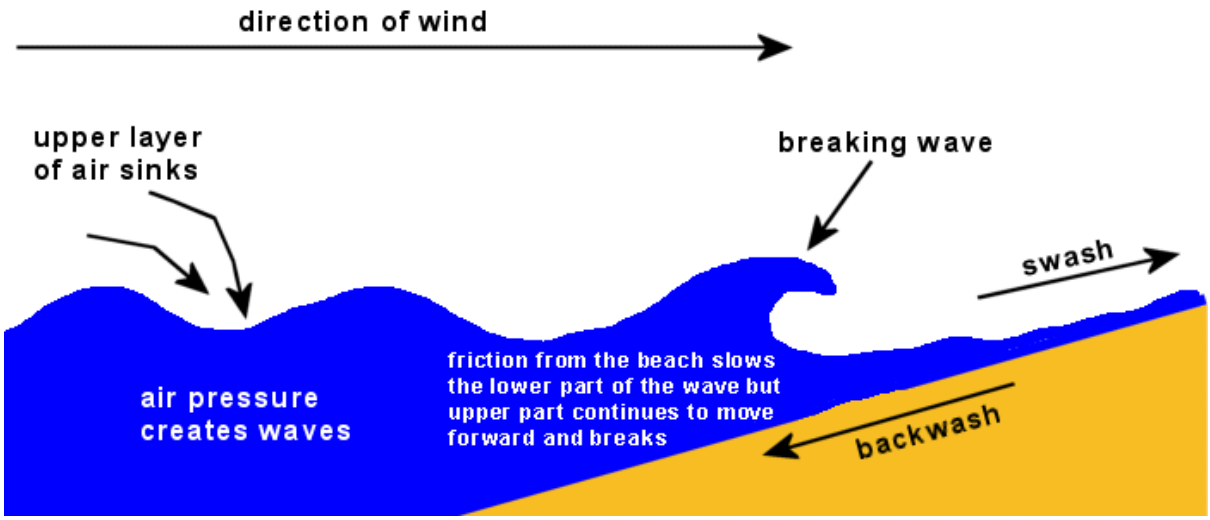

Figure 2.6: Wave breaking (source: the website of geology-learnontheinternet)

2.2.3.3 Undertow

Waves transfer momentum in the direction of travel while propagating across the ocean. The momentum can be defined as a net flux of mass between wave crest and trough. In the surf zone, the momentum becomes significantly larger than that of non-breaking zone due to wave breaking and generation of rollers (Roelvink and Stive, 1989; Nairn et al. 1990). The coastline acts as a closed boundary. Therefore a return flow is observed under the wave trough level to compensate the propagating flux. This strong return current is termed as undertow. Even in non-breaking waves near the shore there is a small return current present. Undertow is primarily responsible for offshore sediment transport during storm events. Measured velocities averaged over a wave cycle under propagating waves in a wave flume is presented in Figure 2.7 to explain return flow above wave boundary layer, *be*..

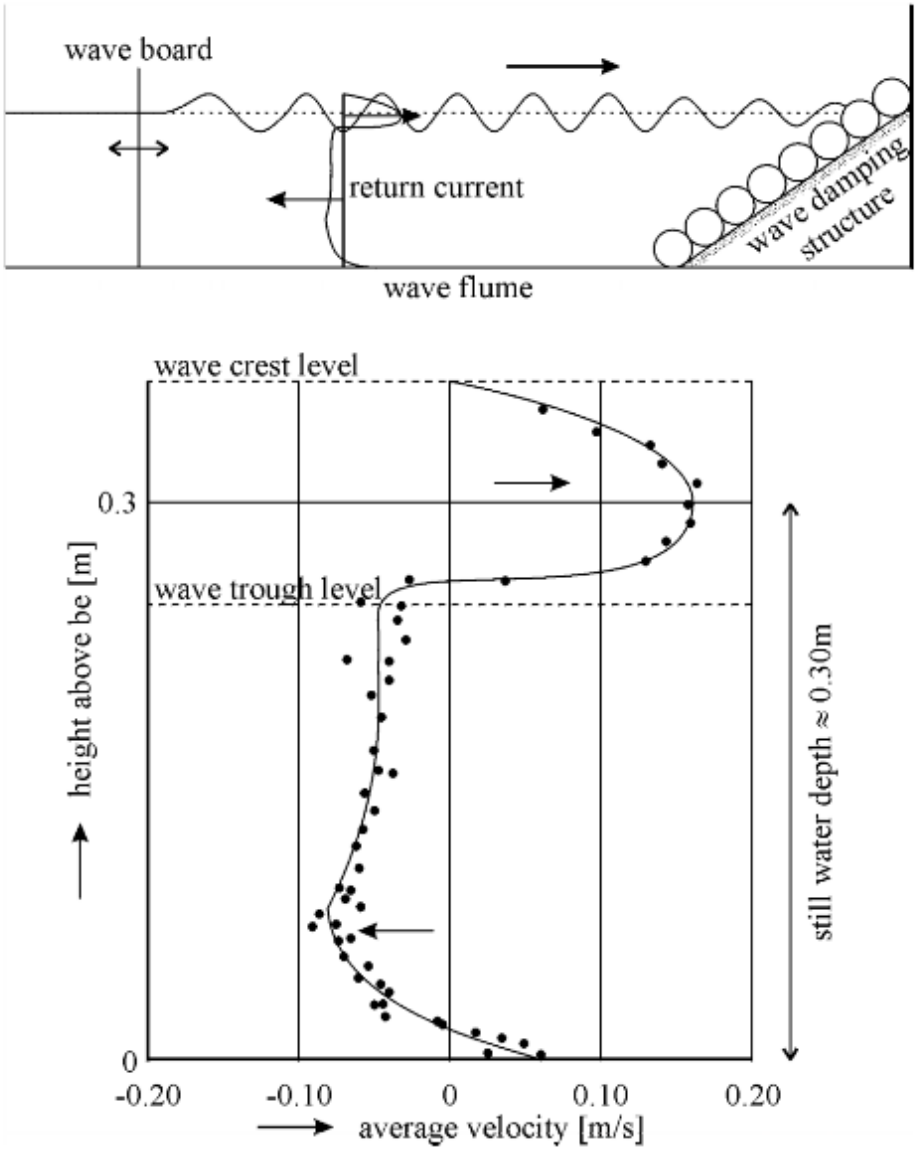

Figure 2.7: Measured velocities averaged over a wave cycle under propagating waves in a wave flume (source: Bosboom J. & Stive M, 2013).

2.2.3.4 Wave set up and set down

Radiation stress is expressed by Longuet-Higgins and Stewart (1964) as the depth integrated and wave averaged excess momentum fluxes due to waves. Change in momentum flux is defined as radiation stress. Radiation stress is responsible for wave forces acting on fluid which results in set-up, set-down and longshore current in near shore area. Wave set-up is referred to the wave-induced increase in mean water level near-shore and similarly wave set-down is a wave-induced decrease of the mean water level towards offshore direction from surf zone to balance the momentum flux. Figure 2.8 is presented for illustration of wave set-up.

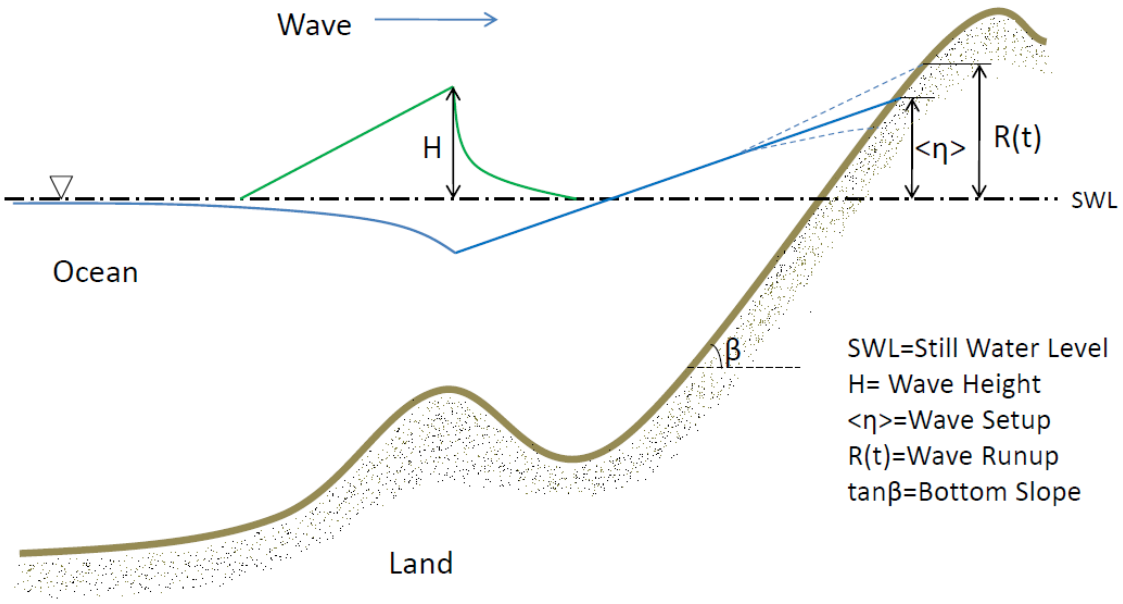

Figure 2.8: Wave set-up (source: the website of hurricanescience)

Time and wave averaged equations for the radiation stresses derived by Longuet-Higgins and Stewart (1964) from the linear wave theory are presented below.

$$S_{xx} = \overline{\int_{-h_0}^{\eta} (\rho u_x) u_x dz + \int_{-h_0}^{\eta} \rho_{wave} dz} \tag{2.3}$$

$$S_{yy} = \overline{\int_{-h_0}^{\eta} (\rho u_y) u_y dz + \int_{-h_0}^{\eta} \rho_{wave} dz} \tag{2.4}$$

$$S_{xy} = \overline{\int_{-h_0}^{\eta} (\rho u_x) u_y dz + \tau_{xy} dz} = \overline{\int_{-h_0}^{\eta} (\rho u_x) u_y dz} \tag{2.5}$$

$$S_{yx} = \overline{\int_{-h_0}^{\eta} (\rho u_y) u_x dz} \tag{2.6}$$

where u_x and u_y are the water particle velocities in x and y direction respectively, p wave is the hydrostatic pressure component of the wave, S_{xx} and S_{yy} are the normal component of radiation stress and similarly S_{xy} and S_{yx} are the shear components of radiation stress. Under the assumption that water is an irrotational fluid, the shear stress due to waves, τ_{xy} is neglected.

Longshore currents are produced as a result of wave forces in the water column due to shear components of radiation stress. The normal component of radiation stress is the reason behind wave set-up and set-down. The difference in mean water level due to set-up and set-down generates cross-shore current.

2.2.4 Wave action balance

Spectral wave action balance equation describes the slow variation of the full spectrum in time and space. Wave action balance takes all individual wave components, the propagation speed of the wave energy into consideration on a fixed grid. The equation computes the action density distribution which is influenced by wind growth, non-linear interactions and wave dissipation, thus changing the spectral shape of energy density [Holthuisjen 2007].

$$\frac{\partial N}{\partial t} + \frac{\partial}{\partial x} c_x N + \frac{\partial}{\partial y} c_y N + \frac{\partial}{\partial \sigma} c_\sigma N + \frac{\partial}{\partial \theta} c_\theta N = \frac{S}{\sigma} \tag{2.7}$$

where N represents the action density as function of angular frequency,σ, and direction,Θ.

$$N(\sigma, \theta) = \frac{E(\sigma, \theta)}{\sigma} \tag{2.8}$$

and c_i represents the transport velocities in x, y, σ and Θ-space and E represents the energy density.

$$E = \frac{1}{2} \rho g a^2 \tag{2.9}$$

in which ρ represents the density of water and g the gravitational acceleration.

2.2.5 Wave Energy balance

Law of conservation of energy is valid for wave system like every other system in our universe. This law is useful to estimate wave transformation as well. The total energy is represented as the sum of potential energy and kinetic energy. Mathematically it is expressed as in Eq. 2.10.

$$E = \frac{1}{8} \rho g {H_{rms}}^2 \tag{2.10}$$

where ρ represents the density of water and g the gravitational acceleration. Each wave component travels with its own velocity c. The group velocity at which the wave energy travels ,is given by ;

$$c_g = \frac{1}{2}\left[1 + \frac{2kh}{\sinh 2kh}\right] c \tag{2.11}$$

where k is calculated using the linear dispersion relation.

If the spectrum is directionally narrow-banded and the peak frequency is constant in space, the Eq. 2.12 can represent the energy balance of the system.

$$\frac{\partial E}{\partial t} + \frac{\partial}{\partial x}\left(E c_g \cos(\theta_m)\right) + \frac{\partial}{\partial y}\left(E c_g \sin(\theta_m)\right) = -D_w - D_f \tag{2.12}$$

where D_w and D_f represent wave energy dissipation due to wave breaking and bottom friction respectively. This equation describes the propagation and dissipation of wave energy for given mean wave direction Θ_m.

2.2.6 Roller Energy Balance

When the wave starts to break and produce surface rollers, a ‘transition zone’ effect comes into existence which introduces a delay between the points where the waves start to break and where the wave set-up and longshore current start to build. This is observed due to the temporary storage of shoreward momentum in the surface rollers.

An energy balance for the rollers is described as follows:

$$\frac{dE_r}{dt} = \frac{\partial E_r}{\partial t} + \frac{\partial E_r c \cos\theta_m}{\partial x} + \frac{\partial E_r c \sin\theta_m}{\partial y} = D_w - D_r \tag{2.13}$$

where E_r is roller energy, D_w is the loss of organized wave motion due to breaking and D_r is the roller energy dissipation.

2.3 Currents

As waves enter the shallow water region, sea currents start to interact with the incoming waves and they become important. The flow situations in time-varying and horizontally varying processes are controlled by different types of governing forces. Explaining shallow water equations will be appropriate to start with to discuss this mechanism.

2.3.1 3D shallow water equations

The shallow water equations (SWE) can be derived from the more general Navier-Stokes equations, consisting of the momentum balance and the mass balance. The following set of equations is known as the 3D shallow water equations or 3D hydrostatic model.

$$\frac{\partial u}{\partial t} + u\frac{\partial u}{\partial x} + v\frac{\partial u}{\partial y} + w\frac{\partial u}{\partial z} - f_{cor}v = \frac{\partial}{\partial x}\left(v_h\frac{\partial u}{\partial x}\right) + \frac{\partial}{\partial y}\left(v_h\frac{\partial u}{\partial y}\right) + \frac{\partial}{\partial z}\left(v_v\frac{\partial u}{\partial z}\right) - \frac{1}{\rho}\frac{\partial p}{\partial x} + \frac{W_x}{\rho} \tag{2.14}$$

$$\frac{\partial v}{\partial t} + u\frac{\partial v}{\partial x} + v\frac{\partial v}{\partial y} + w\frac{\partial v}{\partial z} + f_{cor}u = \frac{\partial}{\partial x}\left(v_h\frac{\partial v}{\partial x}\right) + \frac{\partial}{\partial y}\left(v_h\frac{\partial v}{\partial y}\right) + \frac{\partial}{\partial z}\left(v_v\frac{\partial v}{\partial z}\right) - \frac{1}{\rho}\frac{\partial p}{\partial y} + \frac{W_y}{\rho} \tag{2.15}$$

$$\frac{\partial Uh}{\partial x} + \frac{\partial Vh}{\partial x} + \frac{\partial \eta}{\partial t} = 0 \tag{2.16}$$

$$p = p_a + \int_z^{\overline{\eta}} \rho g dz \tag{2.17}$$

$$\frac{\partial u}{\partial x} + \frac{\partial v}{\partial y} + \frac{\partial w}{\partial z} = 0 \tag{2.18}$$

where u, v and w are velocity in x, y and z directions respectively, ρ is the water density, f_{cor} is Coriolis force , v_h is horizontal viscosity, v_v is vertical viscosity, p is pressure at the location, p_a is atmospheric pressure, W_x and W_y are wave forcing in x and y direction respectively.

2.3.2 Depth average shallow water equation

For simplification it is possible to reduce the full 3D equations into 2D especially when the variations in the vertical flow are minimal. In many cases this approximation is very practical to get fast results by using depth-averaged version of the shallow water equations. In some cases, however, this simplification is inadequate like when there is strong density gradient, e.g. near a river mouth, when there is a strong curvature of flow, as in river bends, or when

the focus is on cross-shore wave-induced currents, where the top part of the vertical distribution of velocity may be onshore directed and the bottom part offshore directed.

The following momentum balance is derived by averaging the set of equations for 3D shallow water equations over the water depth,

$$\frac{\partial U}{\partial t} + U\frac{\partial U}{\partial x} + V\frac{\partial U}{\partial y} - f_{cor}V = \frac{\partial}{\partial x}D_h\frac{\partial U}{\partial x} + \frac{\partial}{\partial y}D_h\frac{\partial U}{\partial y} + \frac{\tau_{sx}}{\rho h} - \frac{\tau_{bx}}{\rho h} - \frac{1}{\rho}\frac{\partial p}{\partial x} - g\frac{\partial \bar{\eta}}{\partial x} + \frac{F_x}{\rho h} \quad (2.19)$$

$$\frac{\partial V}{\partial t} + U\frac{\partial V}{\partial x} + V\frac{\partial V}{\partial y} + f_{cor}U = \frac{\partial}{\partial x}D_h\frac{\partial V}{\partial x} + \frac{\partial}{\partial y}D_h\frac{\partial V}{\partial y} + \frac{\tau_{sy}}{\rho h} - \frac{\tau_{by}}{\rho h} - \frac{1}{\rho}\frac{\partial p}{\partial y} - g\frac{\partial \bar{\eta}}{\partial y} + \frac{F_y}{\rho h} \quad (2.20)$$

Here D_h is the depth-averaged turbulence viscosity. The integration of vertical shear stress gradient over the depth results in the surface shear stress τ_s minus the bed shear stress τ_b. The water level gradient terms follow from the pressure gradients.

2.3.3 Bottom Shear stress

The bottom shear stress is a function of the mean current velocity and the orbital velocity. For current only situations, the bottom stress is described by

$$\tau_b = \rho C_f |\vec{u}|\vec{u} \quad (2.21)$$

where C_f is the friction coefficient which generally depends on the local sediment characteristics and bed formulations, ρ is the water density and $\vec{u}$ is velocity near bed.

2.4 Sediment transport

Morphological changes are mainly controlled by the rate of sediment transport that takes place due to the interaction between waves, currents and the sediment. It can be defined as a function of instantaneous velocity and the sediment concentration in the flow. The interaction between wave hydrodynamics and sediment transport process is very complex. Most of the theory developed for understanding the process is highly empirical. Different theories refer to different empirical parameters that can be verified by laboratory experiments and real data. From the experimental results a range is provided by the researchers for value of the parameters that can be used depending on other factors. The choice of empirical parameters for any practical application is mainly based on experience or by trial and error method.

2.4.1 Sediment properties

The sediment properties are very important for defining the transport mode. Clay, silt, sand, gravel, pebbles and cobbles are commonly found beach materials. The grain size of the material, distribution of grain size, porosity, density, fall velocity etc. influence the transport mechanism.

Most of the properties can be determined by laboratory tests. Fall velocity is be defined as the vertical free fall velocity of a sediment particle in still and clear water. It can be derived by

balancing gravitational force acting downward and drag force of the fluid acting upward. Mathematically fall velocity is expressed as

$$w_s = \sqrt{\frac{4(s-1)gD}{3C_D}} \tag{2.22}$$

where *s* is the relative density of the sediment, C_D is drag coefficient and *D* is grain diameter. If the bottom shear stress is large enough the sediment is transported. To initiate motion the critical shear stress has to be exceeded considering vertical force, horizontal force and moment equilibrium. From the balance following equation can be obtained.

$$(\rho_s - \rho)gD^3 \propto \tau_{bcr}D^2 \tag{2.23}$$

Where τ_{bcr} is the critical bed shear stress, ρ is the water density and $\rho_s$is the density of sediments. From the proportionality of above equation, a critical parameter can be defined.

$$\theta_{cr} = \frac{\tau_{bcr}}{(\rho_s - \rho)gD} \tag{2.24}$$

Here θ_{cr} is termed as Shield parameter and can be determined experimentally. The application of this parameter in transport modelling is narrated further in following paragraph. To understand the transport process more clearly a distinction has been made. Typically transport can be divided into two types depending on the movement characteristics of sediments. They are bed load and suspended load.

2.4.2 Bed load transport

Bed load transport can be defined as the transport of grain materials that move with the flow in a thin layer above the bed. The sediments are relatively larger in grain size and react almost instantaneously to the local flow conditions. The transport is always in the direction of near bed flow.

As mentioned above sediment transport is a function of bed shear stress by the flow acting on the sediment grains. A threshold value of the bed shear stress needs to be exceeded to initiate the motion. This is referred as the critical shear stress or critical Shield's parameter. The dimensionless bed shear stress can be calculated using following equation.

$$\theta = \frac{\tau_b}{\rho g \Delta D_{50}} \tag{2.25}$$

Where τ_b is the bed shear stress, ρ is the water density, g the acceleration of gravity, $\Delta = (\rho_s - \rho)/\rho$. Sheilds A. (1936) published a curve based on his experiment to estimate this critical value using particle's Reynolds number of the system. Bed load transport is related to the Shield's parameter to some power. This method is only valid for uniform flow on a flat bed. Figure 2.9 is the graph published by Sheild (1936).

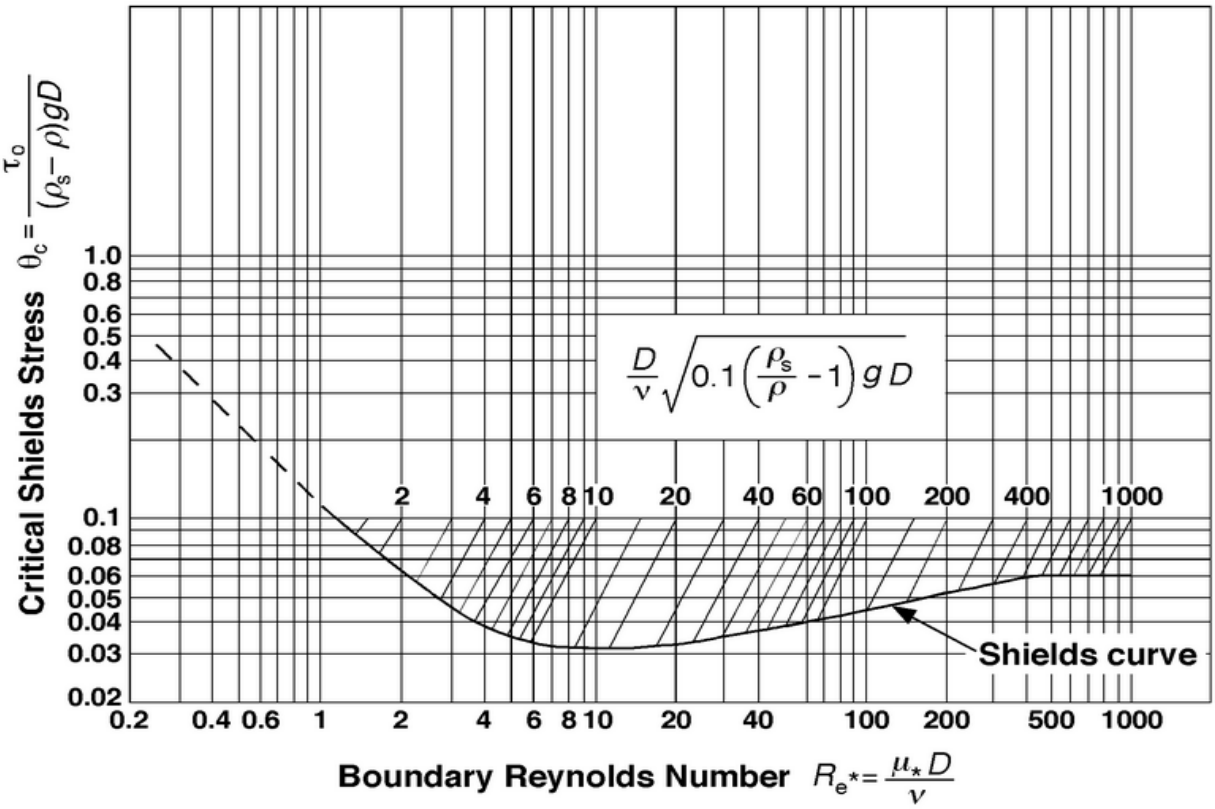

Figure 2.9: Sheild's curve (source: Sheilds A.1936)

Bed slope also has an impact on the amount of transport depending on if it is in the direction of flow or in transverse direction. For rippled beds, the bed shear stress is found to provide both drag and skin friction. Waves interact with the current modifying the bed shear stress, the bed ripples, the sediment mobility and the near-bed current transporting the sediment.
A general form of bed load transport formulations is given by

$$S_b \approx \sqrt{\Delta g {D_{50}}^3}\theta^{b/2}(m\theta - n\theta_{cr})^{c/2}\left(1 - \alpha\frac{\partial z_b}{\partial s}\right) \quad (2.26)$$

Where θ_{cr} is critical dimensionless bed shear stress using Sheild's curve and θ is dimensionless bed shear stress by the flow acting on the sediment grains. The coefficient m represents a ripple efficiency factor, which depends on the ratio of skin friction to form drag and n, may represent a factor for hiding and exposure in graded sediments. $\Delta = (\rho_s - \rho)/\rho$ is the relative sediment density. g is the gravitational acceleration, D_{50} is the median grain diameter and z_b is the bed level. *b* and *c* are empirical factors and after Van Rijn (1984), *b=0* , *c=3~4*.

2.4.3 Suspended load transport

Suspended load transport acts very different from bed load and is not constricted near the bed. The suspended sediments are relatively smaller to be picked up by the flow and remain in suspension while it moves. It does not react instantaneously to the flow or wave conditions as it needs time or space to be picked up or to settle down and thus is called to have 'memory effects'. The orbital motions due to waves are responsible to stir up the fine grains from the bed and to keep them suspended which influences the concentration of the flow. The rest of work is done by currents.

In stationary and uniform conditions, flow can support a certain amount of concentration because the sediment has to be picked up and transported upwards by turbulent dispersion. This is called equilibrium concentration. If the flow is accelerating, the currents will take away the suspended material faster which will result a concentration lower than equilibrium concentration. This means that the flow has capacity to support more sediments than they are present in it. In a decelerating flow, this is vice versa as the capacity to keep the sediments in suspension drops because of the reduced wave action and following turbulence. The concentration will turn out to exceed the equilibrium limit and a fraction of sediments will settle out to keep the balance.

The process of sediment transport is very complex and has lead to lot of assumptions by the scientists and researchers without a complete understanding of the actual process. But the assumptions and empirical formula derived from the experiments carried out so far are considered good enough to understand the practical behaviour of sediment transport and following morphological changes.

2.4.3.1 Equilibrium suspended transport

The sediment transport tends to be in equilibrium with the flow all the time and tries to cope very slowly with the changing bathymetry, sediment properties and flow. It is important to consider how equilibrium concentration is attained depending on varying flow and sediment transport in a (quasi) uniform condition.

The concentration profile can be obtained from the general advection-diffusion equation:

$$\frac{\partial c}{\partial t} + u\frac{\partial c}{\partial x} + v\frac{\partial c}{\partial y} + (\omega - \omega_s)\frac{\partial c}{\partial z} - \frac{\partial}{\partial z}\left(\epsilon_s \frac{dc}{dz}\right) - \frac{\partial}{\partial x}\left(\epsilon_h \frac{dc}{dx}\right) - \frac{\partial}{\partial y}\left(\epsilon_h \frac{dc}{dy}\right) = 0 \qquad (2.27)$$

Leaving out all non-stationary and non-uniform terms this equation reduces to

$$\omega_s c + \epsilon_s \frac{\partial c}{\partial z} = 0 \qquad (2.28)$$

with the general solution:

$$c(z) = c_a \exp\left(-\int_a^z \frac{\omega_s}{\epsilon_s}\partial z\right) \qquad (2.29)$$

Here c is the concentration of sediment, ω_s is the fall velocity and ϵ_s and ϵ_h are dispersion coefficients in vertical and horizontal directions respectively. From various researches carried out to define this dispersion coefficient, various empirical distributions have been invented to represent the case of combined current and waves. A parabolic-constant distribution, with a constant dispersion coefficient in the wave boundary and a parabolic distribution over it is suggested by Van Rijn (1993) which has got immense recognition all over the world.

2.4.3.2 2DH Advection-diffusion equation for sediment

In many cases the focus is on the horizontal variation rather than vertical non-uniformities. For simplification then, the depth averaged advection-diffusion equation can be applied.

$$\frac{\partial h\bar{c}}{\partial t} + \bar{u}\frac{\partial h\bar{c}}{\partial x} + \bar{v}\frac{\partial h\bar{c}}{\partial y} - \frac{\partial}{\partial x}\left(\epsilon_h \frac{\partial h\bar{c}}{\partial x}\right) - \frac{\partial}{\partial y}\left(\epsilon_h \frac{\partial h\bar{c}}{\partial y}\right) = S \qquad (2.30)$$

The source or sink term, S represents the exchange with the bottom and must be considered with some care.

2.4.3.3 Soulsby-Van Rijn formula

Soulsby (1997) developed the formulation by finding a suitable form of the equation that could be fitted to the numerical results of Van Rijn's 1993 model. The formulations are as follows:

$$S_{bx} = A_{cal} A_{sb} u\xi \tag{2.31}$$

$$S_{by} = A_{cal} A_{sb} v\xi \tag{2.32}$$

$$S_{sx} = A_{cal} A_{ss} u\xi \tag{2.33}$$

$$S_{sy} = A_{cal} A_{ss} v\xi \tag{2.34}$$

Where A_{cal} is a user-defined calibration factor, A_{sb} is a bed-load multiplication factor:

$$A_{sb} = 0.05h \left(\frac{D_{50}/h}{\Delta g D_{50}} \right)^{1.2} \tag{2.35}$$

and A_{ss} is a suspended load multiplication factor:

$$A_{ss} = 0.012 D_{50} \frac{{D_*}^{-0.6}}{(\Delta g D_{50})^{1.2}} \tag{2.36}$$

The dimensionless grain diameter, D_* is given by;

$$D_* = \left[\frac{g\Delta}{\vartheta^2} \right]^{1/3} D_{50} \tag{2.37}$$

where ϑ is the kinematic viscosity. The term ξ is a general multiplication factor that governs the power of the transport relation, determines the relative effects of current and waves, and includes a critical velocity:

$$\xi = \left(\sqrt{u^2 + v^2 + \frac{0.018}{C_f} {U_{rms}}^2} - U_{cr} \right)^{2.4} \tag{2.38}$$

$$\text{Here } C_f = \left[\frac{\kappa}{ln(h/z_0) - 1} \right]^2 \tag{2.39}$$

$$U_{cr} = \begin{cases} 0.19 {D_{50}}^{0.1} log_{10}(4h/D_{90}), & D_{50} \le 0.5\ mm \\ 8.5\ {D_{50}}^{0.6} log_{10}(4h/D_{90}), & 0.5 < D_{50} \le 2\ mm \end{cases} \tag{2.40}$$

And U_{rms} is the root mean square orbital velocity.

2.5 Morphological processes

Morphological behaviour is fully controlled by the rate of sediment transport. According to the change in transport rate the bottom keeps updating. The changing bottom influences the rate of sediment transport. Finally depending on the combined action of waves and currents, sediment properties etc. the system tends towards an equilibrium condition and try to maintain it until it experience any change in the system. If there is any change in the controlling factors, the process continues and it always tries to get to an equilibrium situation. The governing equation for the change of bed level z_b is:

$$(1 - \epsilon) \frac{\partial z_b}{\partial t} + \frac{\partial S_{bx}}{x} + \frac{\partial S_{by}}{\partial y} = D - E \quad \ldots\ldots (2.41)$$

Where ϵ is the porosity, S_{bx} and S_{by} are the bed load transports in x and y directions respectively. D is the deposition rate of suspended sediment and E is the erosion rate of

suspended sediment. In a morphological model very often bed-load transport and suspended load transport are not considered separately, in such case the equation reduces to:

$$(1-\epsilon)\frac{\partial z_b}{\partial t}+\frac{\partial S_x}{\partial x}+\frac{\partial S_y}{\partial y}=0 \quad \ldots\ldots(2.42)$$

with S_x and S_y are the transports in x and y directions respectively. By observing the equation it can be seen that a positive transport gradient leas to a negative bed level gradient which means erosion. Similarly a decreasing transport gradient leads to deposition. It is to be noticed that the sediment transport itself is not responsible for any morphological change, but only the gradients in the transport controls erosion or accretion.

2.5.1 Open coast behaviour

Coasts are continuously interacting with waves and wave-driven currents. The most interactive part can be divided between surf zone and swash zone. Surf zone is the wave breaking zone and swash zone is the upper part of the beach between back-beach and surf zone. Swash zone is very dynamic in character and continuously shaped by the incoming waves.

Both long-shore and cross-shore transports play an important role in reshaping a beach profile. Wave-driven longshore currents move sand along the coast and depending on the transport gradients the beaches may accrete or erode. Changes due to long-shore transport gradient take comparatively longer time such as several years to evolve. But cross-shore profile can change dramatically specially during storm events. During storm conditions, swash motions are mainly governed by infra-gravity waves as short wave breaks in the surf zone and only infra-gravity wave persists. As a result, sediments are transported offshore by the cross-shore current with strong undertow and thus the cross-shore profile changes. Dune erosion and consequent over-wash are very typical in this situation. After the storm, during calmer condition the beach tends to recover and come back to its original shape.

An important element in describing dune erosion is the slumping of dry sand and the subsequent transports by the swash waves and return flow. In absence of the swash waves taking away the beach materials, the upper beach would stop to scours and the dune erosion process would slow down considerably.

2.5.2 Morphodynamics of equilibrium profile

The upper shore-face consists of swash zone, beach and dune or coastal cliffs. It is extremely dynamic in nature. It reacts to any changes induced by wave force and instantaneously starts to adjust with new system. Figure 2.10 shows a diagram of beach profile.

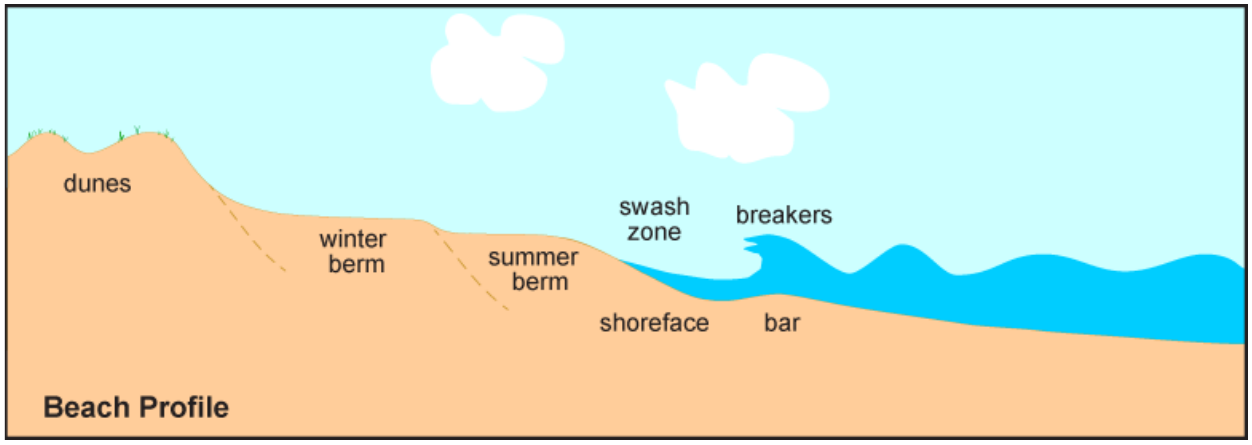

Figure 2.10: Beach profile (source: the website of Long Island University, New York)

An equilibrium profile is attained to cope with new system. Bruun (1954) was the first one to introduce the concept of dynamic equilibrium profile. He proposed an empirical equation for equilibrium beach profile consisting a simple power law relating the water depth, h to the offshore distance, x. The correlation can be presented as

$$h = A(x)^m \tag{2.41}$$

where A is shape factor depending on the characteristics of bed material and m is exponential factor equal to 2/3 .

During an extreme event this equilibrium is disturbed due to large waves that can reach up to coastal bluffs. Because of strong wave actions and subsequent undertow a large amount of sediment is transported to offshore. Sediments eroded from the profile tend to settle somewhere outside the surf zone where return current is not strong enough to transport them further offshore. A bar is formed there which stores the sediments. The new profile takes a parabolic shape according to Bruun's rule with some retreat in coast line. As the storm is over and the waves are back to their regular shape, the new profile seems to be too steep for the new situation. On the other hand, the bar formed outside the surf zone attracts more wave breaking near it. The wave asymmetry and skewness helps to transport the sediments towards shore. The bar supplies required sediments to the waves which results in reduction in its own size and eventually it diminishes. The sediments transported onshore helps to develop a new equilibrium profile with mild sloping beach.

2.6 Numerical models

One of the tasks regarding coastal hydrodynamics involves modelling of wave transformation near shore from offshore. To model these phenomena that waves undergo it is essential to have a good knowledge and understanding of meteorological parameters as they influence the wave transformation process.

Numerical model, which were developed for wave transformation in different time span, can be divided into three generations (Komen et al. 1996). The first generation models were not able to take the non-linear effects into account. The second generation models started to include the non-linear transition by introducing parameters but were not good enough as the solution was obtained using a coupled discrete scheme. The third generation models have

overcome these limitations and can effectively reproduce the significant physical processes with two-dimensional sea state if the model is calibrated properly. SWAN, WAMTECH, HISWA, MIKE are some available software packages that can be used for modelling.

To estimate morphological changes, many empirical formulas and theories have been established by scholars. Though they are well-established formula, they highly depend on the surroundings in which they are formulated. In order to use them in specific case, prior validation is compulsory to ensure acceptable results. This can be done by numerical simulation.

A numerical model is a set of formulae to relate the hydrodynamic forcing to the morphological response for a specific case. The model can be calibrated using some empirical parameters which can be determined from laboratory test or existing field data. Numerical models are very easy, useful and inexpensive way to anticipate the upcoming response of the beach due to any hydrodynamic forcing, thus becoming popular day by day. For numerical modelling, it is important to represent the actual situation by correct approximation of empirical parameters.

3 Erosion Mechanisms in the Arctic

3.1 Arctic coastal erosion

The erosion mechanism due to combined action of wave and current is described in the previous chapter. But the mechanism is not identical to each and every geological setting. The process described there is mainly applicable for sandy beaches in temperate or tropical areas. In the Arctic the situation is different mainly due to the presence of frozen-soil and sea-ice cover.

The sea surface in the Arctic is usually covered by sea-ice during winters. The coastal bluffs there are usually frozen i.e. permafrost, and they are typically covered with snow. That is why thermal properties become important in controlling coastal erosion in the Arctic. Generally no remarkable change in a coastline can be observed in the Arctic during winters. There are two processes in effect behind no coastal erosion during this cold time. Firstly, the freezing temperature turns the sea surface into ice sheet and prevents the waves coming onshore. As the waves cannot reach the bluff, there is no turbulence-induced sediment transport i.e. erosion is impossible. Secondly , snow, having low conductivity of heat, act as insulation layer over the dunes for air temperature and solar radiation. During summer the melting of permafrost turns the soil into a thawed mass moving down-slope and thereby causing erosion. But this process is delayed by the snow present over the bluffs by influencing the thawing of permafrost.

3.2 Erosion mechanisms

To describe the erosion of permafrost two concepts developed by Are (1988) are immensely supported by the researchers. These are named as “Thermo-denudation” and “Thermo – abrasion”. Both of them do not take place at the same time. But one single coast can experience both of the processes depending on surroundings and other factors in its lifetime. A detailed illustration of the processes is given in the following paragraphs.

3.2.1 Thermo-denudation

In summer both air temperature and solar radiation becomes intriguing factor for permafrost erosion. In the beginning of summer, the temperature starts to rise above freezing point and the ice starts to melt. The sea ice is melted first and waves can now reach to the shore. The protective insulation shield on bluffs no longer exists as snow over there also starts to melt. This leads to melting of permafrost underneath. The thawing of exposed permafrost sometimes form gullies within the bluffs. This melting process loosens the beach material as they turn into flowing slurry and thus responsible for the reduced strength and stability of the bluff material.

As a consequence the bluff is no more stable with the slope that it was before. Therefore the top part of the cliff collapses because of instability induced by its own weight. The sediment available from the toppling of the cliff is deposited at the foot of the dune or coastal bluff. The process of cliff erosion due to thawing of permafrost is termed as Thermo-denudation.

No large waves are needed for this kind of erosion. But wave has an important role on taking away the deposited sediments on the beach that becomes available from breaking of bluff. If the sediments are not taken away by wave actions the bluff attains a slope that is stable enough to the corresponding condition and erosion stops. But if the waves continue to transport the sediments offshore, then the procedure keeps continuing. A schematic diagram is presented in Figure 3.1 to explain the process.

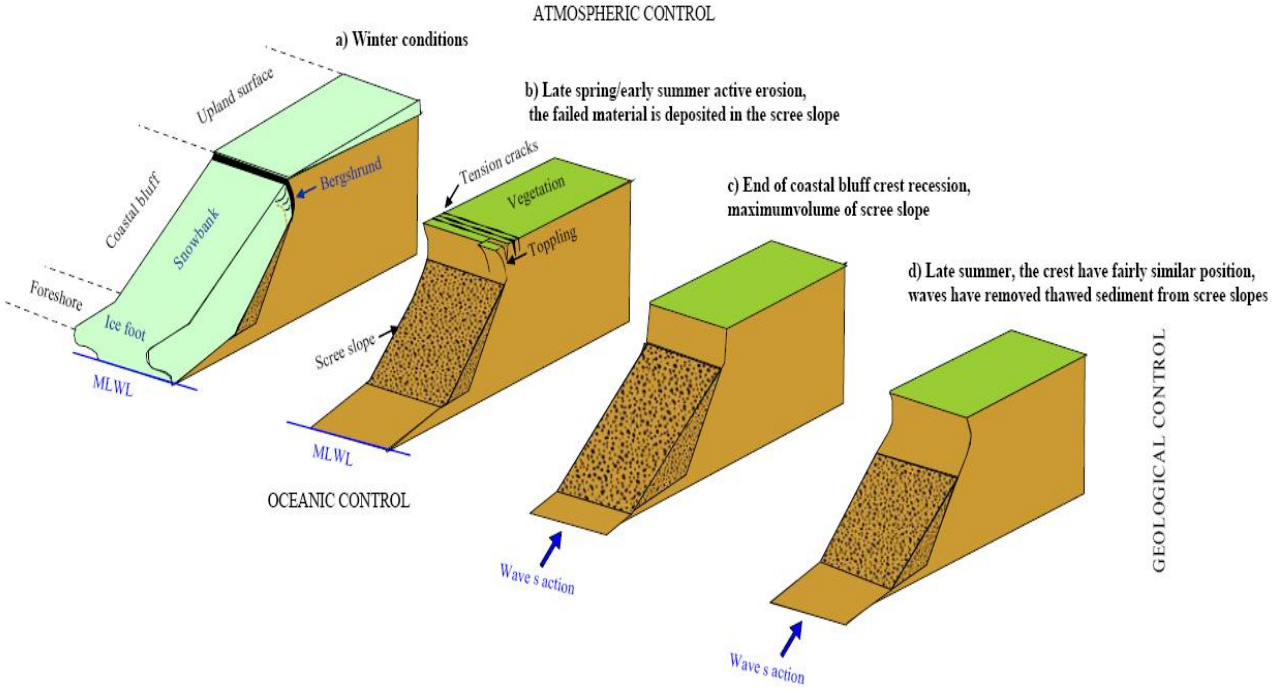

Figure 3.1: Conceptual model of thermo-denudation (After Brundsen and Lee,2004;sea-cliff geomorphological process-response system)

3.2.2 Thermo –abrasion

The second process, thermo-abrasion is initiated by the combined mechanical and thermal actions of waves. The waves generate turbulence at the bottom of the cliff. The strong plunging waves form a wave-cut notch at the foot of the shore-face. With further deepening of this notch the cliff is hollowing out leaving a cornice overhanging the beach. Finally at some point the overhanging part of cliff becomes unstable enough leading to block failure. The waves remain active to remove the deposited materials from shore-face and continue to dig a new notch. Thus the process continues. Figure 3.2 is presented to explain this process.

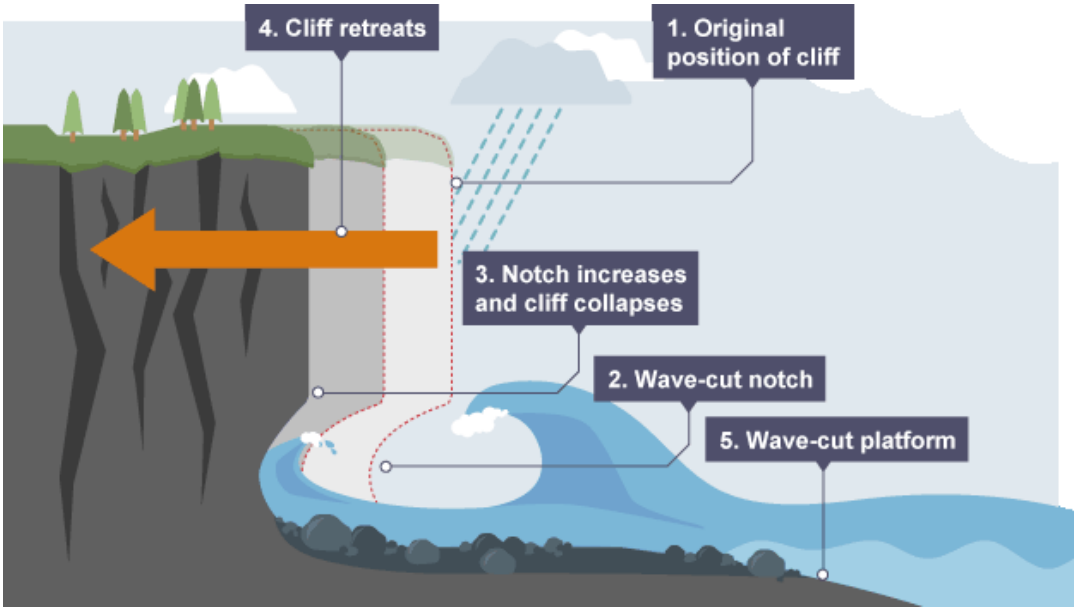

Figure 3.2: Conceptual model of Thermo-abrasion (source: the website of BBC-education)

3.3 Modelling of Arctic coast

There are very few numerical programs available to model the erosion process in an Arctic coast although not very accurately. The thermal properties become necessary and the geotechnical process needs to be combined with wave action of the system. The failure of a block can be modelled using geotechnical formula for stability with a probabilistic calculation. But to combine the wave actions with geological process controlled by specific thermal properties of sediments is a complicated task and calls for further research. The current study approaches to observe if it is possible to model an Arctic coast for erosion using a numerical tool that is available in this field.

4 Modelling Arctic coastal erosion

In this chapter the numerical modelling tools used for this study is narrated. The theory and formulations used by these tools and their applicability for this study is described to give the readers insights to the numerical modelling process.

4.1 SWAN

To get the boundary conditions in nearshore area from offshore wave data, a wave model is essential. Simulating WAves Nearshore (SWAN) has been used in the current study for this purpose. The SWAN is a wave modelling tool to compute random, short-crested wind generated surface gravity waves of a two dimensional area. This is a third-generation spectral wave model to simulate wave transformation while travelling towards the shore from deep ocean. It is a standalone open source program developed by Delft University of Technology, The Netherlands.

SWAN computes the wave energy and associated changes in wave heights, shape and direction for each grid by resolving wave action balance with sources and sinks. It analyses the wave spectral change due to the wind generation, white capping, wave breaking, energy transfer between waves, and variations in the ocean floor and currents. SWAN does not calculate wave-induced currents. The inputs required to set-up a basic model are bathymetry of the area, wind velocity and direction, wave parameters at offshore boundary, etc. Guidelines are available to prepare the code of commands for user-specific condition. There is no limitation for size of domain. But SWAN is recommended mainly for transition from ocean scale to coastal scale.

The model features provided by SWAN are mentioned below.

- Wave propagation in time and space, shoaling, refraction due to current and depth, frequency shifting due to currents and non-stationary depth.
- Wave generation by wind.
- Three- and four-wave interactions.
- White capping, bottom friction and depth-induced breaking.
- Dissipation due to aquatic vegetation, turbulent flow and viscous fluid mud.
- Wave-induced set-up.
- Propagation from laboratory up to global scales.
- Transmission through and reflection (specular and diffuse) against obstacles.
- Diffraction.

SWAN does not account for Bragg-scattering and wave tunnelling.

SWAN can produce outputs like one or two-dimensional spectra, significant wave height, wave periods, mean wave direction and directional spreading, one or two-dimensional spectral source terms, root-mean-square of the orbital near-bottom motion, dissipation, wave-induced force, set-up, diffraction parameter etc.

4.2 X-beach

For numerical modelling of coastal erosion, X-beach is going to be used as a tool in this study. This section is intended to describe the functionalities of this modelling tool in short. It is developed by a consortium of UNESCO-IHE, Deltares, Delft University of Technology and the University of Miami. It models the near-shore processes such as morphological changes, near-shore currents, wave propagation, sediment transport etc. and is aimed to estimate the effect on the near-shore area, beaches, dunes and back-barrier during time-varying storm and hurricane conditions. It is intended as a two dimensional process-based tool to compute the natural response and to predict the vulnerability of a coast to dune erosion, overwash and breaching. The step it follows is shown by a schematic diagram in Figure 4.1.

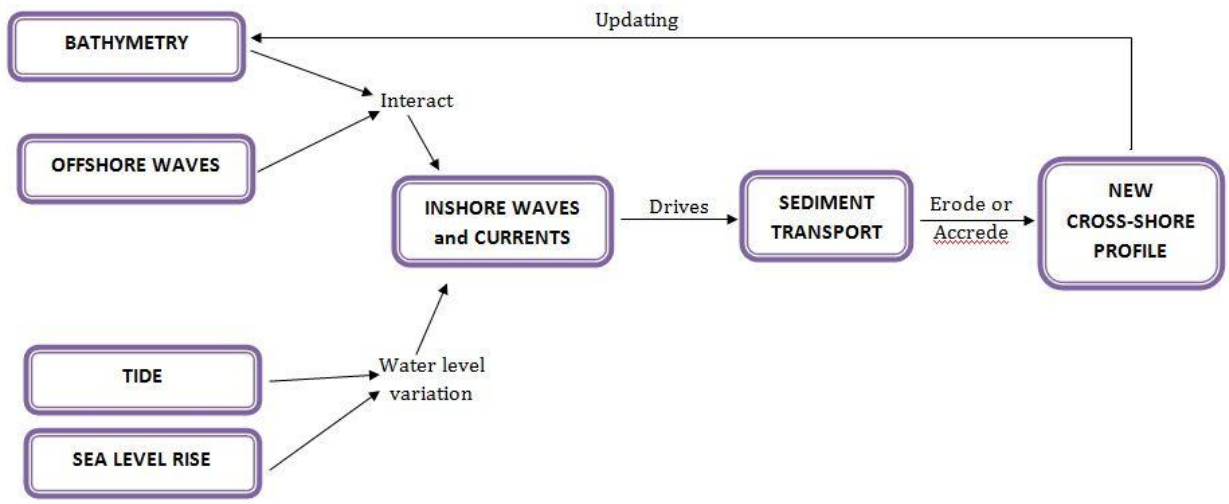

Figure 4.1: Schematic diagram of X-beach program

This tool is developed to model sandy beaches with tidal influences. No thermal properties of the beach material are taken into consideration. This already implies a limitation to use of this tool for an Arctic coast since sediment properties and erosion mechanisms are highly controlled by thermal properties of beach material there. For this thesis, a case study is assumed for the coast in Varandey, Russia experiencing coastal erosion due to storm event. The modelling of Varandey coast is going to be carried out for the storm that took place in the month of July. The permafrost is anticipated to melt during late winter or early summer. In summer, the coast no longer shows Arctic behaviour and sediment transport mechanism especially during storm condition is governed by avalanching. That is why the beach starts to act as a typical sandy beach. As the storm of interest in this study is in July, the use of X-beach in this setting may be justified.

The model applies formulations for short wave envelope propagation, non-stationary shallow water equations, sediment transport and bed update. A newly developed time-dependent wave action balance solver is also introduced so that no separate model is needed to simulate the propagation and dissipation of wave groups. It can also predict wave-current interaction in the short wave propagation by solving various wave breaking dissipation models.

The nonlinear interaction of waves and current in shallow water is the reason behind forming an undertow which contributes a lot to bed shear stresses and offshore sediment transport. The Generalised Lagrangean Mean (GLM) approach is implemented to represent the depth-averaged Eulerian flow velocities. It combines a time-dependent wave action balance with the nonlinear shallow water equations (NSWE). It is a well-known concept behind sediment transport that wave induced turbulence stir up the particles from bed and current is responsible for transportation of this suspended particles. The equilibrium sediment concentration is obtained from computed hydrodynamics using the pick-up function (Reniers et al. (2004). Suspended sediment concentration acts as a source term for the 2DH advection-diffusion equation. Two sediment transport formulas are available to compute transport vectors. Thay are - Soulsby-van Rijn (1997) and Van Rijn (2007). Bed level changes are updated from sediment transport gradients.

An important mechanism- Avalanching is also implemented in the model by introducing a pre-defined threshold slope both for dry and wet points. The transport of sediment from dry dune face to the wet swash zone is controlled by slumping and slumping of sand during dune erosion is triggered as the slope exceeds this threshold value. This phenomenon also plays a role to model the morphological update of the dunes. A schematic diagram of X-beach modules is presented in Figure 4.2.

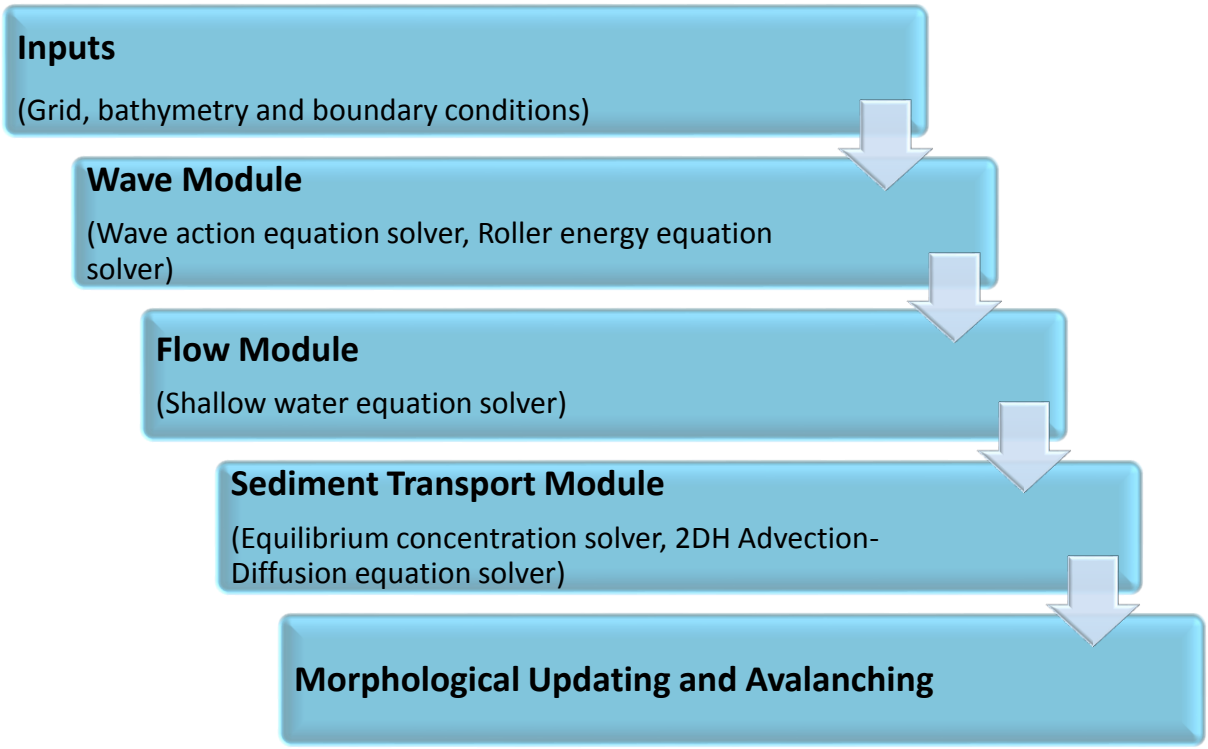

Figure 4.2: Schematic diagram of X-beach modules and corresponding theory

As the inputs for an X-beach model, it is important to define boundary conditions provided by the wind, wave and surge models and the main output generated by the model will be the time-varying bathymetry. The numerical implementation is mainly first order upwind in combination with a staggered grid. The model scheme utilizes explicit schemes with an automatic time step based on Courant criterion to ensure numerical stability of the solution.

The model is aimed to provide sensibly accurate stable solutions in a reasonable computational time.

Details of initial and boundary conditions specifically applied to model the study area are illustrated in following text.

5 Chapter 5: Case Study: Varandey, Russia

5.1 Introduction

For this thesis, a case study is considered for Varandey, Russia. A model is going to be set up to simulate the coastal erosion of the area under consideration for storm event. The results from the simulation are compared later with full-scale observations to validate the model. This chapter provides a short introduction of the area under consideration. The source and reliability of the data used for setting up the model in the current study are also explained.

5.1.1 Area description

The location for this study is chosen as Varandey, Russia. Emerging hydrocarbon industry in Varandey has made this area more attractive to commercial investors. Varandey seaport and settlement located near the coast are used extensively for logistic support of oil industry. Various types of industrial activities are coming into existence in the area day-by-day making it more vulnerable to geomorphologic changes. The coastal infrastructures to be installed by these projects are under threat because of active coastal erosion process. This issue has attracted the researchers and scientist because of its long-term variable coastal erosion. Therefore a detailed understanding of the process has become necessary to ensure safety of these structures and also to avoid any long-term adverse effect.

The location selected for the purpose of the current study is the coast of Varandey, Russia. The Pechora Sea (Russian name - Pechorskoye More) is a south-eastern extension of the Barents Sea located in the European part of Russia. The coast is located on the Pechora sector of the Barents Sea in north-west Russia. The tentative co-ordinate of the area is 68°47'33"N and 57°58'10"E. The area is indicated on the map in Figure 5.1.

Figure 5.1: Location of the Varandey area. (source: Google map API)

Varandey coastline is differentiated into three geographic sectors by two rivers - VarandeiskayaGubaand the Peschanka. The 90 kilometer long coastline can be subdivided into three regions named "Pesyakov", "Varandey" and "Medynskiy" according to their geographical variability. Figure 5.2 shows these three area in a satellite image.

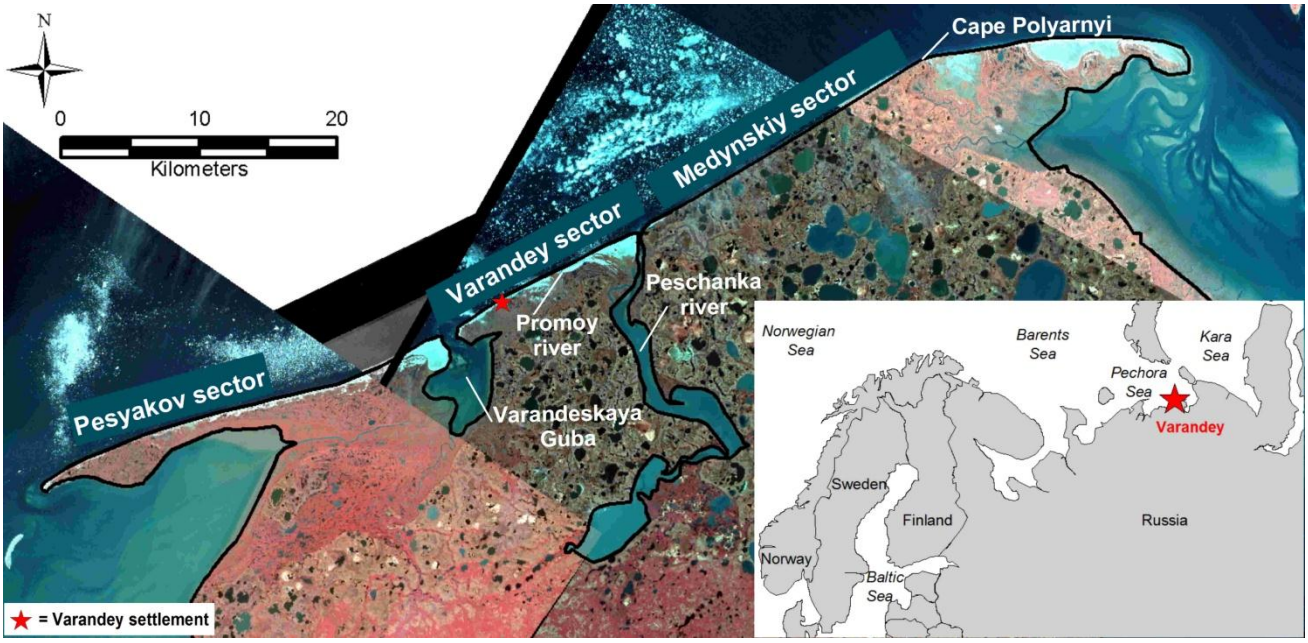

Figure 5.2: Location of the Varandey area. Pictures: SPOT images from 1998 (on the left) (Source:E. Guegan ,2013).

The coast of Varandey was affected severely by storm in July, 2010. Medynskiy sector of the coast is approximately 25 kilometer long. The eastern part of this sector is observed to show maximum coastal erosion. The current study focuses mainly to this part of Varandey coastline.

5.1.2 Geomorphology

Field investigations by various researchers describe the geology and geomorphology of the coastal profiles. Both "Pesyakov" and "Varandey" area are observed to have 5m to 12 m high dunes with marine terrace and sandy beach. But "Medynskiy" is a bit different from other two sectors. It has a fairly continuous bluff. It is composed of a 5 to 15 m high marine terrace which reaches the sea forming 3 to 10 m high coastal bluff. On the lee-side of the bluff snow banks are found to persist until late July (Ogorodov, 2005). This coastal bluff is subjected to erosion by wave action. The existence of a small beach width can be explained by this wave action and characteristics of beach materials. The beach materials are not course enough to resist the erosion and maintain a wider beach.

A sketch from E. Guegan (2013) is shown in Figure 5.3 to give a visual of the beach profile of Medynskiy sector.

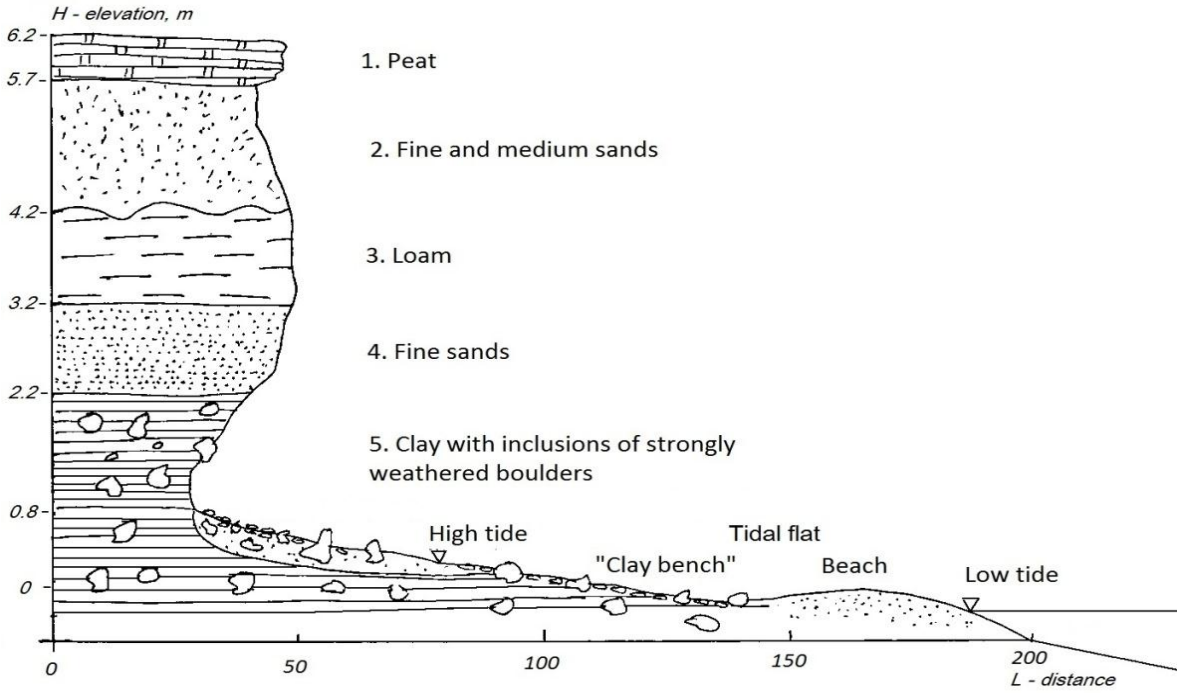

Figure 5.3: Geological-geomorphological profile of the thermal abrasional coast of "Medynskiy" sector, modified from (Ogorodov, Unpublished results-b) (Source: E. Guegan,2013)

Some photos from eastern part of Medynskiy area is shown in Figure 5.4 to give the readers a practical feeling of the existing area.

Figure 5.4: Photos from eastern part of Medynskiy area (Source: Ogordov S.A.,2013)

5.1.3 Erosion observations

Large variation in erosion rates of Varandey has drawn the attention of researchers. The coast has been observed for long and the satellite images are available from year 1968. Further field investigation has been carried out by various researchers to improve the knowledge on erosion mechanisms. The rate of erosion varies along the coast. The eastern part of the coast shows maximum erosion. The report by E. Guegan (2013) is found very important to get information on the history of erosion rate. Figure 5.5 is presented below to give an idea on the variability of average erosion rates along the Varandey coast which is collected from above mentioned report.

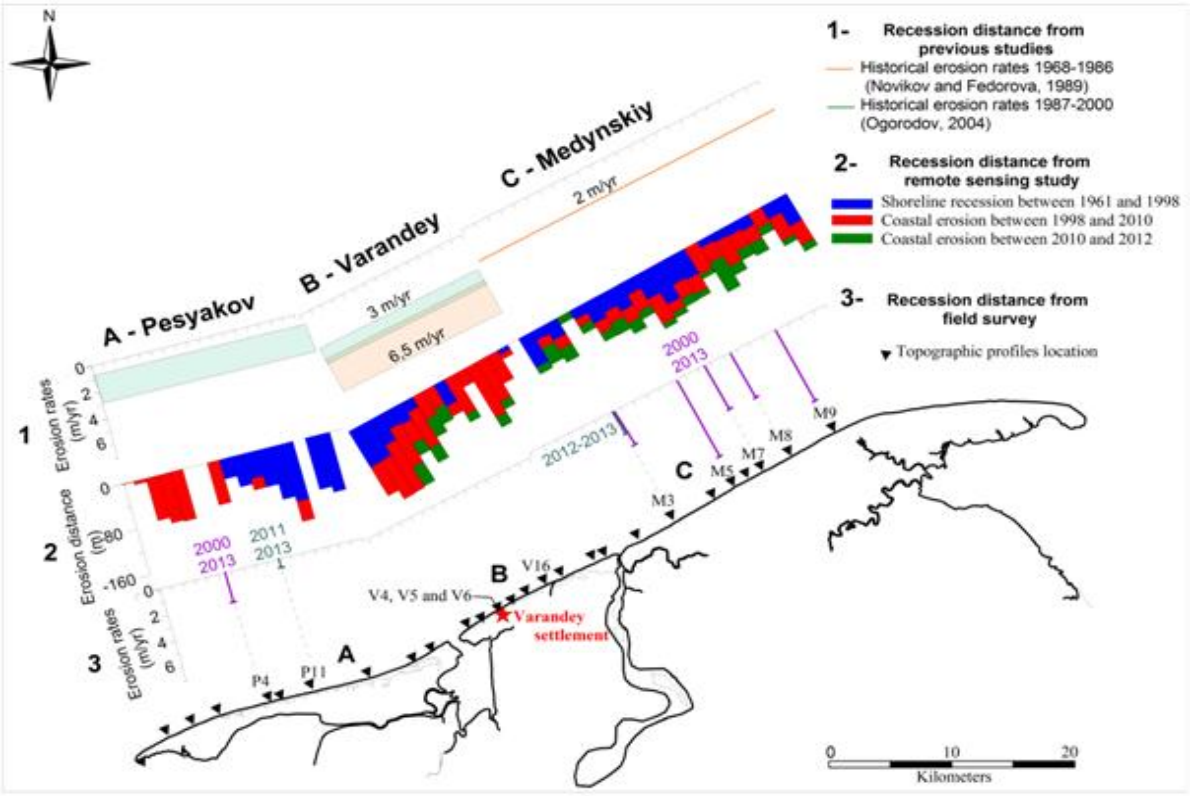

Figure 5.5: Erosion rates along Varandey Coasts; A – "Pesyakov", B – "Varandey", and C – "Medynskiy". (Source : E. Guegan ,2013).

To understand the coastal processes it is important to have knowledge on hydro-meteorological data of the area as they influence coastal dynamics. This area shows Arctic behaviour during winter season. The sea surface near the coastline remains covered with floating or land fast ice and thus no waves can reach to the coast due to freezing sea surface. The ice forms an insulation layer for the dunes as well. During summer, the snow cover does not exist anymore and thawing of permafrost eventually leads to down-slope movement of thawed mass due to instability of soil. This eroded mass is deposited at the foot of the coastal bluffs. The waves can reach to the shore now as the sea ice disappears allowing waves to approach the coast and play their role to active erosion process. Both thawing of permafrost due to increasing air temperature and the wave actions are responsible for the coastal erosion. Therefore ice-free period is very important in coastal dynamics.

Figure 5.6 describes annual average temperature range for the area. This graph is obtained based on the temperature recorded during year 2000 to 2012 from the website of "World Weather Online". Though it does not provide any information about long term variation of the air temperature of the area, it gives a good idea about the monthly variation of temperature within a year. In Figure 5.6, the average high temperature is shown with a red line and average low temperature with a blue one.

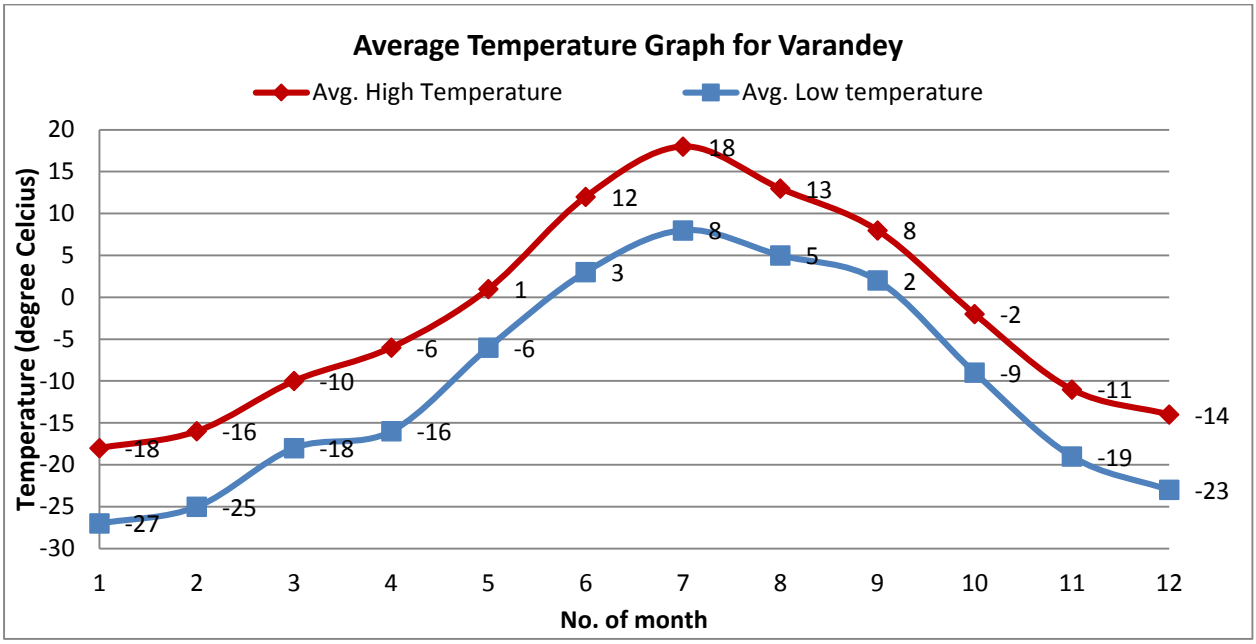

Figure 5.6: Average temperature graph for Varandey area (source: website of world weather online)

The average highest air temperature can be noticed in the month of July whereas the average lowest temperature can be observed in January. June to September can be considered as summer days. January to May and October to December can be considered as winter period. The presence of snow to the lee-side of the dunes has been observed until July in Medynskiy. The ice-free season usually is considered as from July to October (E. Guegan ,2013).

The ice free period is considered as the period with active erosion. The Arctic geodetic settings are responsible for two different erosion mechanisms – Thermo-denudation and Thermo-abrasion. The rise in temperature initiates thawing effect and eventually thermo-denudation process. No severe wave condition is necessary for thermo-denudation. This type of erosion is expected to continue through whole summer. But during storm conditions high waves can reach the coastal bluffs and wave-cut notch triggers block type of failure. This process, termed as 'thermo abrasion' can contribute to larger rate of erosion with harsh changes in coastline.

A drastic change in coastline was observed during 2010. A catastrophic storm on 24th July 2010 is considered as main reason behind this. The coastal bluff which was linear in 2010 turned into a curved one as investigated on 2011. The thermo-abrasion type of failure was evident at site. The block type of failure indicated towards erosion by high and strong waves. Figure 5.7 shows a comparison between satellite images taken in 2010 and 2011.

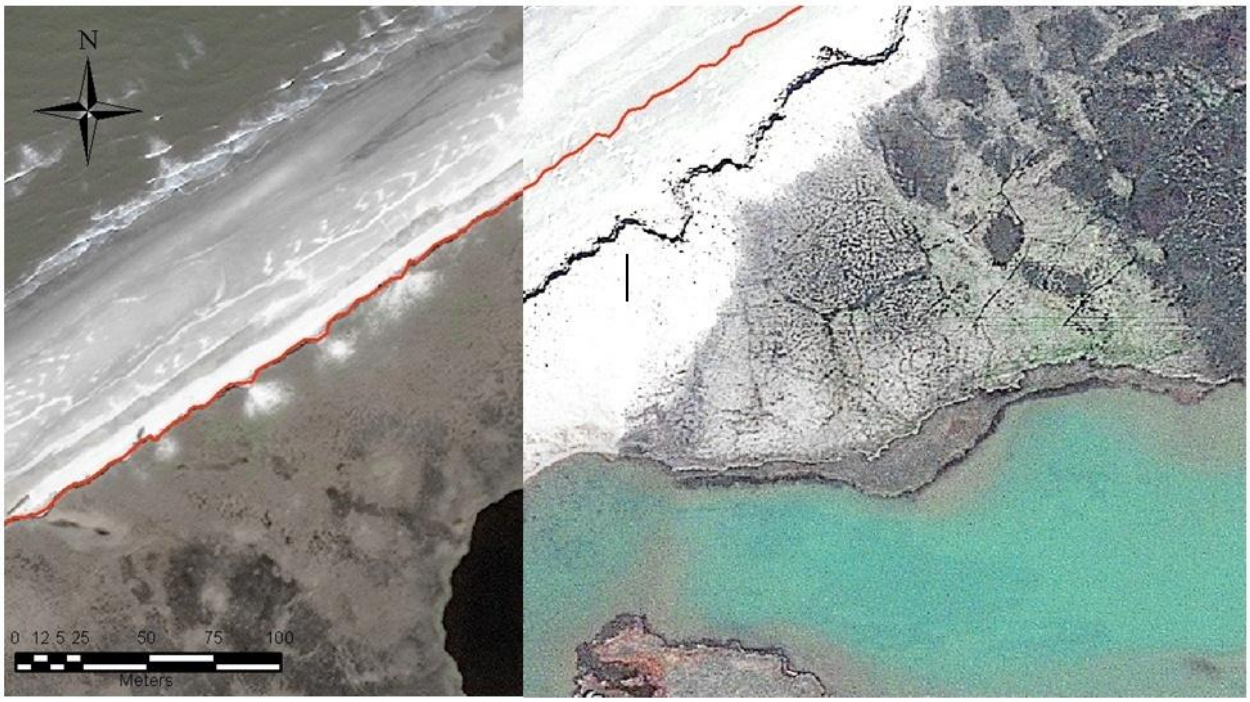

Figure 5.7: The difference of geometry of the coastline from 2010 to 2011. (Source:E. Guegan ,2013).

There has been a lot of research on measuring coastal erosion rates and understanding the natural processes behind this. Coastal Storm Modelling System (CoSMoS) is one of the recognized numerical modelling tools to model thermo-abrasion process for estimation of Arctic coastal erosion taking thermal effects into consideration. There is a lot of scope to improve the tools so that coastal erosion can be modelled better using numerical modelling approach to represent the actual behaviour of the coast.

5.2 Description of the problem

The erosion can be divided into two types – erosion due to longshore sediment transport and erosion due to cross-shore sediment transport. In case of a storm condition, cross-shore transport of sediment is the prime reason for coastal retreat. The sediments supplied by the degradation of coastal bluff are transported offshore by strong waves. A storm surge can magnify the rate of erosion. If a surge is combined with high tide, it can produce a vigorous height of water level near the shore. The high energetic waves are then capable of eroding dunes. Overwash of dunes is quite common during this kind of extreme events. During any storm event, the erosion can be considered solely depended on cross-shore transport by ignoring the longshore effect. Therefore in assessing coastal erosion due to storm only situation, cross-shore transport is calculated.

Investigations on understanding the erosion mechanism is still going on. Arctic geodetic setting makes it critical to model this kind of coast. Both thermo-abrasion and thermo-denudation takes place on the same coast depending on other climatic factors. There is currently no model available to model these phenomena successfully. Thermo-denudation can be compared with the avalanching process of soft silty cliff. The slumping failure of silt cliff material looks similar to thermo denudation type of failure. But regardless of similarity in outlook, no scientific proof based on experiment has been established to support this idea.

On the other hand, wave cut notch by thermo abrasion following the mechanical erosion process can be modelled using wave transformation and sediment transport formulations as long as the thermal factors are allowed to be neglected. But intensity of notch that can make a block to fail cannot be determined utilizing the available theory. This is where a coupling of geotechnical process with other processes becomes essential.

This study is an approach to numerically model the coast for erosion due to extreme events (i.e. focusing on cross-shore sediment transport) especially bluff or dune erosion. As the study area selected shows Arctic behaviour during winter, the model is developed to simulate the summer condition with ice-free period. X-beach is used as numerical modelling tool which is mainly developed to compute dune erosion in sandy coast due to storm. A model is generated to simulate the coastal erosion of Medynskiy area and thereby to observe if it can resemble the existing behaviour of this Arctic coast.

5.3 Approach

To generate the model data regarding bathymetry, wind, waves, tide and sediment properties are essential. The first step towards the task is to obtain these data from different source. The model is intended to set up using the hindcast data from the storm on 24th July 2010. The records for wind, wave and tide for that specific time is used to simulate the model. A tentative sediment characteristic is estimated to match the existing situation based on written communication with Emilie Guegan, PhD student, NTNU, SAMCoT. The measured erosion rates obtained from other sources is found useful to validate the model prepared. It is very important to verify the reliability of the results before progressing further. The amount of erosion found from model run is compared to measured value for this purpose.

The wave data is available far offshore from the area of interest. To reduce the computation time and grid size for coastal erosion analysis, transition of wave data from ocean scale to coastal scale is required. Wave modelling tool, SWAN is utilized for this purpose. The result from SWAN is used as input for main model. For coastal erosion analysis, X-beach is selected. Only near shore area is modelled with X-beach. The upper shore profile could not be obtained for the continuous coastline. That is why only one representative dune profile is chosen for analysis.

After checking the sensible behaviour of underlying physical processes associated with output parameters, model is found convincing enough to simulate the area of interest with certain reliability. As the model is ready to give results, a sensitivity test is carried out to observe the impact of wind stress over the computational domain. Model is run with different wind speed and the results are noted to deduce the relation of this term to output.

Another analysis regarding the sensitivity of critical slope for avalanching is performed. The significance of both the threshold values for wet and dry slope is studied and their consequence over the result is presented. This sensitivity test will contribute to a better understanding of the model developed.

5.4 Selection of X-beach as modelling tool

For numerical modelling of coastal erosion, it is a prime task to decide upon a tool that is suitable for the specific case of Varandey. As the coastal erosion during a storm event is going to be modelled, attention is paid to select a tool that can predict cross-shore sediment transport rate and consequent dune erosion. X-beach is a two-dimensional process-based tool to model dune or bluff erosion in a sandy tidal beach by an extreme event with reasonable accuracy and reasonable computation time. The behaviour of the coast and predominating erosion mechanism are also kept in mind while choosing a numerical modelling tool. X-beach is found to imitate the process for dune or bluff erosion by calculating the possibility of avalanching to that of existing coastline. This phenomenon can be considered similar to thermo-denudation to some extent. In thermo-denudation, soil from dune gets loose as a result of melting permafrost which is termed as thawing effect. Then it fails by its own weight and eventually washed away by wave actions. Avalanching considers slumping of sand causing dune erosion when the slope exceeds a critical value.

5.5 Data

The objective of this study is to model cross-shore coastal erosion using X-beach. To get the boundary conditions to be applied in X-beach, another wave modelling tool, SWAN is used as well. For any numerical modelling some data are required as inputs. For this analysis the required data are:

- Bathymetry and Cross-shore profile
- Wind and wave data
- Tidal data
- Sediment characteristics
- Rate of erosion in a known storm event

The following section narrates the source, explanation and reliability of data that are used extensively for both SWAN and X-beach analysis to carry out this study.

5.5.1 Data for SWAN analysis

5.5.1.1 Bathymetry and Cross-shore profile

MIKE, another software powered by Danish Hydraulic Institute (DHI) is used extensively to obtain bathymetry data. MIKE C-map is used as a tool to extract bathymetry of the study area. Jeppesen chart is a worldwide electronic chart database providing information on depth and tidal variation. MIKE C-map uses this information to create the bathymetry of the area someone interested in. MIKE Zero is then used for processing of this bathymetry data. The area under consideration is modified according to user's point of interest and additional bathymetry information (if available) can also be added to match the existing field condition. Finally generation of mesh and interpolation of depth data is done to create a new bathymetry file which is further processed by Surfer11 to convert it to a suitable format (.dat) which can be used as input for SWAN or X-beach.

Figure 5.8 shows the bathymetry of the study area used for wave transformation.

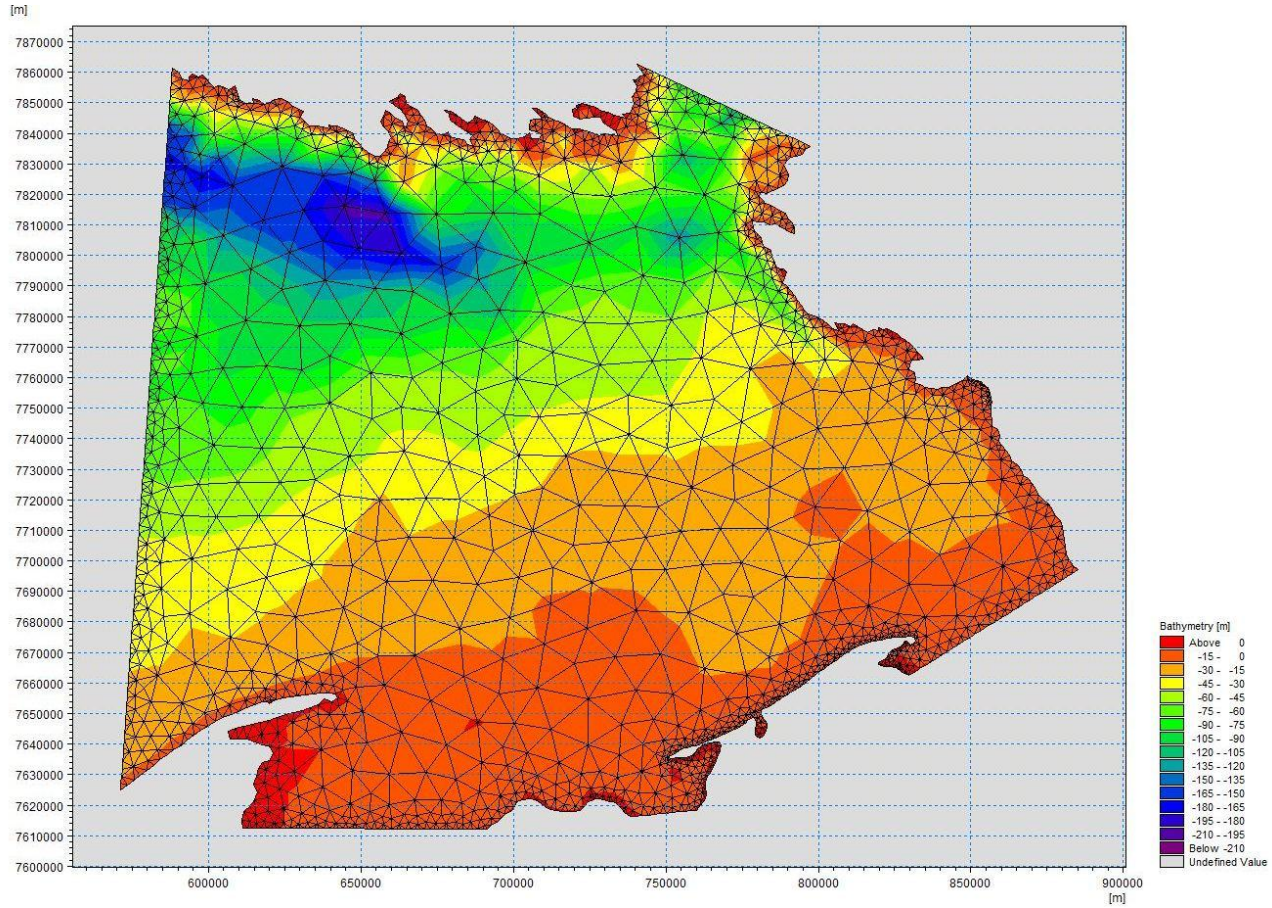

Figure 5.8: Extracting bathymetry map using MIKE zero

About 314 kilometer by 250.5 kilometer domain is selected to extract the bathymetry. This huge area has to be investigated to get wave conditions at the boundary of computational area for X-beach. The resolution of the bathymetry is finalized as 104mx83m considering the limitation of virtual memory of computer system and the amount of data to be handled. Figure 5.9 shows the interpolated bathymetry of the area based on the data extracted from MIKE C-Map.

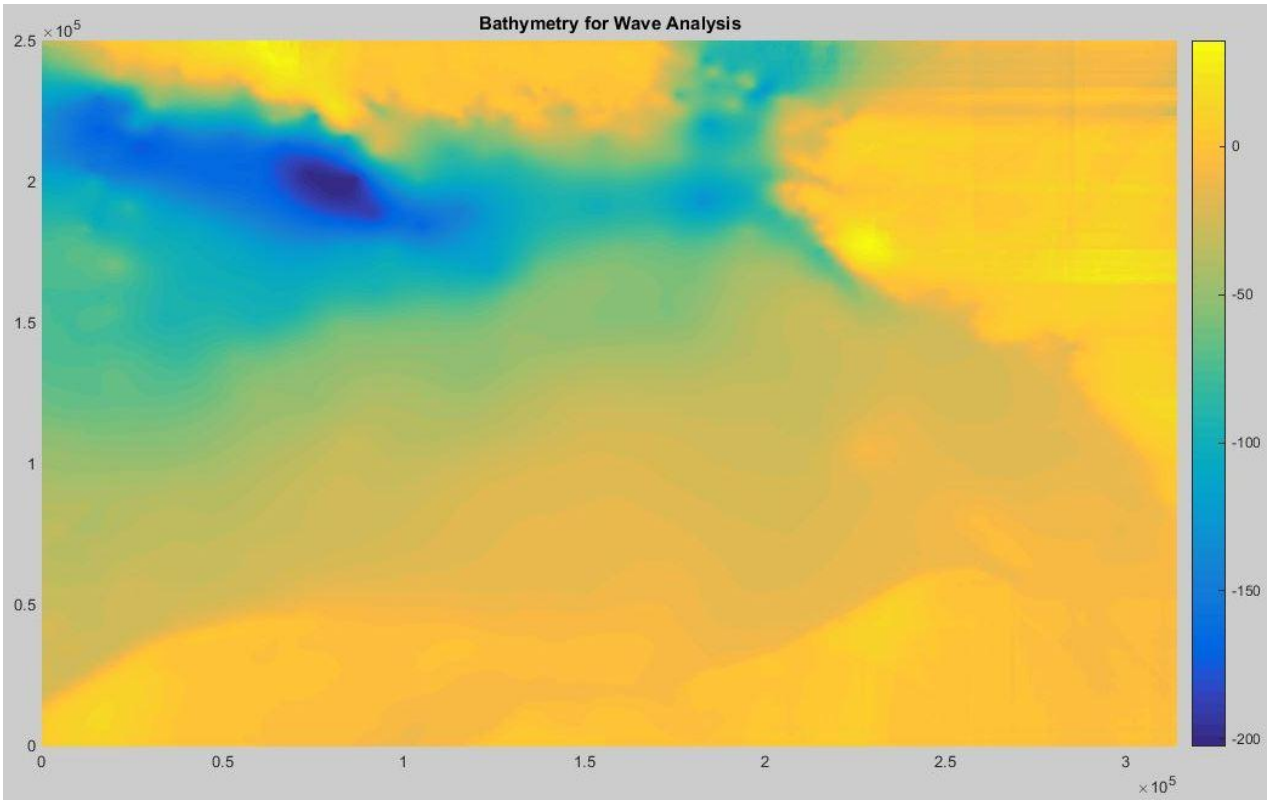

Figure 5.9: Interpolated bathymetry map for wave modeling

From the figure above, it can be seen that the study area is more or less protected by land from east and north directions. The only possible direction of incoming wave to enter the domain is from west boundary of the domain. The north-west part of the domain is the deepest with average depth of about 180m.

5.5.1.2 Wind

For wind-generated sea waves, the wind speed and direction play an important role to wave parameters. Fetch length, wind speed and water depth together determine the wave properties using wave-energy balance. Annual average wind speed is calculated as 22.3 km/h for year 2000 to 2012 according to the information by "World Weather Online" website. In year 2014, the maximum wind speed recorded was 90 km/h on 20 April according to the information provided by the online website "TuTiempo".

A 24 hour long catastrophic storm took place in Varandey on 24 July 2010. The consequence of the storm on coastal erosion was widely noticeable and thus provide important information for this study. That is why attention is paid to the wind and wave conditions of that particular event only. Wind data are collected for the month of July 2010 from both Norwegian Meteorological Institute (NMI) and European Centre for Medium-Range Weather Forecasts (ECMWF).

The data NMI provided is at the coordinate of 70.46^{o}N and 52.64^{o}E which is far offshore from the coast under this study. In Figure 5.10 the red arrow points towards the area of study and the black star indicates the location of wave gauge. The wave gauge is located about 285.15 kilometres to NW (310^{o}) of the study area.

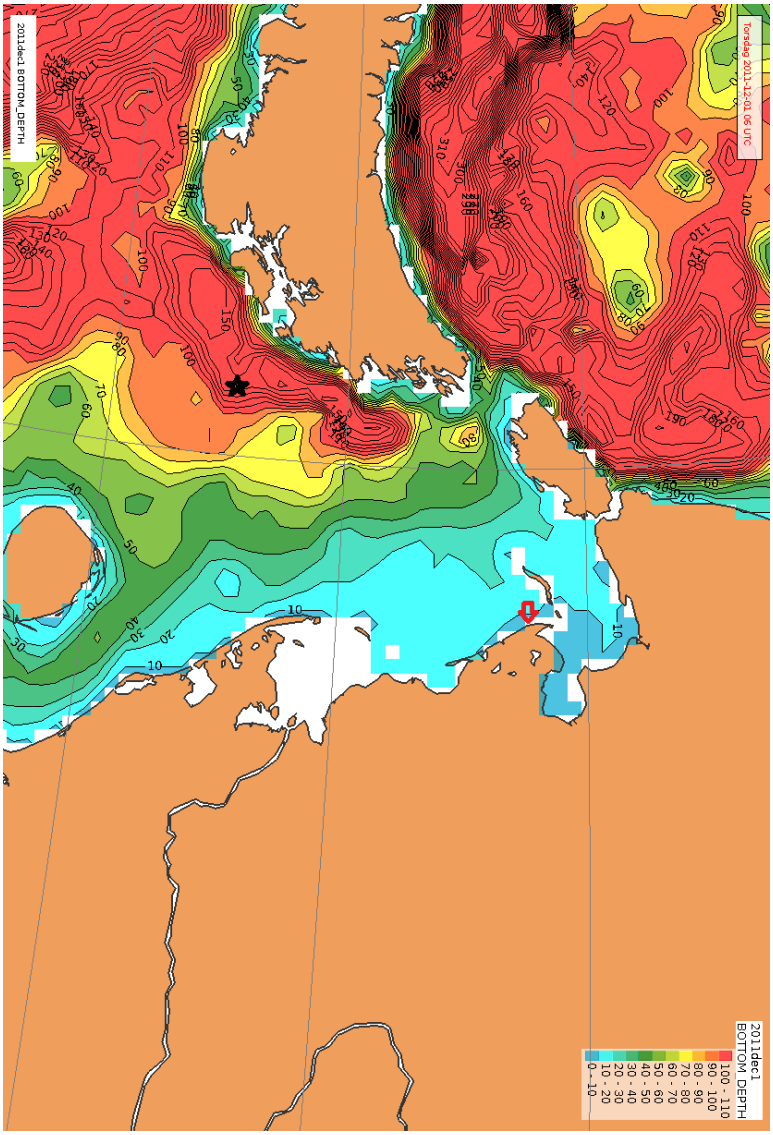

Figure 5.10: Location of hindcast data from NMI (source: NMI)

Wind speed and direction at different elevations are provided by NMI for each 3 hour interval. This information is used for wave modelling which will be further discussed in the section 5.5.1.3.

Wind data at 10 meter elevation is obtained for 12 hours interval from the website of ECMWF also. The data are downloaded from publicly available ERA interim report from their website. The data from NMI and ECMWF is compared for the month of July in Figure 5.11. They are found to follow the same trend.

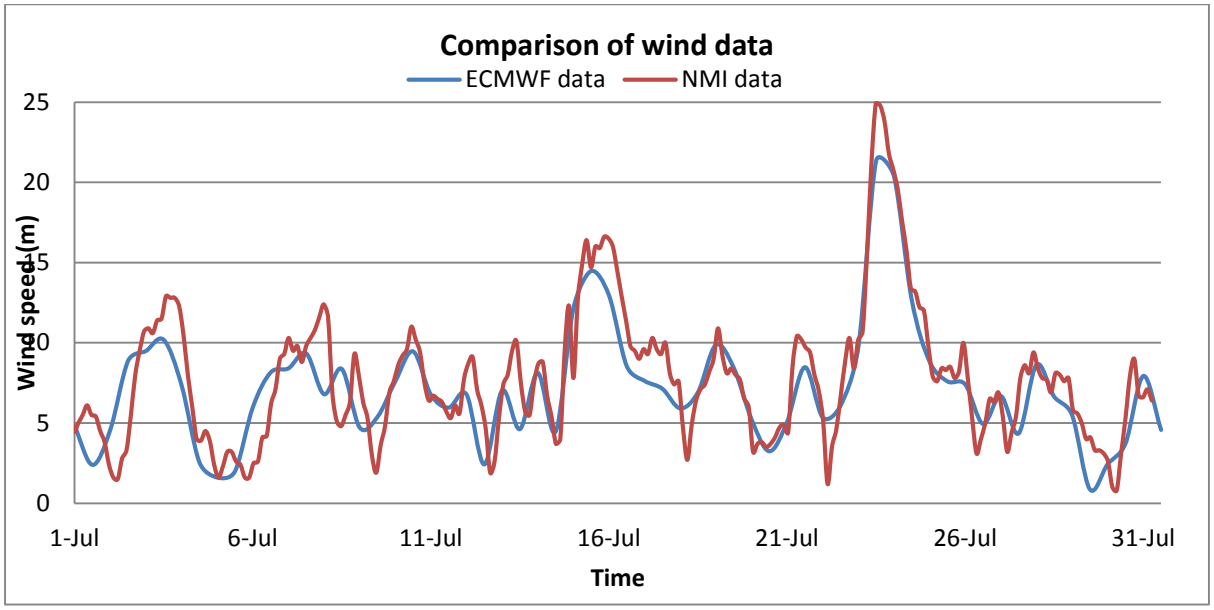

Figure 5.11: Comparison of wind data from NMI and ECMWF

Though they follow the same trend, but data from NMI is used for analysis. The data provided by ECMWF is for 12 hours interval whereas the data from NMI is for 3-hour interval. That is why the wind data from NMI is expected to represent the variation in wind field more accurately. Therefore NMI wind data is used for wave analysis. A windrose diagram for the month of July 2010 is presented in Figure 5.12 and 5.13 to get an idea of predominant wind direction. The predominating direction is observed to be NW to W.

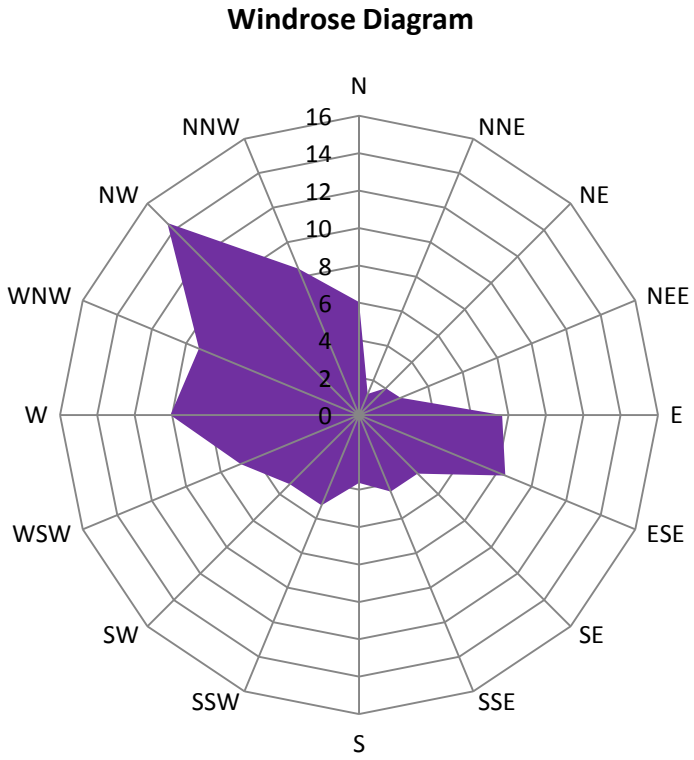

Figure 5.12: Windrose diagram for all wind speed

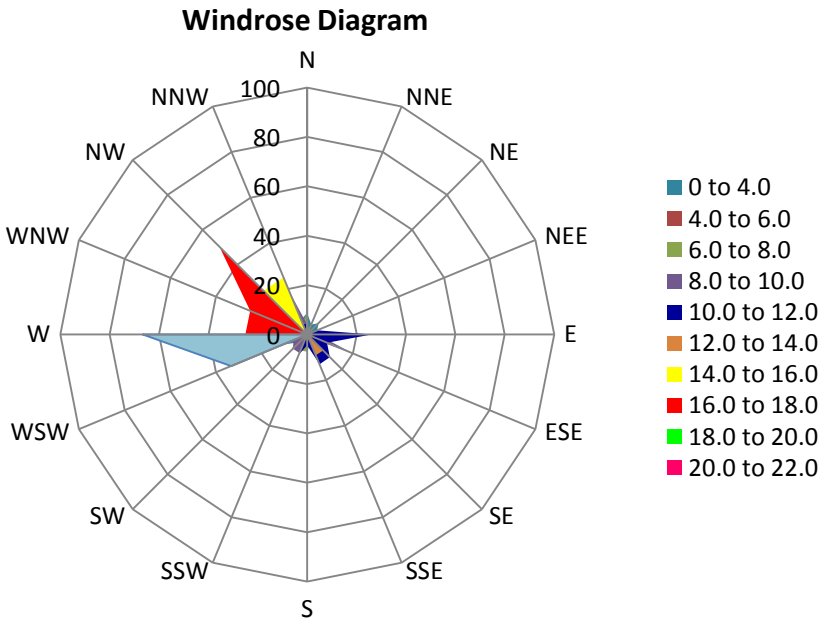

Figure 5.13: Windrose diagram for different group of wind speed

5.5.1.3 Wave

Coasts are exposed to waves only in ice-free seasons. Wind generated waves are defined by wind direction, wave fetch and water depth. The area concerned is protected from significant waves coming from North, east and south because of land boundary and shallow depths. The longest fetch can only be observed from NW to WNW direction which can produce the waves without any obstacle because of land boundary and give the largest contribution to wave energy amount.

As mentioned earlier only in summer time, the waves can trigger the erosion process as they can reach the shoreline. In winter, sea ice prevents the waves from reaching onshore and thus they have no effect on erosion. This is why only ice-free months, i.e, from July to October, are the main focus of this study.

Wave data are collected for the month of July 2010 from Norwegian Meteorological Institute (NMI) at the same point as wind data, see Figure 5.10. Sea state is defined for each 3 hour and the parameters of JONSWAP spectrum for wave for each sea-state during July 2010 are collected. The wave data are used to prepare the waverose diagrams presented in Figure 5.14 and Figure 5.15. From the diagrams it is evident that the predominant direction for wave is from NW to WNW.

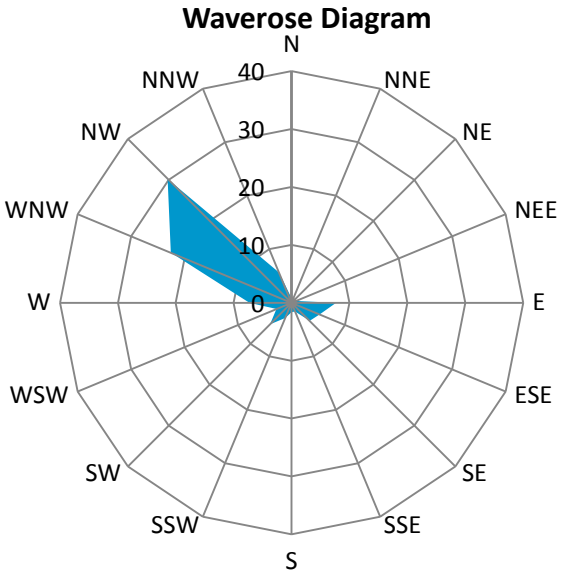

Figure 5.14: Waverose diagram for waves in July,2010

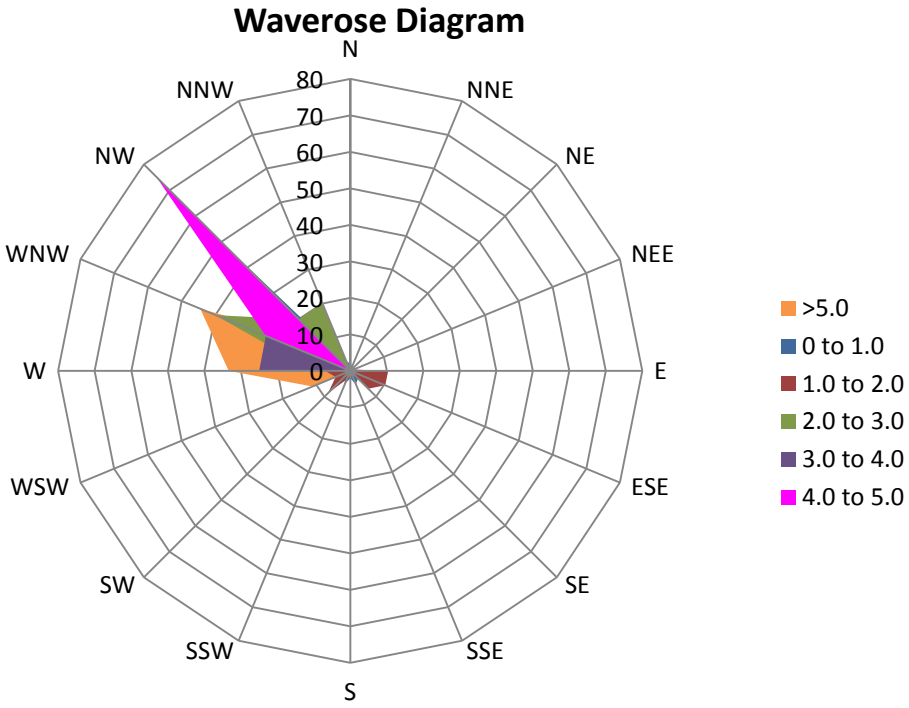

Figure 5.15: Waverose diagram for different wave height groups in July 2010

5.5.2 Data for X-beach analysis

5.5.2.1 Bathymetry and Cross-shore profile

For modelling of coastal erosion, comparatively smaller area with increased resolution is taken under consideration. Bathymetry data extracted from Jeppesen chart using MIKE C-Map are used again. But the Jeppesen chart provides bathymetry for area under water only. For coastal erosion analysis the cross-shore profile of upper shore face with dune is necessary. To incorporate the dune profile, bathymetry data are introduced to represent the

beaches and dunes. The correction made it possible to get a full cross-shore profile of coastal area. The tentative shore profile utilized for the erosion analysis is assumed based on the figure 5.3 and presented in Figure 5.16. Figure 5.17 shows bathymetry of the area selected for X-beach run with manually incorporated values.

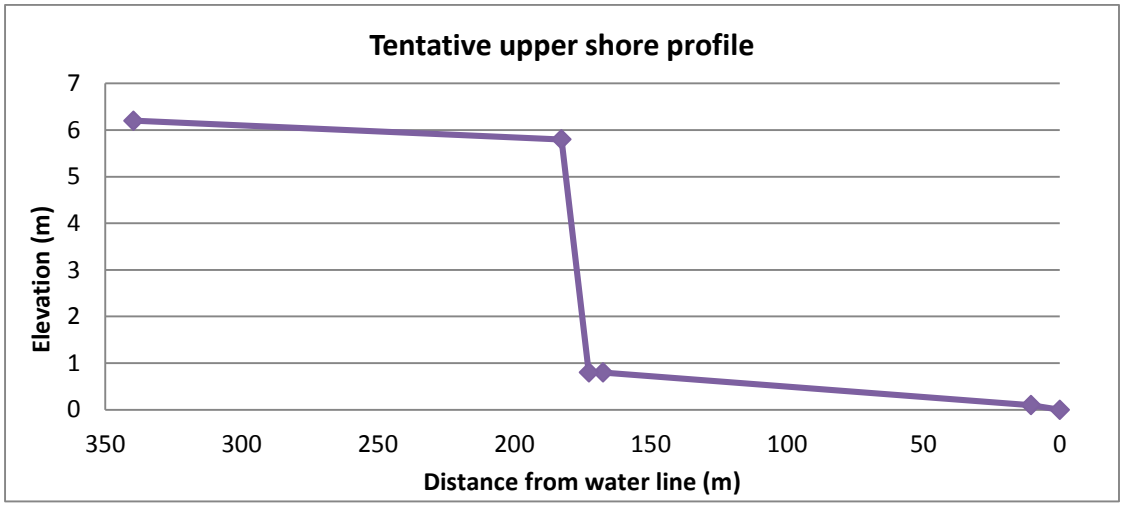

Figure 5.16: Assumed dune profile (refer to figure 5.3)

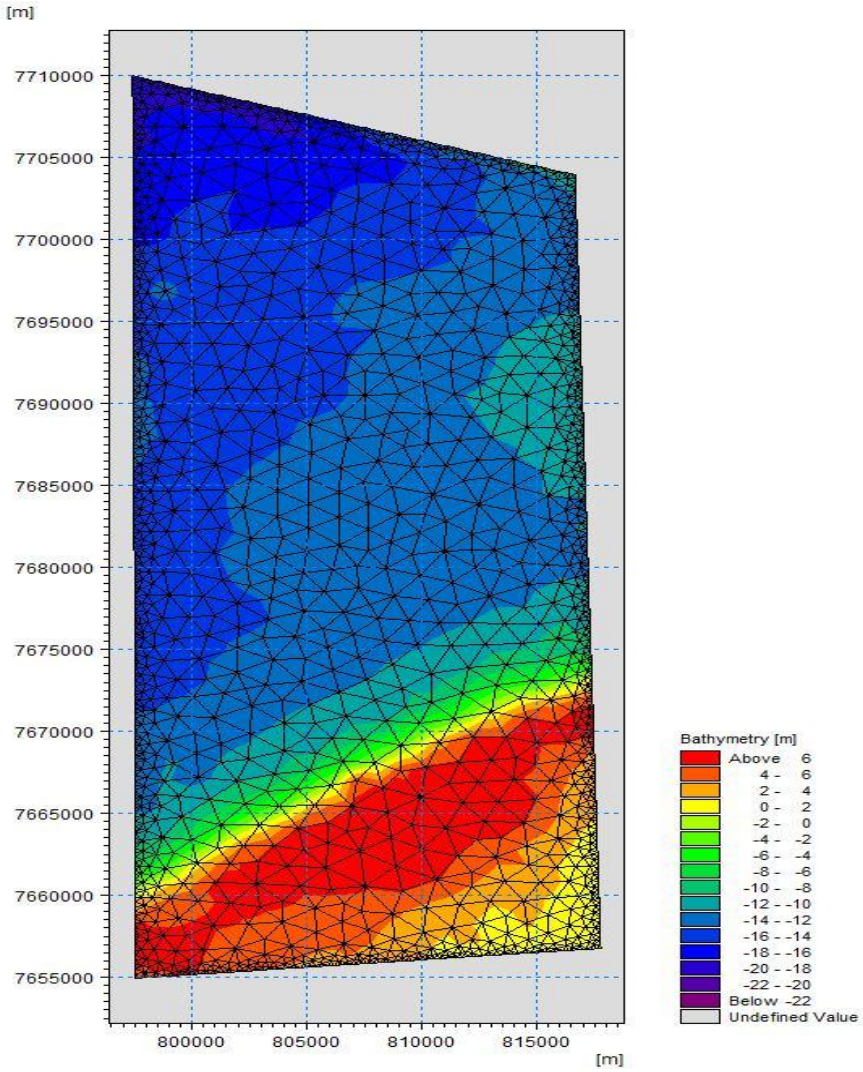

Figure 5.17: Bathymetry map for X-beach

Special attention is given to the location of incoming wave boundary. It is made sure that the result from SWAN for wave modelling can sufficiently represent the boundary condition for coastal erosion analysis.

5.5.2.2 Wind

The data described in section 5.5.1.2 is used for transforming offshore wave conditions to a nearshore boundary condition using SWAN. But for coastal erosion analysis data somewhere near the shore is considered more relevant. That is why for X-beach analysis wind data for comparatively near the area of interest is obtained from the website of ECMWF. The co-ordinate of the point is 69°15'0.00"N and 58°30'0.00"E. The location is shown in Figure 5.18.

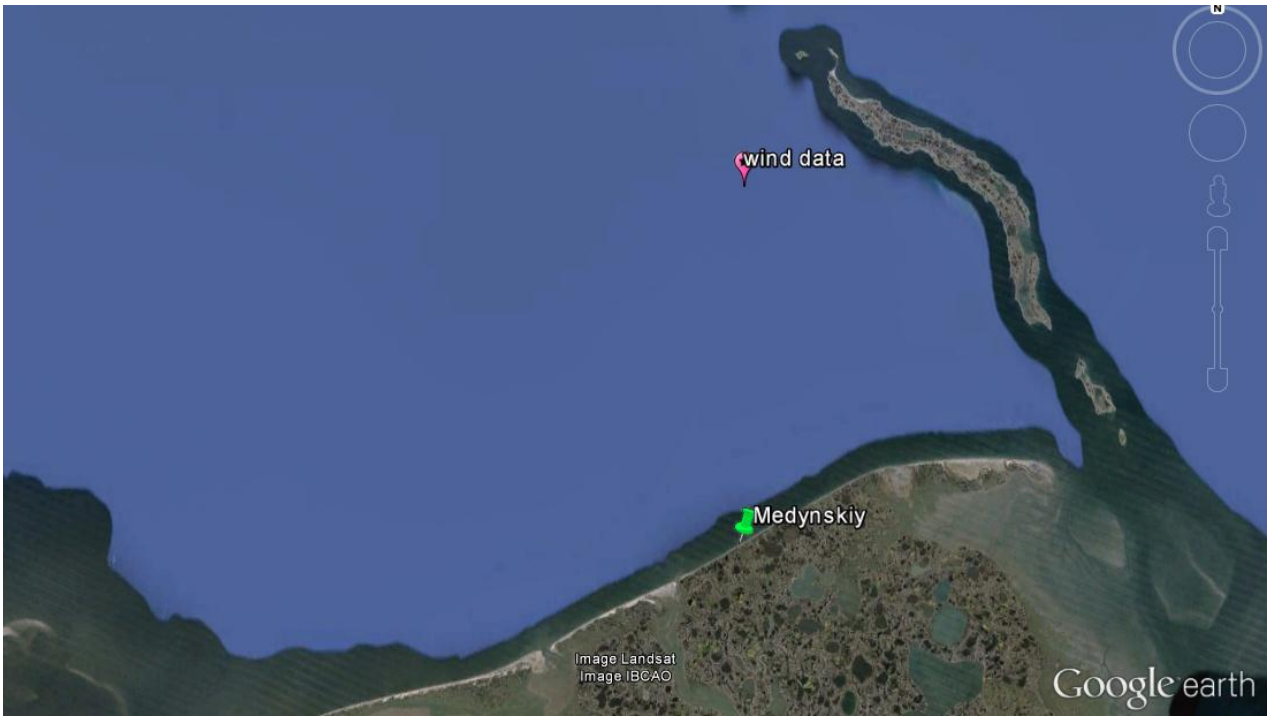

Figure 5.18: Location of hindcast wind data for erosion analysis

The wind speed is observed to vary from 10 m/s to 22 m/s during the storm period. The graph in Figure 5.19 gives good suggestion to select the range of wind speed for erosion analysis. The wind direction is found to vary from 274^{o} to 305^{o} during this period.

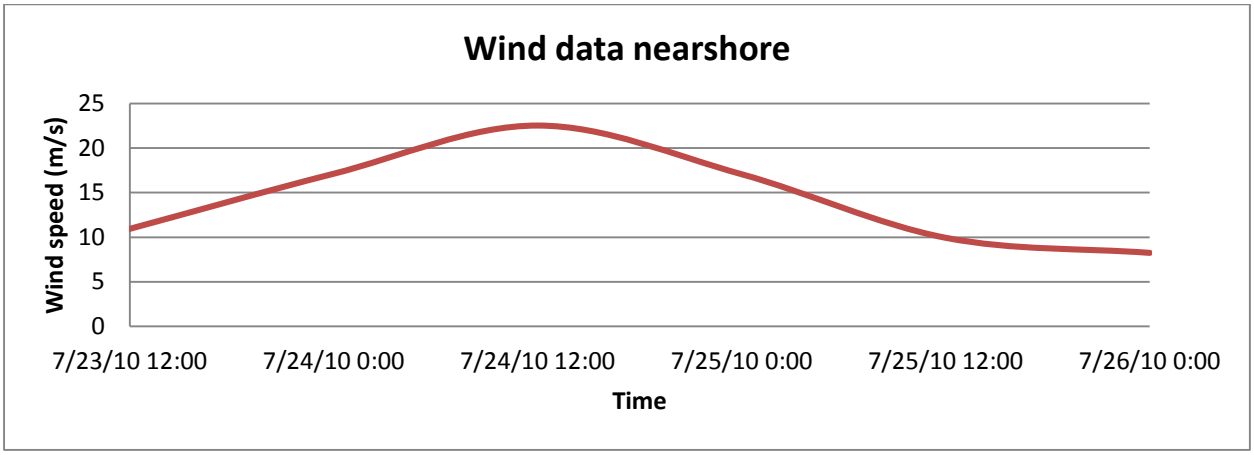

Figure 5.19: Wind data from 23 July,2010 to 26 July,2010

5.5.2.3 Wave

As mentioned earlier, the wave conditions for X-beach analysis is derived through wave transformation from offshore boundary to near-shore boundary using SWAN. During the storm on 24th July the maximum wave height of 12.1 m was observed coming from west direction. The wind direction varied from WSW to WNW for the 24 hour long storm period. For the analysis of coastal erosion, wave data from 23rd July 21:00 to 25th July 00:00 has been considered important to represent the storm situation. The details of SWAN analysis is explained in the following chapter.

5.5.2.4 Tidal data

Water level of the Pechora Sea is influenced by tides. Near the area of Varandey, mixed semidiurnal tidal fluctuations are present. The tidal variation is shown in Figure 5.20 for 10 June to 10 July of 2010 below using data from a tidal station named BukhtaVarneka located near the study area.

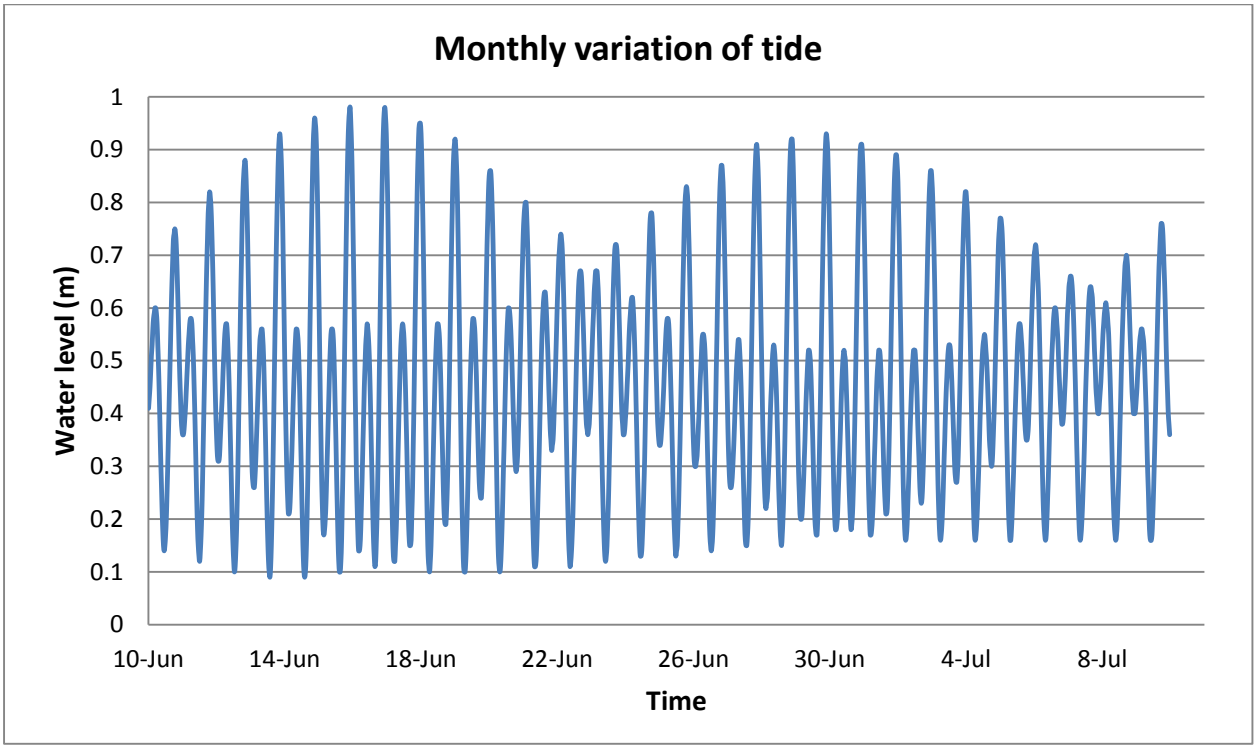

Figure 5.20: Monthly tidal variation recorded at BukhtaVarneka from 10 June, 2010 to 10 July, 2010

The coast of Varandey experiences a tidal sea level changes ranging about 1 to 1.2 meters. (E. Guegan, 2013). Storm surge combined with spring tide can give a high water level that can influence the coastal bluff erosion. The sea level rise of 1.75 m and higher relative to mean sea level is referred as the extreme storm surge.

The observations for sea level are taken by Russian meteorological service (Methods,1957) while sea surface is free of fast ice in the Baltic elevation system. The mean annual sea level (MASL) is calculated as -0.3m based on these data. The high energetic waves combined with water levels are the most crucial part of coastal dynamics.

The catastrophic storm in July 24th, 2010 was produced by the influence of the powerful cyclone over the southern part of the Barents Sea moving from the North Atlantic to the Kara Sea. Strong north-west and west-north-west winds with velocities higher than 25 m/s generated 9 m-height wind waves at the entrance of the Pechora Sea. As a result, storm surge occurred along the southern coasts of the Pechora Sea with the sea level rise of 3.6 m in the Baltic elevation system or 3.9 m relative to mean sea level of Varandey which was exceptionally high. This was registered as a record-breaking maximum of storm surge level. Duration of the storm was approximately 24 hours. The previous strongest storm surge was registered on the February 7th, 1978 with the sea level rise of 2.65 m. Extreme storm surges are expected usually in August – October. During the period wind speeds are observed to be stronger compared to other time of the year and wave fetch are longest too due to the absence of sea ice. The combination of these two factors causes the highest probability of storm surges. According to this explanation, the event of 2010 was unanticipated as it took place on July 24th.

The tidal information is also obtained from tidal database of MIKE C-map. The water level time series of 24th July 2010 is considered useful for this simulation. There was no tidal station very near to Medynskiy coast. Therefore information from other tidal stations which are located bit far away is used. There are four tidal stations which are considered useful initially. This is obvious that none of them will accurately represent tidal condition of the interest area in this study. But unavailability of required data compelled to use this approximation which may impose certain level of unreliability on the results. The tidal stations considered are Khabarovo, BukhtaVarneka, Bugrino and Reka Pechora (shown in Figure 5.21). The co-ordinates of the tidal stations are mentioned in Table 5.1.

Table 5.1: Co-ordinates of tidal stations

Sl.	Name of tidal station	Latitude	Longitude
A	BukhtaVarneka	69°42'2.30"N	60° 4'20.75"E
B	Khabarovo	69°38'52.84"N	60°24'59.26"E
C	Reka Pechora	68°23'8.77"N	54°25'48.94"E
D	Bugrino	68°47'52.84"N	49°16'11.06"E

Figure 5.21: Location of different tidal stations near Varandey (Source: Google map API)

The time series from all of them are compared to decide upon which one will be the most relevant regarding the concerned area. The water level fluctuations from all four stations are plotted against each other to take an informed decision. The Figure 5.22 shows the difference among them.

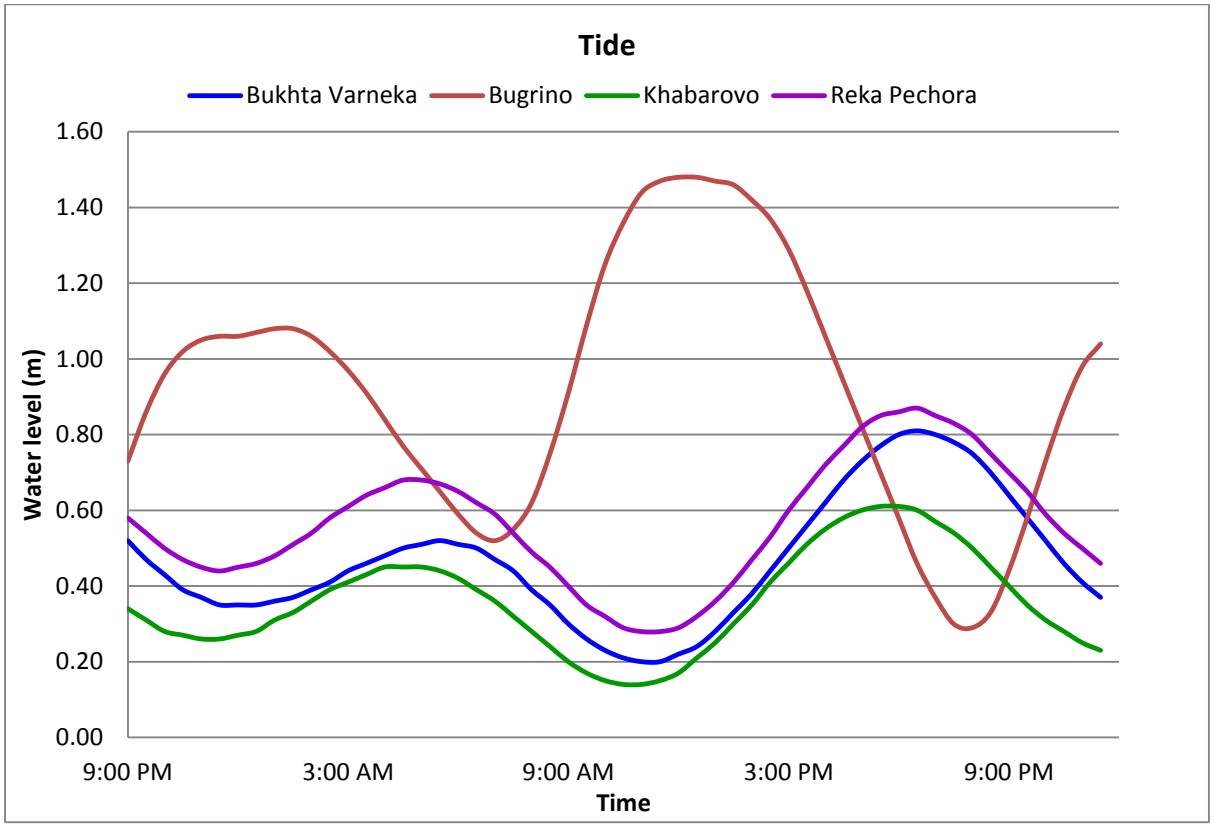

Figure 5.22: Tide level comparison from different tidal stations

From Figure 5.22, it can be observed that three of the stations show tidal variation which are completely in phase except Bugrino. Bugrino, which shows a tidal variation out of phase with others, is anticipated to be influenced by local effects. BukhtaVarneka is comparively near the coastline and the open coast situation unaffected by any nearby land resembles the intended location of this study better. After the comparison of the tidal records, it is decided that the data from Bukhta Varneka is the most relevant in this case and thus used for simulation.

It is already mentioned above that 3.9 meter of storm surge relative to mean sea level was observed during the storm. The storm surge combined with high tide results in the most devastating effect on shore face. When astronomical tide is combined with surge level during a storm the water level rise is termed as storm tide. For the current study this is done to take the sea level rise into consideration. The surge level is added to tidal level to get the storm tide during the high tide period. 3 hours of high tide condition is considered to be replaced by storm tide. Figure 5.23 represents the comparison between recorded tidal level at BukhtaVarneka and tide value with surge effect utilized in modelling of coastal erosion.

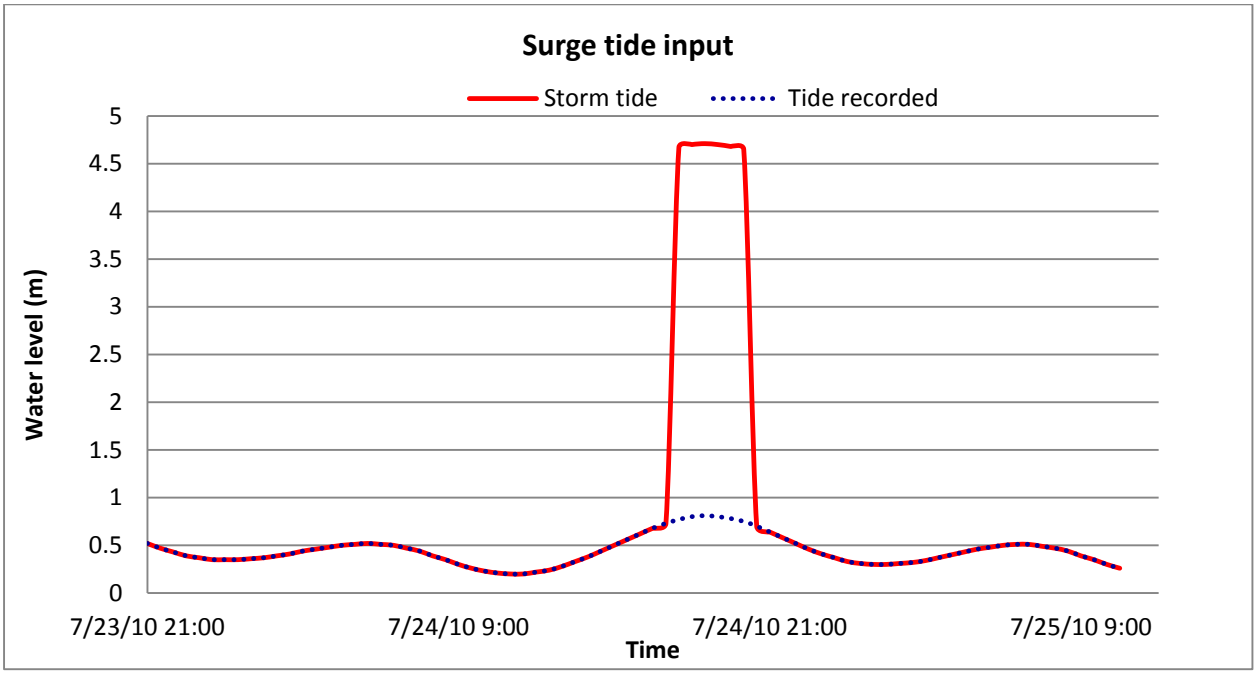

Figure 5.23: Recorded tidal level at BukhtaVarneka and storm tide value applied in model

5.5.2.5 Sediment characteristics

Emilie Guegan, a PhD student NTNU/ SAMCoT, has been conducting a research in the same area from 2010-2012. Part of her work was to explore the geomorphological aspect of the area. Field work carried out by Emilie Guegan provides her a better understanding on sediment properties. She used samples retrieved by coring and drilling to determine the water content and particle size distribution. The findings from her research is found very useful to estimate a suitable soil density, porosity, D_{50} and D_{90} which are used for simulation of coastal erosion though sample from the particular location is not available. The soil is mainly ice-rich silt. The sediment properties are mentioned in Table 5.2 as suggested by her through written communication.

Table 5.2: Sediment properties

Properties	Value
Soil density	1300 kg/m3
Porosity of frozen soil	0
Porosity of unfrozen soil	0.3
D_{50}	0.007 mm
D_{90}	0.011 mm

5.5.2.6 Rate of erosion in a known storm event

From the findings of E. Guegan (2013), the average rate of coastal erosion is obtained for the 15 kilometer long coastline of Medynskiy. The calculation is based on satellite images and field observations. The average rate of erosion was found to be 19.6 m/yr near Medynskiy area from 2010 to 2011 with a maximum of 60m/yr. Unfortunately no data for erosion due to storm only could be obtained. The storm that took place on 24th July was very disastrous as such event was never been recorded in previous 50 years. The erosion rate in 2010 was exceptionally high compared to other years before and after 2010. That is why it is assumed

that most of the erosion in year 2010 was due to this severe storm. The model is validated using this data.

Finally a sketch is presented in Figure 5.24 to give readers an overall idea of analysis domain for both SWAN and X-beach run.

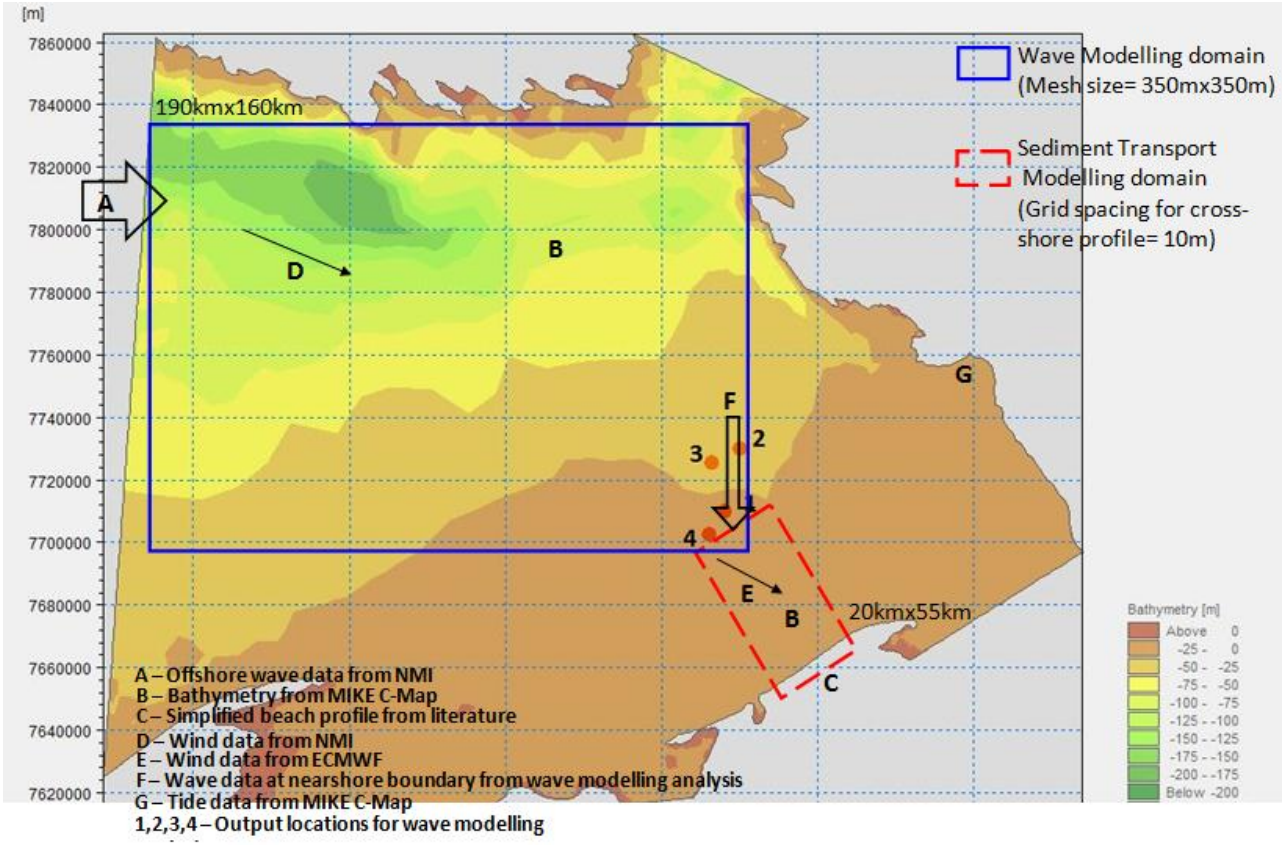

Figure 5.24: Domain for numerical modelling

6 Analysis and Results

In this chapter, the details of setting up a numerical model for coastal erosion and calibration of the model are explained. The outcomes from the simulation of newly generated model is presented and discussed further.

6.1 Task description

The model simulation is divided into two parts:

1. Wave modelling using SWAN
   - To obtain near shore boundary condition from offshore boundary condition.
2. Erosion analysis using X-beach
   - To set-up the model and analysis of dune erosion using boundary conditions from previous analysis
   - This part can be further divided in two tasks;
     a) Calibration of model for available data
     b) Sensitivity analysis of wind stress and avalanching parameters

To model the coast, data from 23rd July 2010 21:00 to 25th July 2010 10:00 are utilized. The time for which the model simulated the conditions is in total 39 hours. The storm on 24th July is the target of the simulation and the duration of this storm was 24 hours. But to investigate the full impact of the storm it is necessary to run the model for an extra time that is required by waves applied as input at the boundary to reach the coast.

A summary of the model simulation run is presented in Figure 6.1

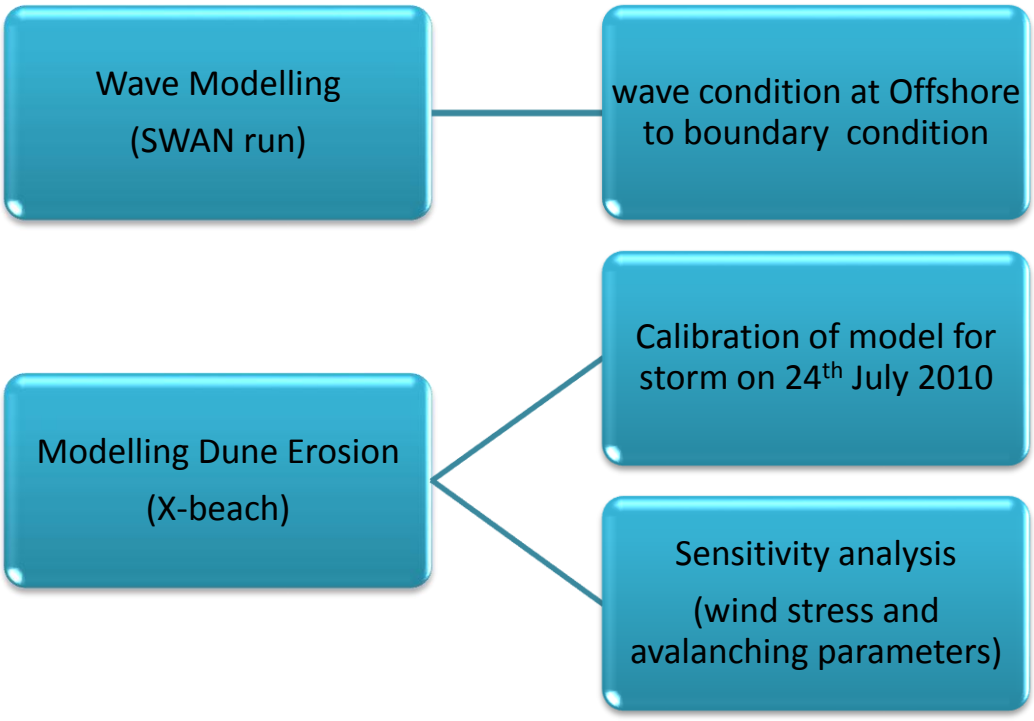

Figure 6.1: summary of simulation runs

6.2 Wave Modelling

Because of the large distance of wave gauge from study area, it is necessary to get the wave condition in a near-shore area. To get the wave parameters in area near the boundary of computational domain for X-beach, modelling tool for wave transformation is used. SWAN is a well-recognized wave modelling program and comparatively easier to use for this kind of wave transformation process. For wave analysis SWAN (Version: 41.01A) has been used.

6.2.1 Model set-up for SWAN

6.2.1.1 Bathymetry grid and output location

About 190x160 sq. km of computational area is selected for analysis to make sure that wet points are covered only. The bathymetry map with figures and details are already discussed in section 5.5.1. Four points in the domain are chosen for outputs to compare the transformed wave condition and to define the boundary wave conditions for x-beach program. The co-ordinate and depth of these output locations are mentioned in Table 6.1 and their locations are marked in Figure 6.2.

Table 6.1: Co-ordinate and depth of SWAN output locations

No. of output	Latitude	Longitude	Depth(m)
1	69º21'45.9936" N	57º52'35.976"E	23.90
2	69º32'8.5668"N	58º3'40.835"E	28.38
3	69º 30' 22.7052"N	57º 49' 9.156"E	27.05
4	69º 18'7.4232"N	57º 44' 23.46"E	22.31

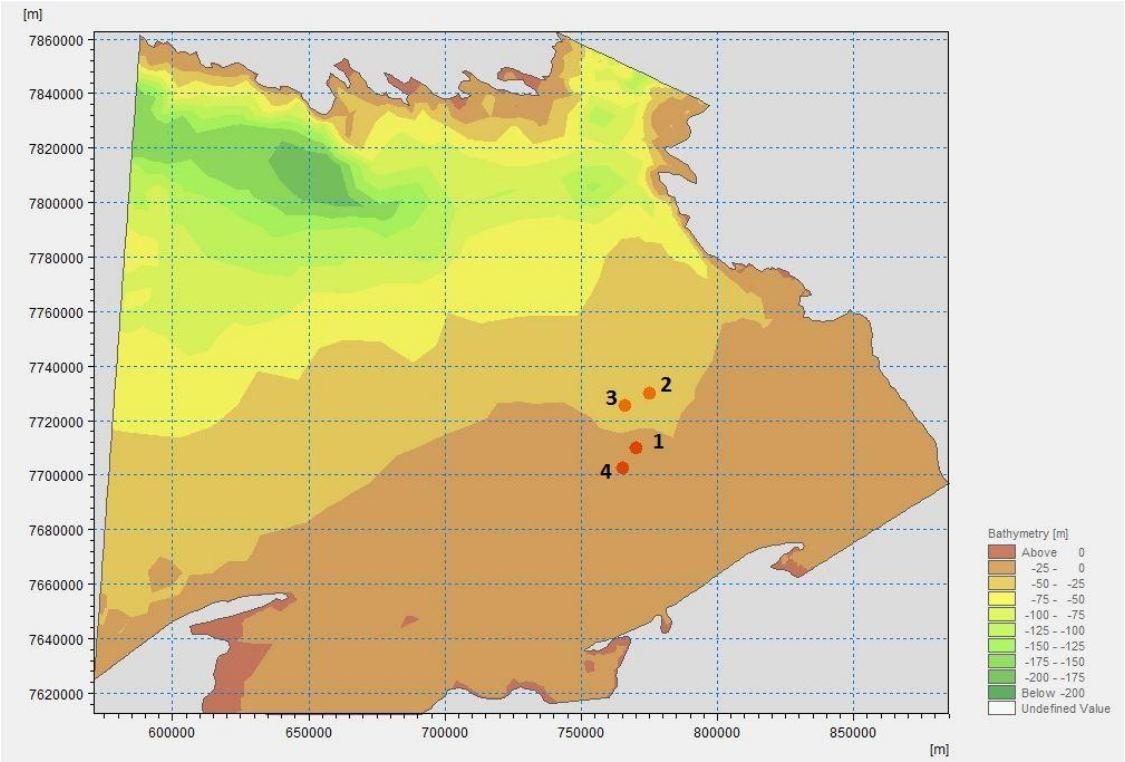

Figure 6.2: Location of outputs considered for SWAN run

6.2.1.2 Boundary conditions

A constant wind speed and associated direction is applied to whole domain instead of individual local wind speed at each grid. As main focus of this study is to model the coastal erosion, this is considered to be acceptable because of time limitation.

A threshold of 5.0m for wave height can be identified as a storm situation for this study. According to this consideration, a total of 27 hours wave conditions are to be analyzed to capture complete effect of the storm. The significant wave height (Hs) for corresponding 27 hours are plotted to get an overall idea about the behaviour of waves that are entering the domain. The inputs for wave modelling with 9 different conditions are mentioned in Table 6.2. The significant wave heights at offshore boundary considered during storm period is plotted in Figure 6.3.

Table 6.2: Wave and wind data at offshore boundary

sl.	Significant wave height, Hs (m)	Peak period, Tp(sec)	Peak direction, Theta p(degrees)	Wind speed at 10m elev., W10(m/s)	Wind direction, D10 (degrees)
1	5.2	9.2	257	21.1	239
2	10.4	13.5	272	24.9	254
3	12.1	14.9	272	24.8	265
4	11.6	14.9	272	23.8	278
5	10.4	14.9	287	21.8	284
6	9.1	13.5	287	20.8	287
7	7.9	12.3	287	19.6	292
8	6.8	12.3	302	17.6	297
9	5.6	11.2	302	15.8	304

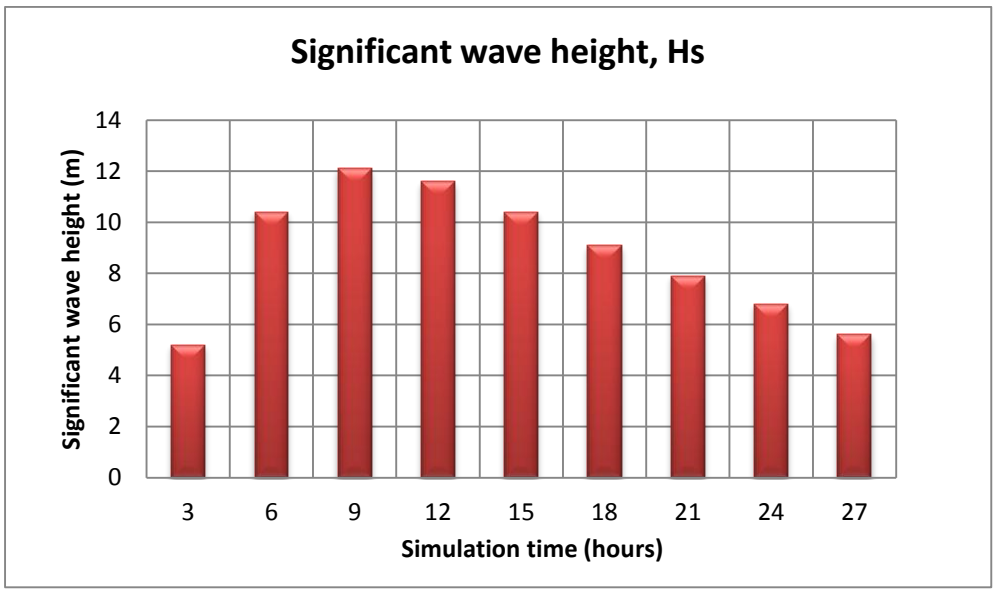

Figure 6.3: Plot of significant wave height at offshore boundary

In writing the code for SWAN run, nautical convention of direction is used. Spectral wave directions are considered for a limited directional sector only. From the observations of windrose and waverose diagram in section 5.5.1.2 and 5.5.1.3, it is evident that most of the energy is coming from the sector between 200 degree and 330 degree. That is why computation has been made limited to this sector to minimize computation time. The waves are to enter the region through west boundary and considered as constant along the boundary. The full code is attached in the appendix A.

6.2.1.3 Computational domain

Computational area with different grid size has been experimented to get an idea how fast the solution converges and to decide upon a fixed grid size that gives an accurate enough boundary condition to represent the near-shore area. The grid size is decreased as long as the result converges to an acceptable order of accuracy. Table 6.3 shows how decreased grid size influences the outcome. The wave condition number 5 is used for this comparative analysis.

Table 6.3: Comparison of results from analysis with different grid size

Trial	Grid size	Grid no.	Hsig for point 1	Hsig for point 2	Hsig for point 3	Hsig for point 4
1	1000mx1000m	190x160	9.38	8.60	8.94	9.89
2	500mx500m	380x320	9.58	8.73	9.03	10.17
3	350mx350m	543x457	9.68	8.78	9.09	10.29
4	200mx200m	950x800	9.64	8.75	9.07	10.26

Keeping in mind various factors such as- expected accuracy of the result, virtual memory capacity of the computer used and reasonability of computation time, a 350mx350m grid size is finalized for wave analysis.

6.2.2 Outputs from SWAN

Graphs are prepared comparing the significant wave height (Hs) and peak period (Tp) from all output locations. It is found that the results are almost in same order as the points are located very close. The variation is due to difference in depth between two points. The table with outputs is presented in the appendix A. Figure 6.4 and 6.5 shows the variation of significant wave height and peak period for different output locations respectively.

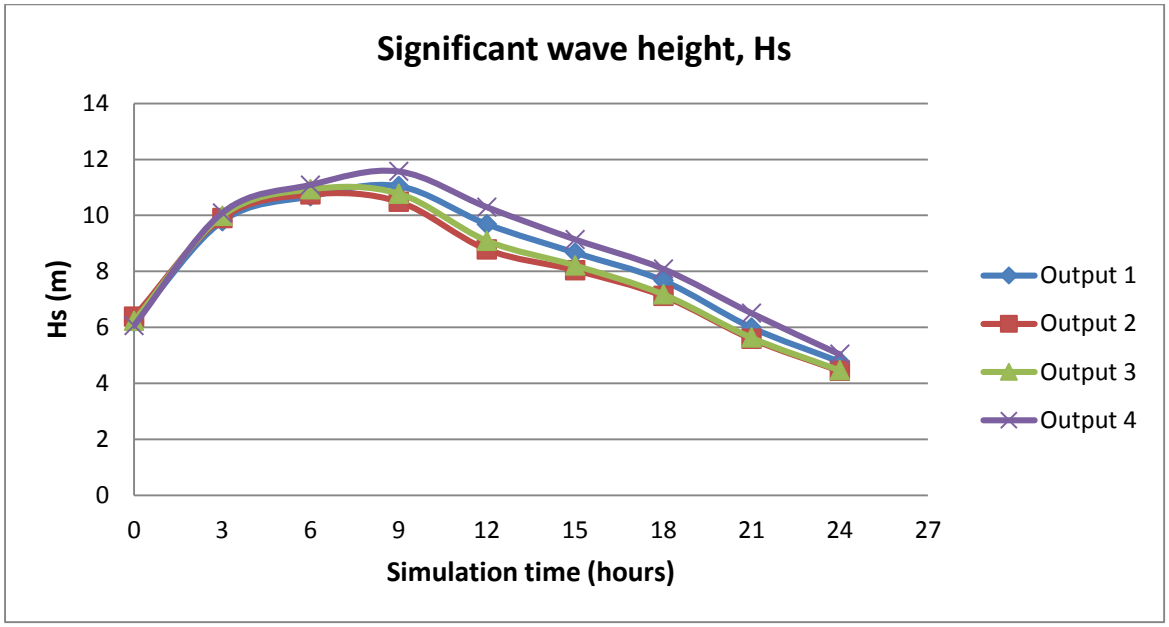

Figure 6.4: Comparison of significant wave height (Hs) at different output locations

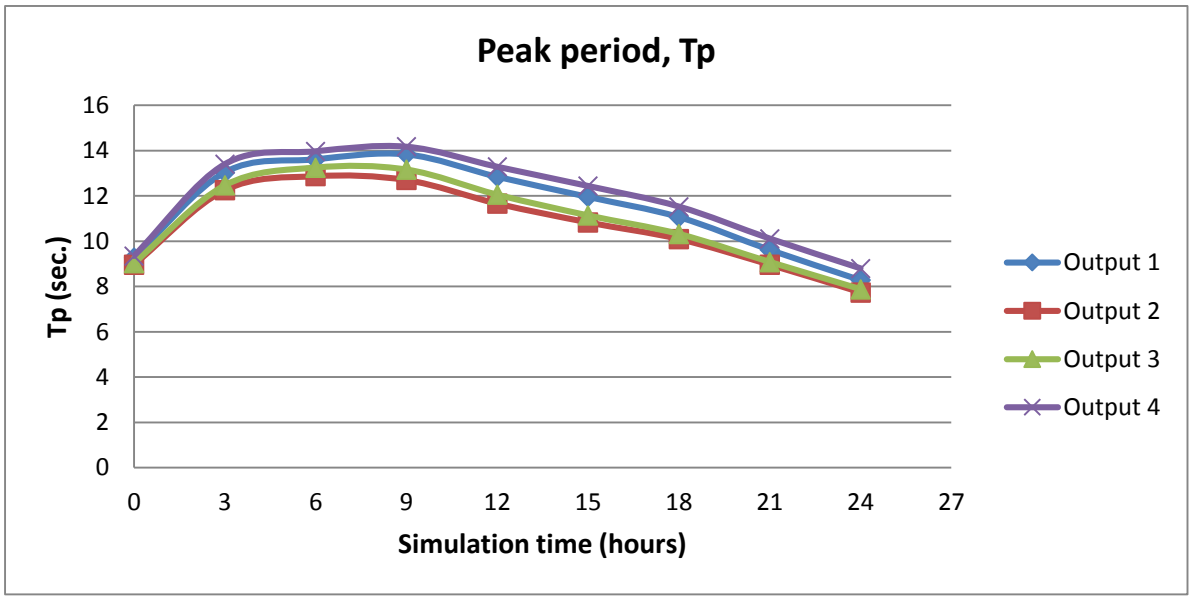

Figure 6.5: Comparison of peak period (Tp) at different output locations

As mentioned in the earlier section, the study area is surrounded by land surface to the east and north direction. The waves are entering to the region from west boundary. The upper left corner of the west boundary is comparatively deeper than the lower left part. The average depth of that region is 180 m. Wave enters from this boundary and starts to deflect according to wave transformation theory. Also the wind generated wave inside the domain influences the wave spectrum. The wind-generated wave depends mainly on fetch length as a constant wind speed and direction is considered and is predicted to develop more as the wind is passed further inside the domain. The lower left corner of the computational domain has shallower depth and waves coming from this part refracts early towards the land situated nearby. That is why waves entering the domain from upper left corner and the wind-generated wave are mainly contributing to the waves present in the area of intended outputs.

As the wave approaches further it reaches the shallower part and starts to feel the bottom more. This is the region where shoaling comes into effect. The increase in wave heights is pretty obvious and can be verified by a closer look into the colour-grading plot of the results in Figure 6.6. The yellow marked area shows the highest wave height.

After this region the waves cannot move further in the same direction because of existing land mass and then spreading of wave energy together with refraction comes into action. The waves are supposed to increase in height due to refraction. The opposite effect i.e. decrease in height is expected due to diffraction. The wave angle changes direction due to refraction and diffraction as well. The joint effect of these two phenomena while travelling through the existing topography decides the emerging wave properties near-shore. In most of the cases under this study, the wave heights are found to decrease relative to input wave height near the boundary of the study area. The plot gives fairly clear idea about the effect of wave transformation processes all over the domain.

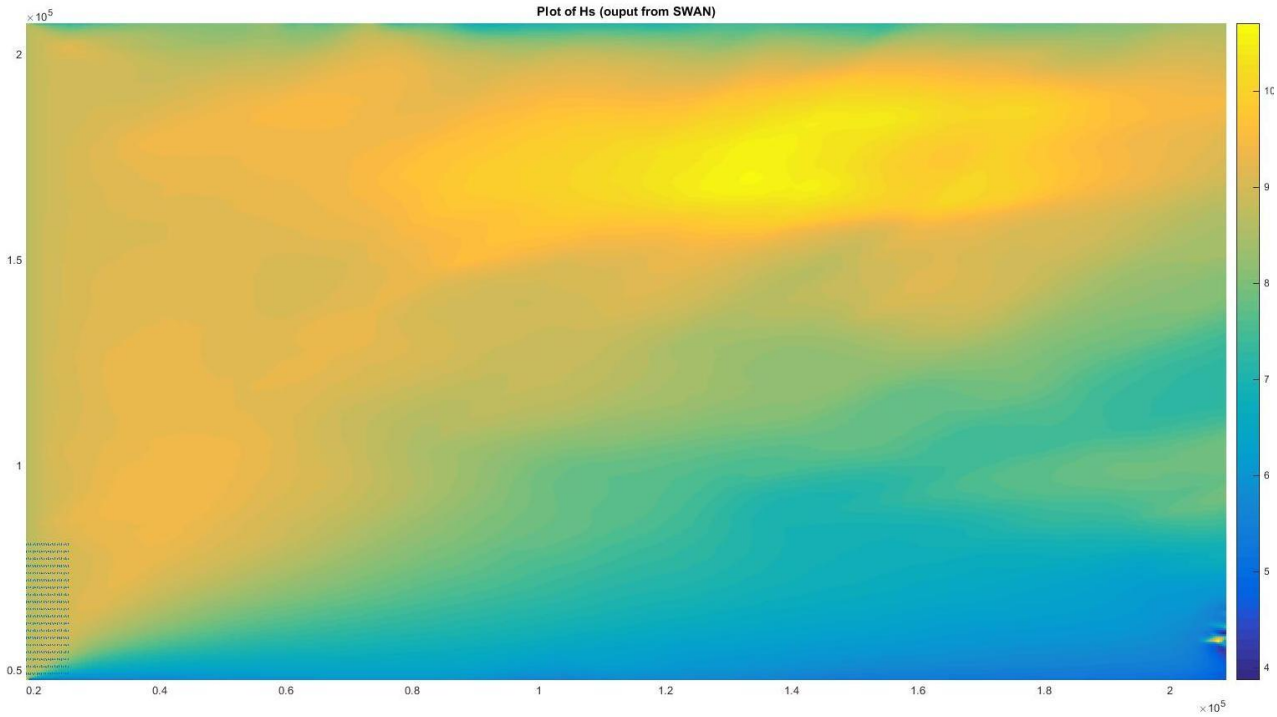

Figure 6.6: Colour-grading plot of resulting wave heights after SWAN run with wave condition 5 (refer to Table 6.2)

The result can be supported by the concept of physical processes underlying wave transformation and considered to represent the situation in a right way. The outputs from this analysis are used as boundary condition for setting up coastal erosion model.

6.3 Modelling dune erosion

As mentioned earlier, to model coastal erosion of the area under this study, X-beach is used as a numerical modelling tool. Since the objective is to model the coast for storm events with dune or coastal bluff erosion this numerical tool is considered appropriate to simulate the situation. The boundary conditions obtained from SWAN analysis is utilized to reduce the computational domain and thereby to reduce the computation time.

6.3.1 Model set-up for X-beach

The input parameters for X-beach run are described in the following text. All of the input parameters to setting up the model can be grouped into six categories.

1. Grid and bathymetry

The first task to generate a model is to define a grid system with known bed level that follows specific guidelines. The bathymetry needs to be provided in a matrix form so that each row represents a cross-shore profile. The first column should represent the offshore boundary.

No field data for accurate dune profile exists. Therefore a representative upper shore profile has been assumed. As the upper beach profile is estimated depending on the available information in the literature, it is not expected to be very accurate. The variation in erosion rate along the shoreline cannot be studied. That is why only one cross-shore profile is modelled. To keep the computation time reasonable, optimal grid spacing is used. The optimal grid spacing in cross-shore direction for bathymetry is selected as 10.0 meter.

Because of interpolation of bathymetry data the abrupt change in slope at the foot of dune was converted to mild one. This is corrected manually to provide X-beach the correct pattern of beach profile.

2. Boundary conditions

Waves

The results from SWAN analysis is used as wave conditions in offshore boundary. The output from points 1 and 4 are more relevant for X-beach analysis as they are located near the boundary line of computational domain. Therefore the parameters of JoNSWaP wave spectrum for the worst case scenario between these two points are considered as input here.

Wind

A time-varying wind input is not applied to avoid complexity of the model set-up. Instead a constant value of wind parameters throughout the simulation time is provided to evaluate the wave growth effect on dune erosion. The wind properties are collected from the website of ECMWF for near shore. The details have been discussed in section 5.5.2.

A representative value for wind data is chosen from the record of 24 June 2010. The wind direction is selected as 290^{o} at 10m elevation for model run. The model has been run with different wind speed to analyze the impact of implementation of wind stress in momentum balance on erosion rate. A comparison of the results from models with different wind speed and without any wind stress is carried out.

Tides and surge level

The tidal variation of BukhtaVarneka is used as inputs. From 23 July, 21:00 to 25 th July, 10:00 total 39 hours are considered. A surge level of 3.9 meter was observed near the southern coasts of Pechora Sea during the storm on 24 July 2010. This surge level is included to get the effect of increase in water level on coastal bluff erosion. As the storm duration was

24 hours, but the surge level is added to tidal level during high tide only. Figure 5.23 is used to explain the water level variation imposed at boundary to accommodate both surge and tidal variations.

3. Physical parameters (water properties, sediment properties)

For most of the physical parameters default value from the program has been used. For instance density of water is applied as 1025kg/m3, air density as 1.25 kg/m3 and wind drag coefficient=0.002.

For sediment properties estimated values are used as explained in previous chapter. Uniform D_{50} sediment diameter, uniform D_{90} sediment diameter, porosity and density of sediments are the important sediment parameters that are used for modelling erosion.

4. Numerical parameters

Maximum courant number is allowed to be 0.9 for numerical calculation. Lax-Wendroff scheme is used for numerical analysis. To select the simulation time, another important phenomenon had to be taken into account. It is observed that the wave front needs 7:30 hrs to reach the shoreline from offshore boundary. That is why simulation time has been increased by 12 hours to get the full effect of the 27 hours wave condition. Total simulation time now becomes 39 hours. In the script, code is provided with instruction for recording the results after each 15 minutes time interval.

5. Morphological parameters

To take the avalanching effect into account it is necessary to provide the program a realistic limiting value for both wet and dry slope. The critical slope controls the avalanching and thereby amount of erosion. It is a difficult task to select appropriate values for these parameters as no field data is available. The calibration of model depends on these parameters. The value is kept on changing as long as the output is found to match the existing scenario. The output is compared to known erosion rate for the known event to validate the model. A sensitivity analysis is carried out to demonstrate the effect on final result due to these parameters.

6. Others

Threshold depth for drying and flooding, Chezy coefficient and threshold water depth for concentration and return flow etc. are some parameters that cannot be counted. All of these parameters are empirical and always vary within a range. No significant effect on the result of model can be observed due to small variations in their value during calibration run. Therefore reasonable assumptions are made for these inputs. Table 6.4 presents a sum up of all the input parameters used.

Table 6.4: Description of input parameters in X-beach run

Keyword	Description	Value	Remarks
tstop	Stop time simulation	140399 sec	
tint	Time interval output global values	900 sec	
CFL	Maximum Courant no.	0.9	
scheme	Switch numerical scheme for wave action balance	2	Lax-Wendroff
rho	Density of water	1025 kg/m3	Default
rhos	Density of sediment(no pores)	1300 kg/m3	Site data
rhoa	Air density	1.25 kg/m3	Default
Cd	Drag coefficient	0.002	Default
por	Porosity of sediment	0.30	Site data
D50	Uniform D50 sediment diameter	0.000007 m	Site data
D90	Uniform D90 sediment diameter	0.000011 m	Site data
wetslp	Critical avalanching slope under water	0.1	Governing parameter
dryslp	Critical avalanching slope above water	1	Governing parameter
C	Chezy coefficient	65	Assumed
hmin	Threshold water depth for concentration and return flow	0.20 m	Assumed
eps	Threshold depth for drying and flooding	0.01 m	Assumed
waveform	Option for wave-shape model	2	Vanthiel-VanRijn formula
form	Equilibrium sediment concentration formulation	2	Vanthiel-VanRijn formula

6.3.2 Calibration run

The model is run several times with varying parameters to observe the impact on result. Finally it is calibrated to produce the erosion estimated from field data. Thus the model is validated. With the above mentioned parameters the model generates about 20.0 m of dune erosion ignoring wind stress in computational domain. From previous literature it is known that the average rate of erosion was found to be 19.6 m/yr for 2010 and maximum rate of erosion was observed to be 60 m/yr. Though data regarding dune erosion due to storm only is not available, the yearly rate gives an idea of the range for erosion. The result from X-beach model falls within the range.

The change in upper beach profile due to storm derived by X-beach calibrated model is shown in Figure 6.7.

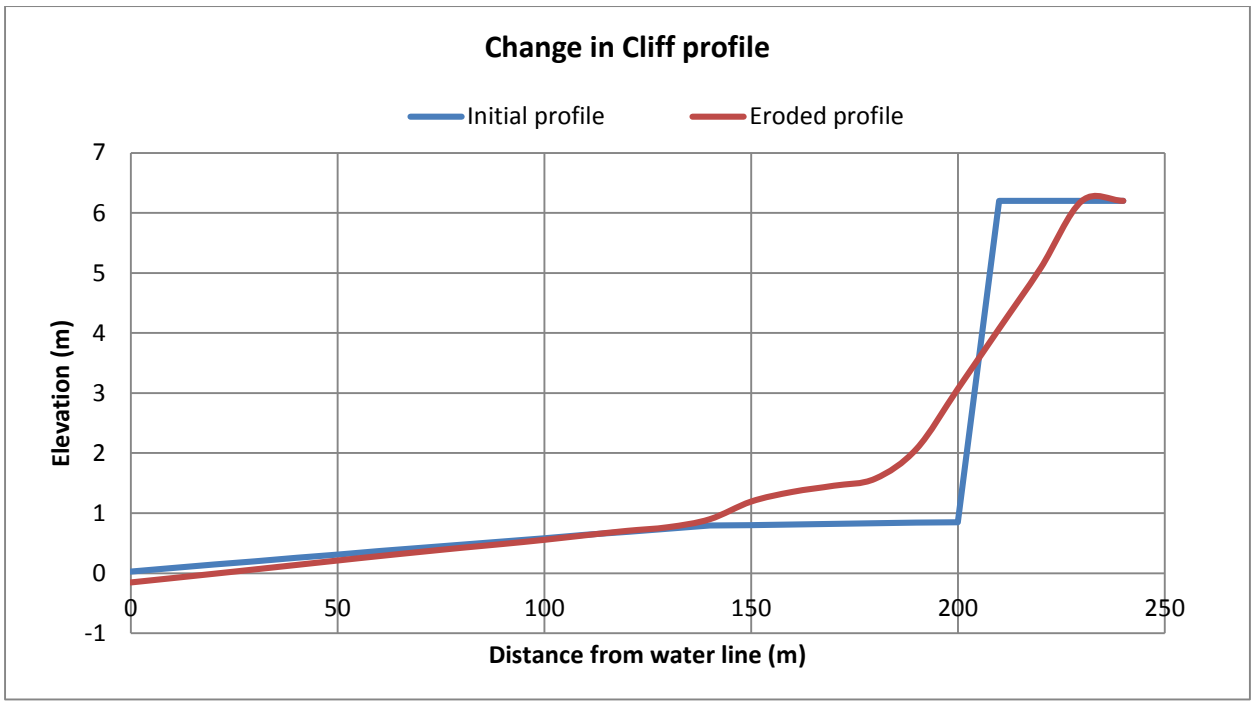

Figure 6.7: Initial cross-shore profile and eroded profile

The wave energy and roller energy variation along the cross-shore profile are examined to understand the wave dynamics behind erosion process. The wave energy decreases as the wave front approaches near-shore. This is due to breaking of individual waves with comparatively higher wave heights. At the shore-face wave energy diminishes which refers to breaking of all waves. At this point roller energy is found to be maximum which is expected according to theory as the roller energy comes from breaking waves. The Figure 6.8, 6.9, 6.10 and 6.11are presented to show these features.

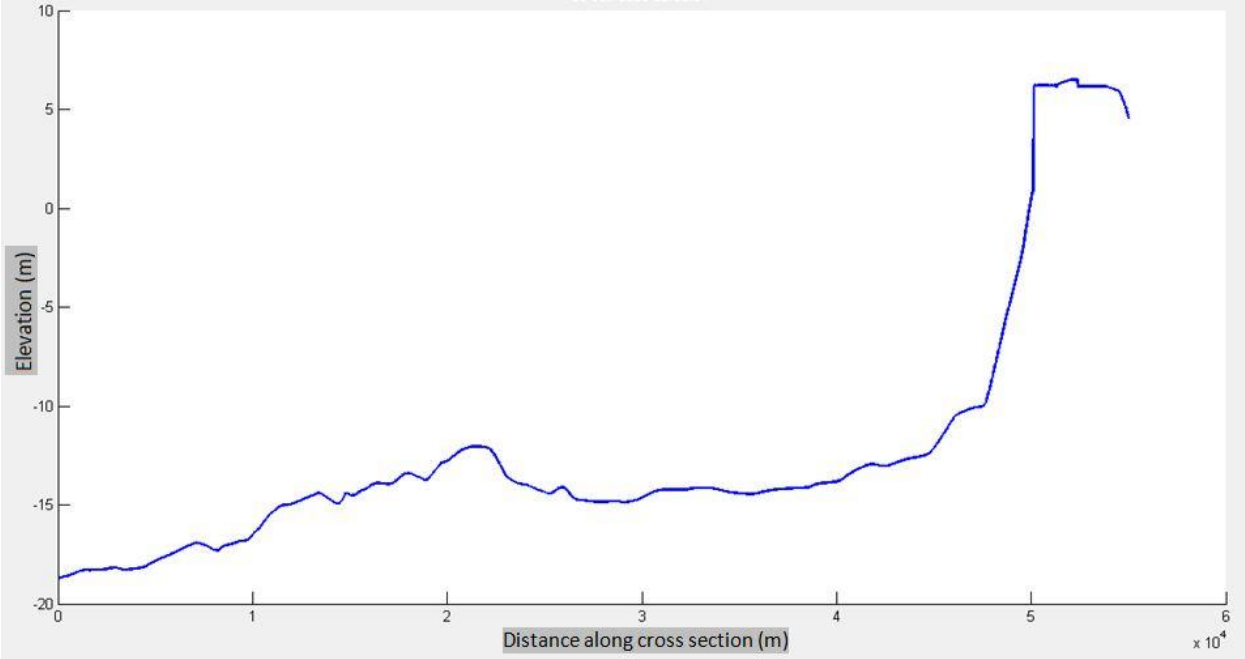

Figure 6.8: Cross-shore profile from X-beach

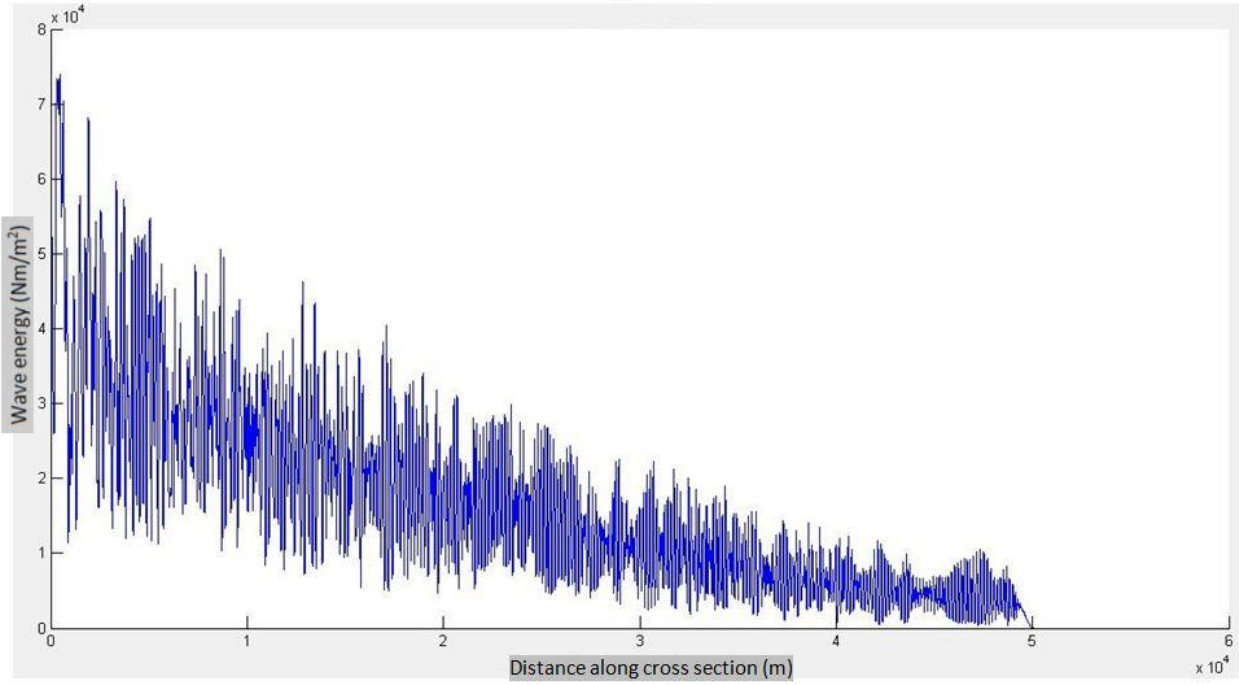

Figure 6.9: Wave energy

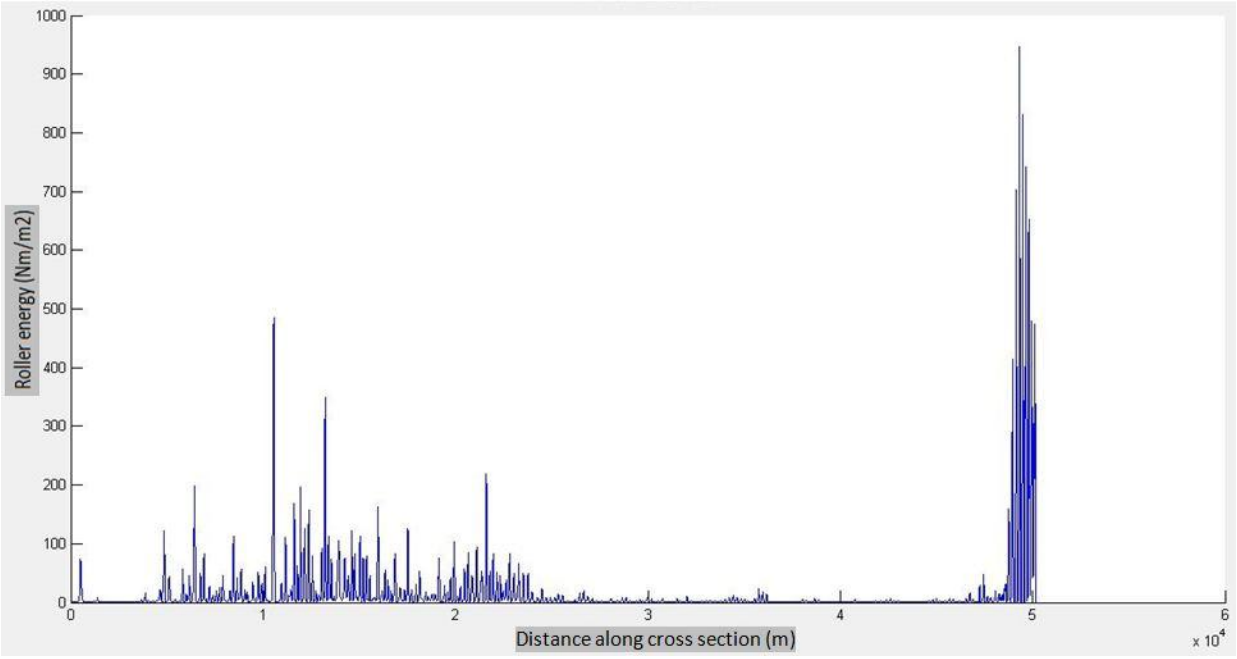

Figure 6.10: Roller energy

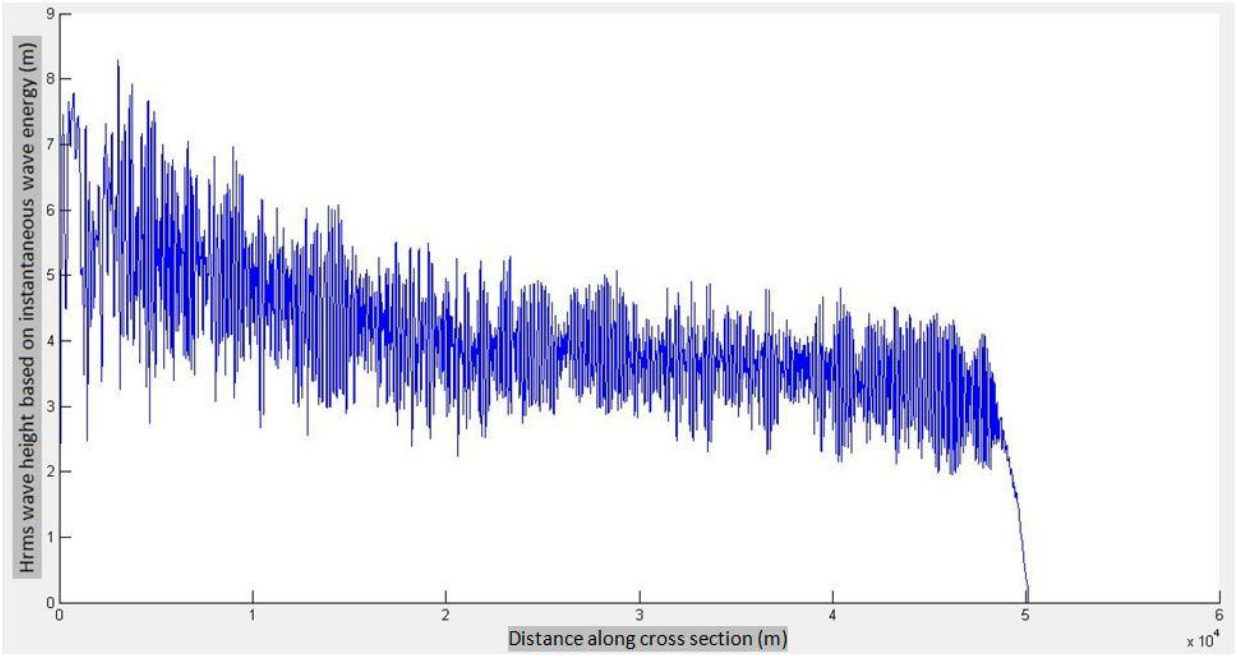

Figure 6.11: Root mean square wave height, Hrms Based on instantaneous wave energy spectrum

6.3.3 Sensitivity analysis

A sensitivity analysis is also carried out to demonstrate the wind effect on erosion. The erosion rate of cliff profiles for different wind speeds (including the case of no wind) coming from the direction of 290^{o} according to nautical convention are plotted in Figure 6.12. It is expected that the existence of strong wind will produce wind generated waves within the domain which will make the waves more intense. Therefore increase in erosion can be expected for this case compared to the wave condition where wind effect is absent. The comparison of result from models supports this idea.

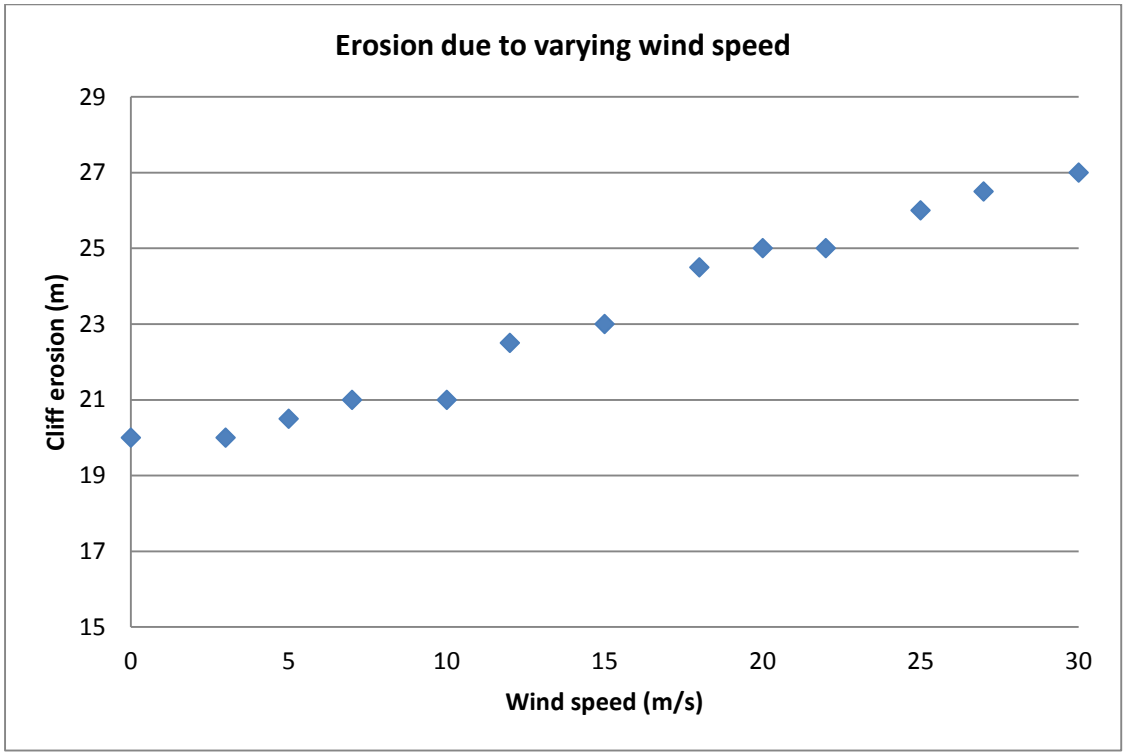

Figure 6.12: Sensitivity analysis for wind speed

To demonstrate the results, Figure 6.13 is attached here showing eroded profiles with three different wind speeds.

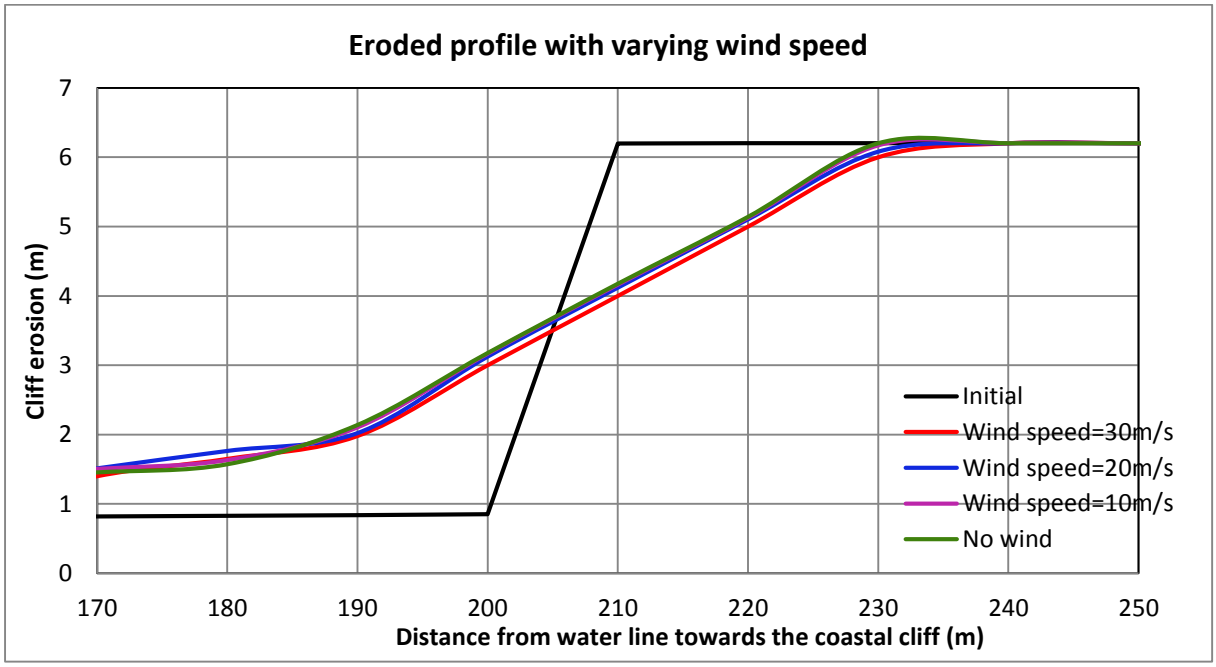

Figure 6.13: Comparison of eroded profiles with different wind speed

The model is run with different wind directions varying from 260^{o} to 360^{o} for wind speed 10 m/s. This is done to observe the impact of wind direction on cliff erosion. Figure 6.14 shows the results.

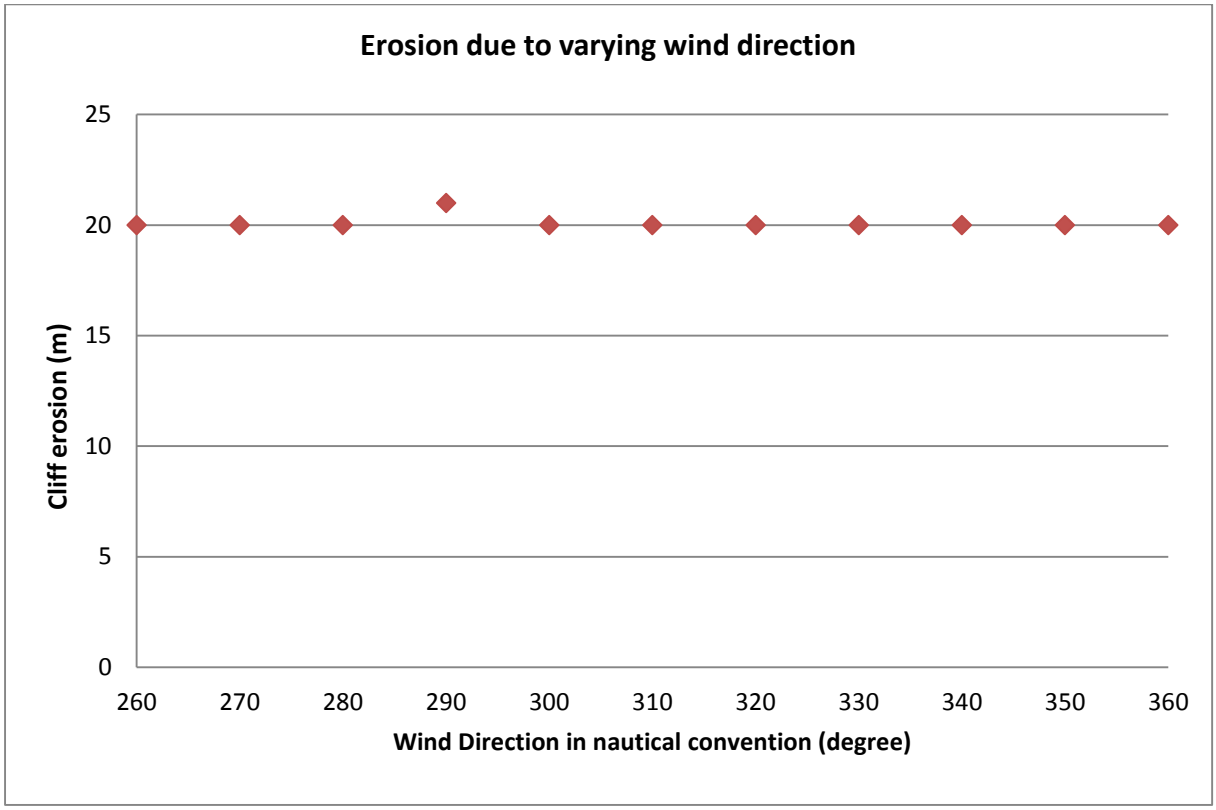

Figure 6.14: Sensitivity analysis for wind direction

Figure 6.14 shows the highest erosion of 21 m for wind coming from 290°. For winds from other directions no noticeable variation in cliff erosion was observed. The wind from 290° is to perpendicular to the coastline and thereby produces maximum cross-shore effect as the wind-generated waves contributes positively to the direction of offshore waves. On the other hand, when wind comes from other than 290°, the erosion analysis with one-dimensional cross-shore profile does not take into account the effect of wind component other than the shore normal direction and thus excludes the effect of wind on cross-shore transport of sediments. Only normal to the shore component of wind is active for generation of offshore waves and does not vary the result too much. To conclude, the erosion analysis with one-dimensional cross-shore profile is not useful to study the impact of wind direction. For this purpose an erosion analysis with two-dimensional bathymetry will be helpful.

Another sensitivity test is done to characterize the impact of avalanching parameters on X-beach model. The lower value of critical slope refers that the slope is less stable and the dune is more vulnerable to erosion. The two parameters 'dryslp' and 'wetslp' are the governing factors here. The 'dryslp' parameter refers to the critical avalanching slope above water and 'wetslp' parameter is same but below water. They control the avalanching of the dune material. Both of the parameters are tested to observe the variation of erosion rate due to their altering value.

The 'dryslp' parameter is found to vary within a range from 0.1 to 2.0 according to X-beach manual. With increase of critical slope, no significant change in erosion is observed from the results. Figure 6.15 represents this effect. The amount of cliff erosion is expected to vary. But

the result does not match the expectation. The reason may be that the specific cross-shore profile used here is not being affected by this parameter. Further analysis with different cross-shore profile will be helpful to decide on the impact of this parameter on cliff erosion. For now no clear conclusion can be drawn from this result.

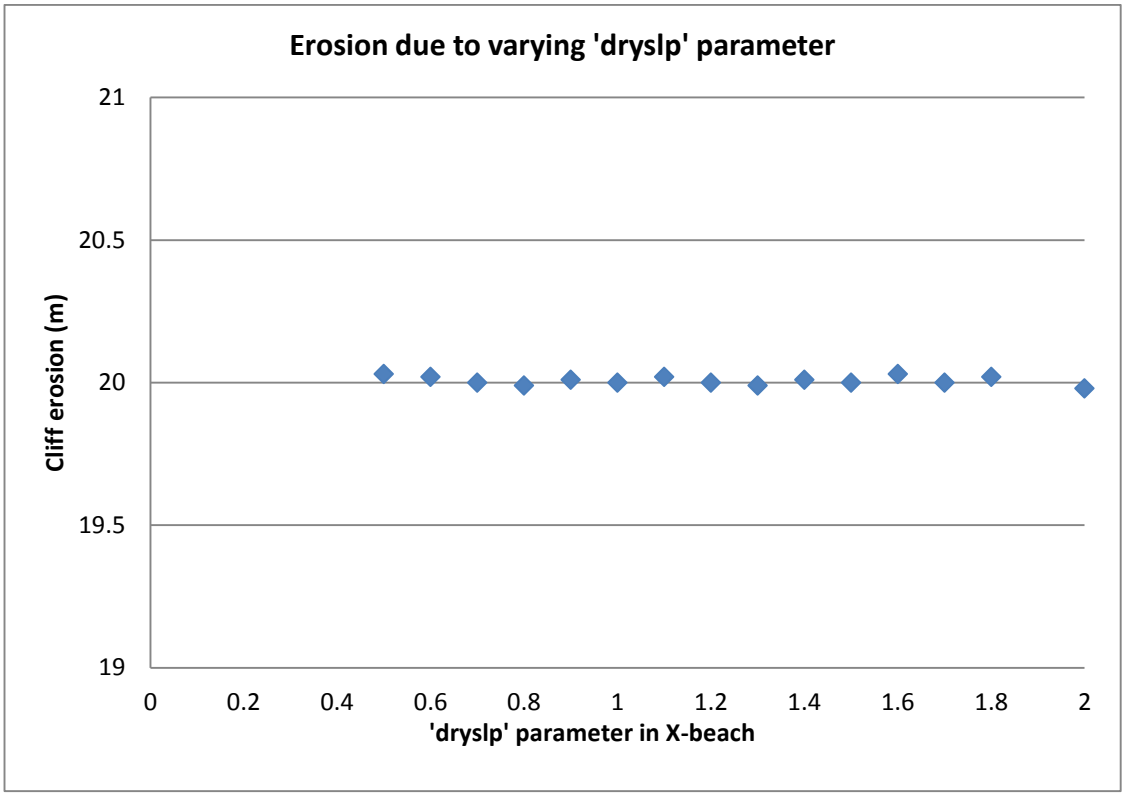

Figure 6.15: Sensitivity analysis for critical dry slope parameter

The ‘wetslp’ parameter ranges from 0.1 to 0.3. The resulting erosion for various ‘wetslp’ value is also observed. It is evident from Figure 6.16 that the erosion changes very rapidly for ‘wetslp’ varying 0.1 to 0.2. But after that the rate of change in erosion decreases as the ‘wetslp’ is reduced further. Still the rate of erosion shows a decreasing trend. The eroded profiles with different ‘wetslp’ values are plotted in Figure 6.17.

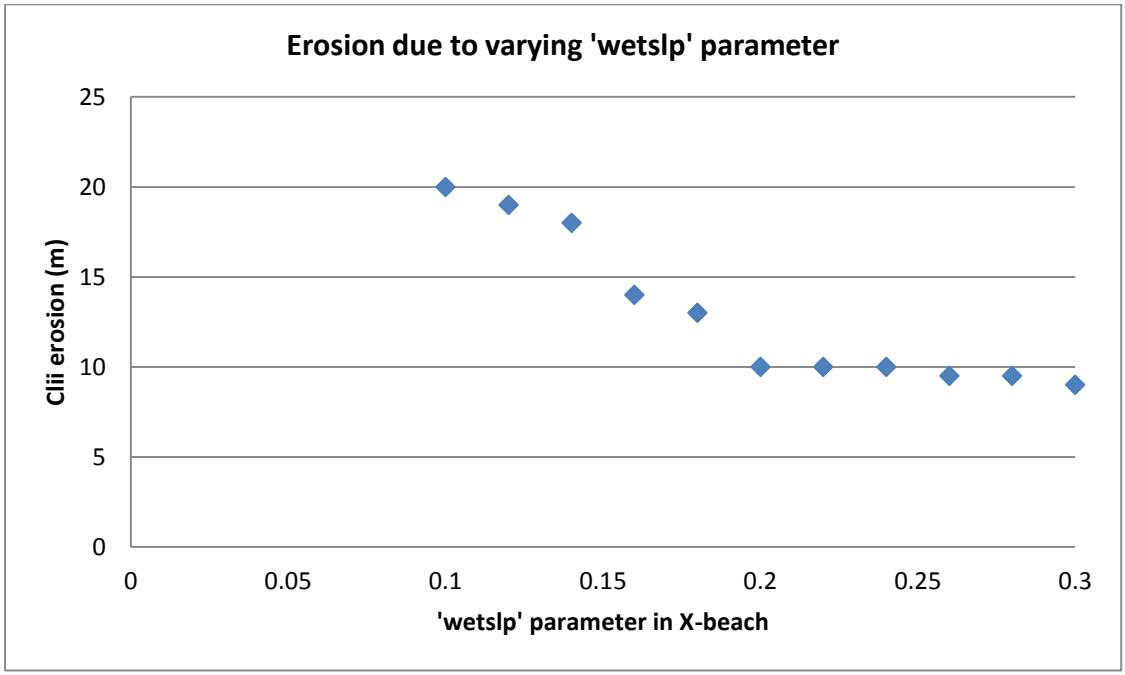

Figure 6.16: sensitivity analysis for critical wet slope parameter

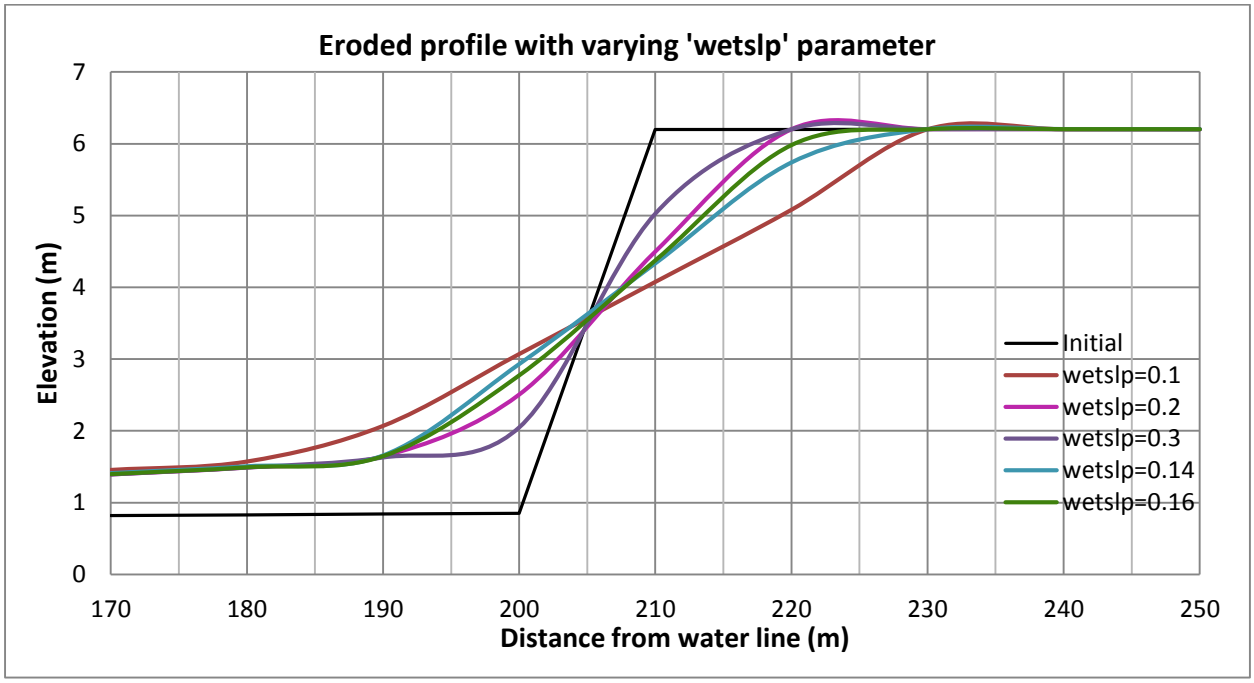

Figure 6.17: Comparison of eroded profiles with different 'wetslp' parameter.

6.3.4 Coastal erosion analysis using two-dimensional bathymetry

Finally the model is run for once using two-dimensional bathymetry with the parameters of calibrated model to get an idea of applicability for larger area. Later the 2D model is run with two different wind directions to study the effects of varying wind directions on coastal erosion. The grid spacing along cross-shore direction is kept unchanged (10.0m) and the grid spacing along the longshore direction is chosen as 1018.0m. The model generated using X-beach is shown in Figure 6.18 with the position of boundary relative to coastline and Figure 6.19 shows directional wave-grids considered for the numerical domain.

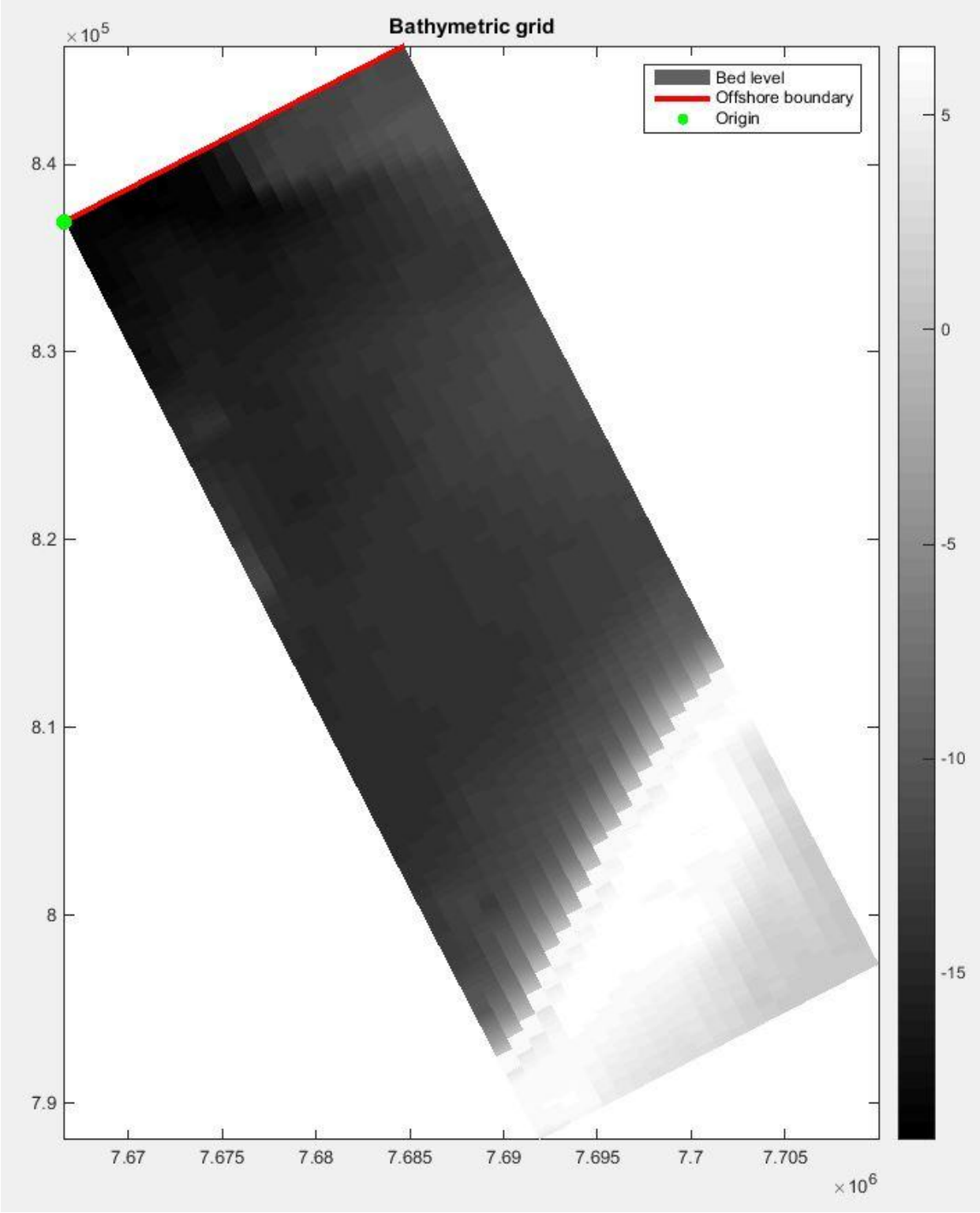

Figure 6.18: Model domain generated using X-beach

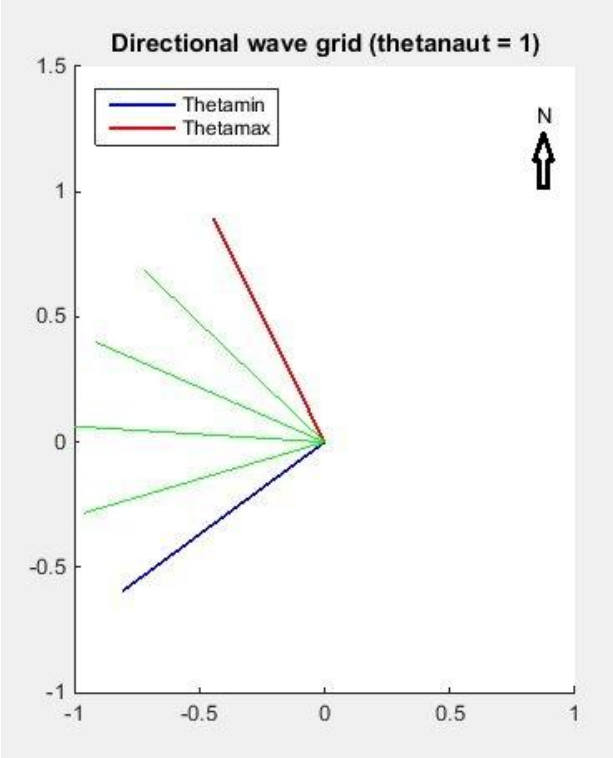

Figure 6.19: Distribution of directional wave grid considered by X-beach model (using nautical convention)

For two-dimensional bathymetry, X-beach can show animation of changing behaviour of different properties within the domain. Some snap shot from the animation of results from the simulation run are presented in the following text.

Figure 6.20 shows the variation in water level due to tide and storm surge during the simulation period. In Figure 6.20 (e), (f) and (g) the storm surge coming towards onshore can be seen clearly.

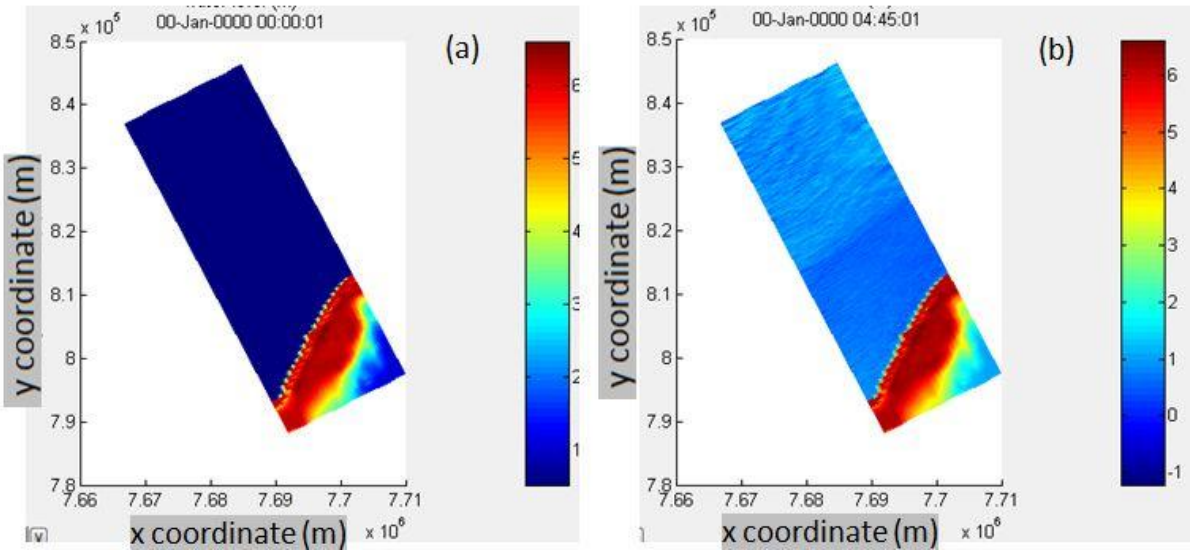

Figure 6.20 : Water level variation due to tide and storm surge (continued)

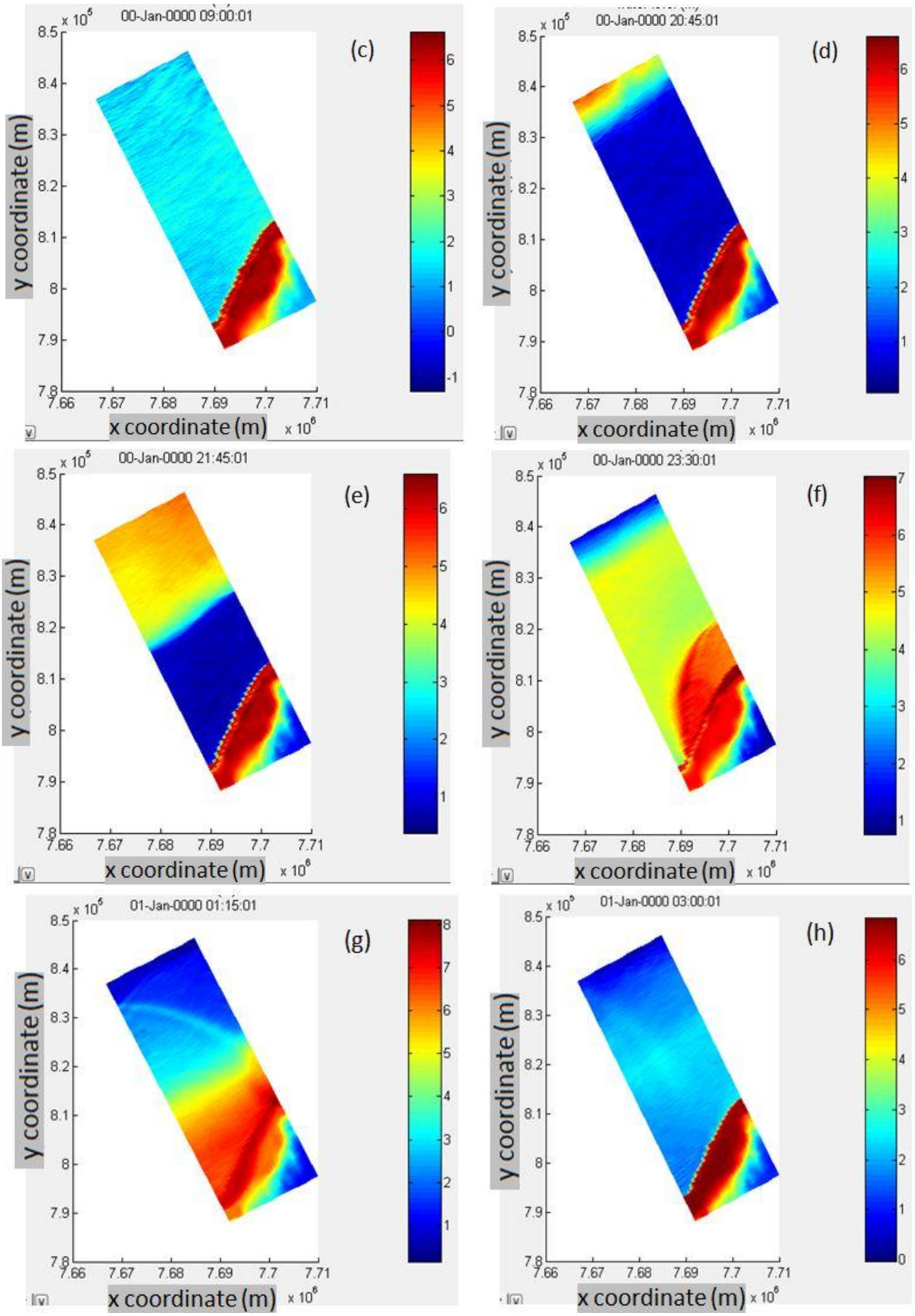

Figure 6.20 : Water level variation due to tide and storm surge

Figure 6.21 shows the variation in wave energy captured for three different time step. Figure 6.22 represents the instanteneous root mean square wave height (H_{rms}) computed using wave energy for different grid by X-beach.

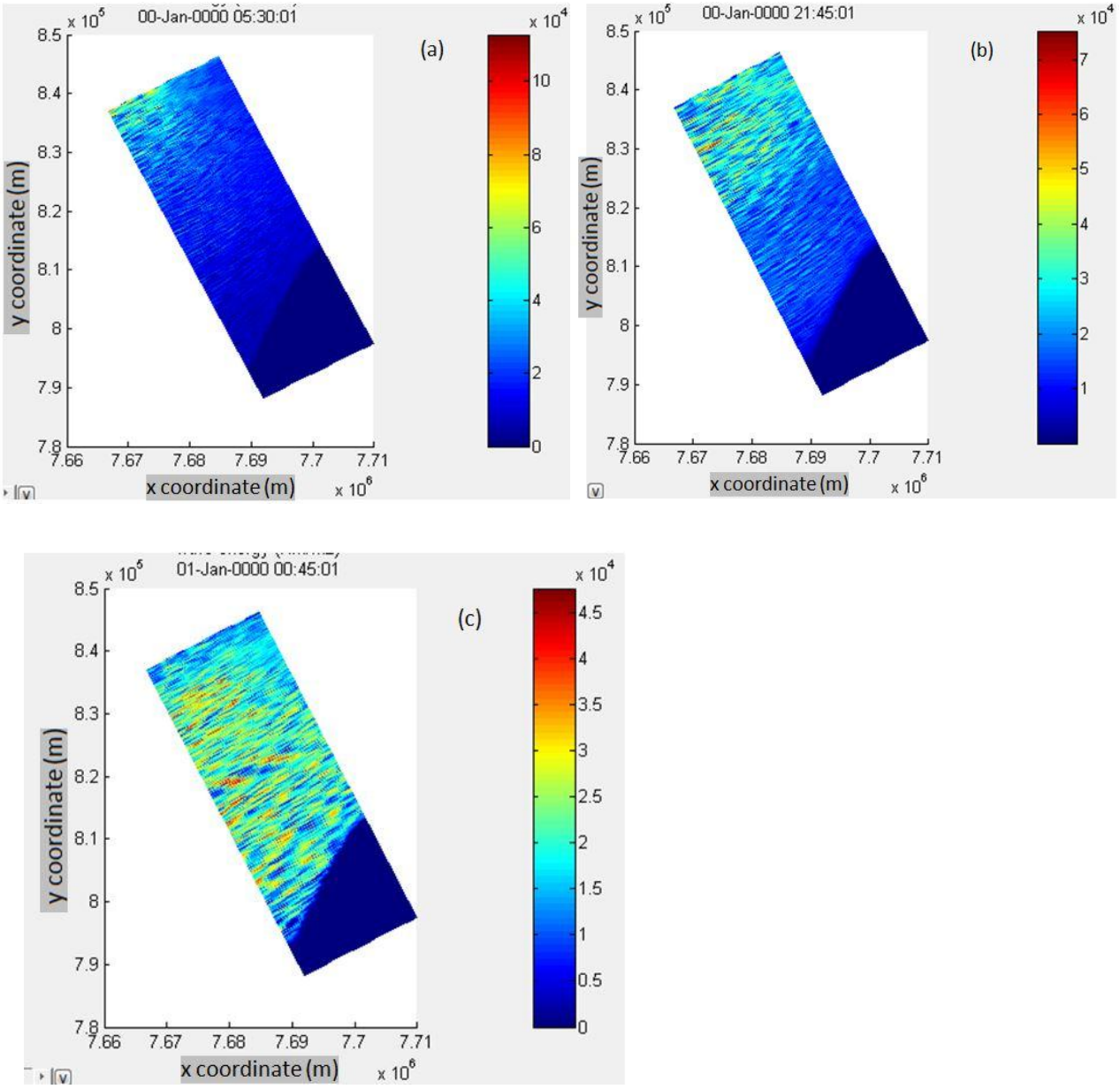

Figure 6.21: Wave energy variation

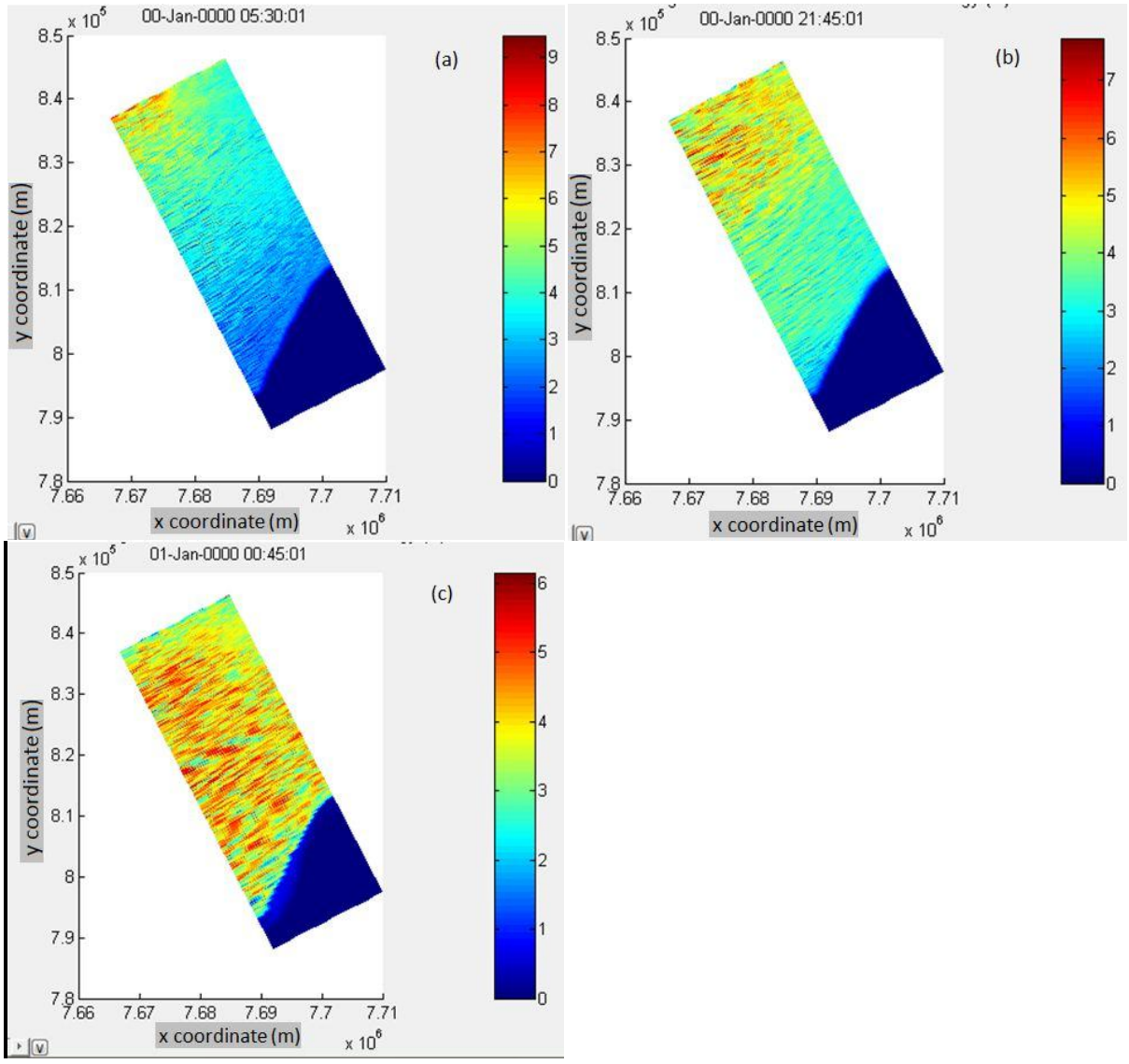

Figure 6.22: Root mean square wave height, Hrms Based on instantaneous wave energy spectrum

Figure 6.23 represents the change in bed level. The initial shoreline is shown using a blue line in Figure 6.23 (a) and the final shoreline after simulation is indicated with a green line in Figure 6.23 (b).

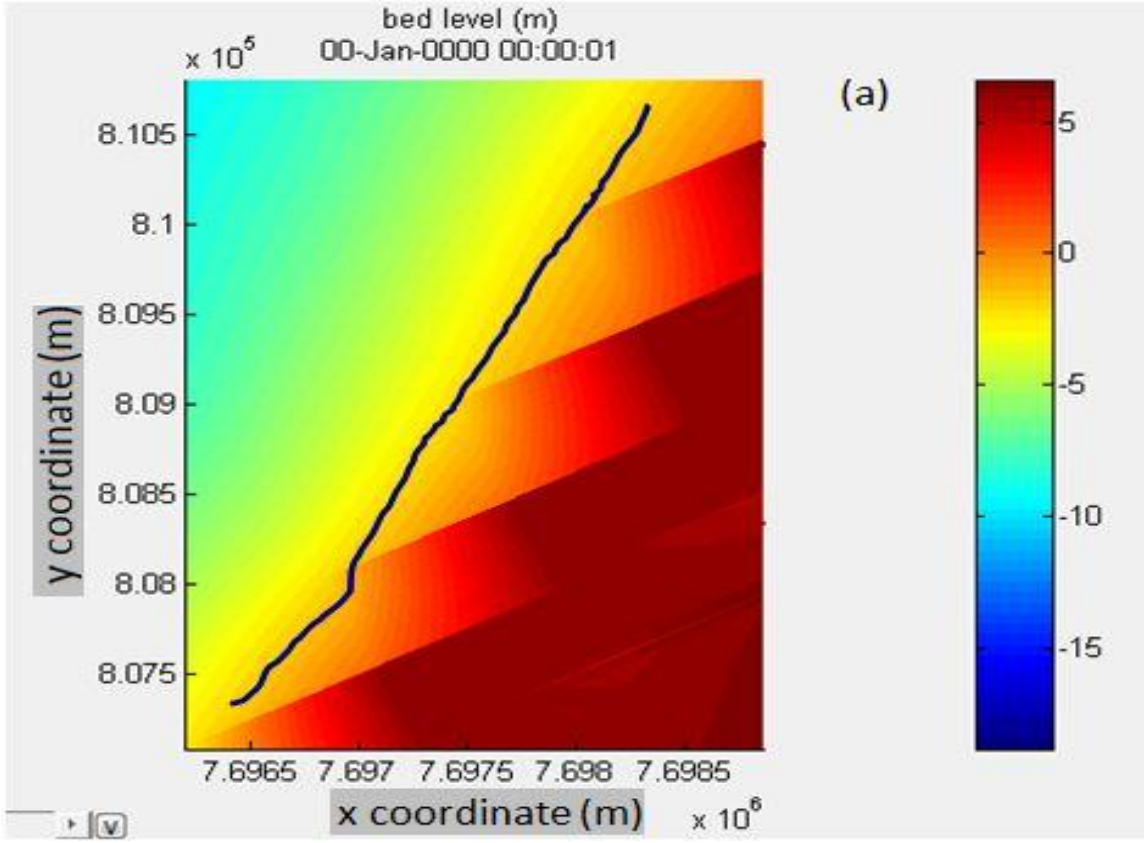

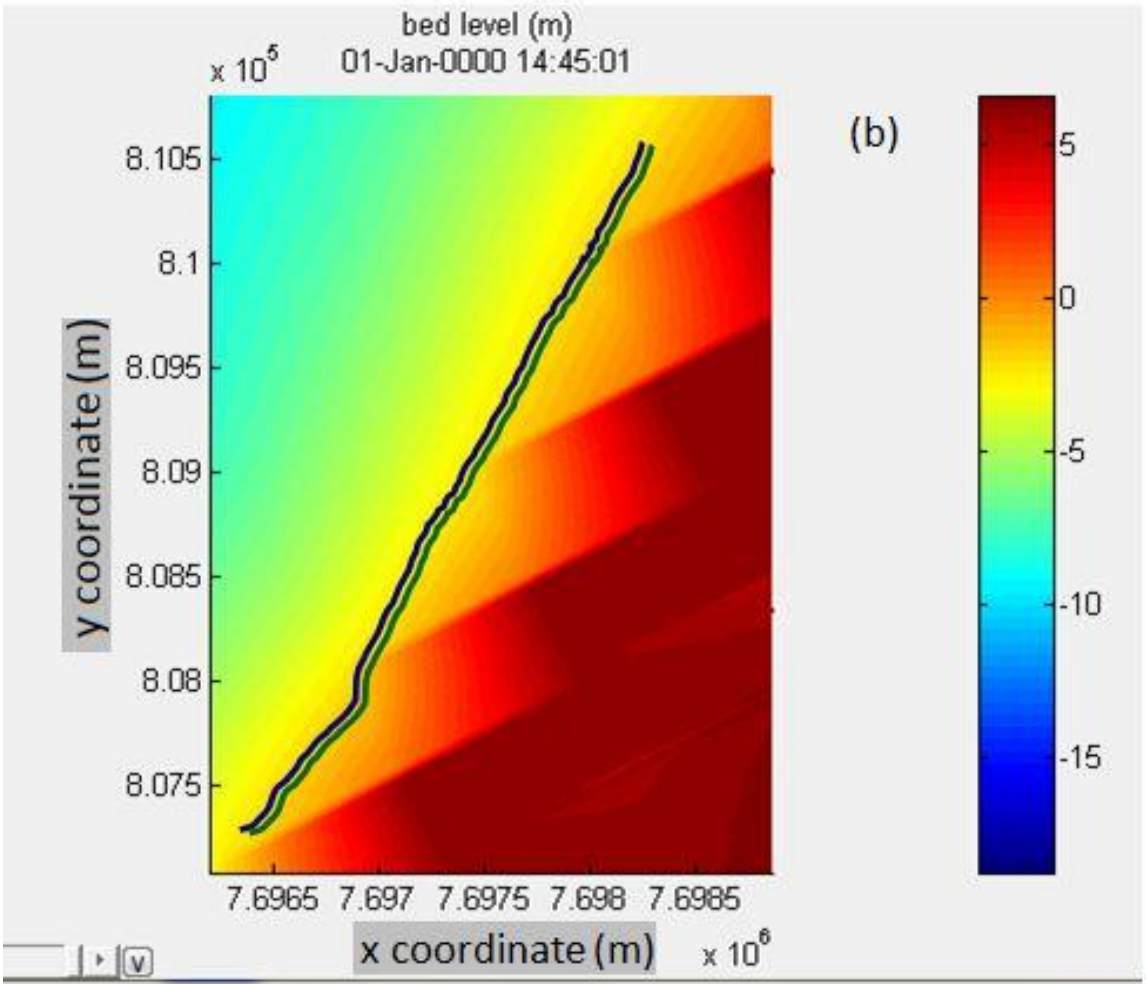

Figure 6.23: Change in bed level

Beacuse of the large size of domain for X-beach analysis, it is difficult to measure the change in shoreline or cliff erosion from this 2D colour plot. But the change can be measured using plots for different cross-shore profiles as described in previous text. From this it can be concluded that a 2D analysis for coastal erosion using X-beach can be a useful tool to simulate larger coastal area.

Erosion analysis is carried out with this two-dimensional bathymetry to observe the effect of wind direction. Wind velocity of 20m/s coming from both 290^o and 340^o nautical direction is applied for separate run. Figure 6.23 shows the comparison between the erosion profiles from these two conditions.

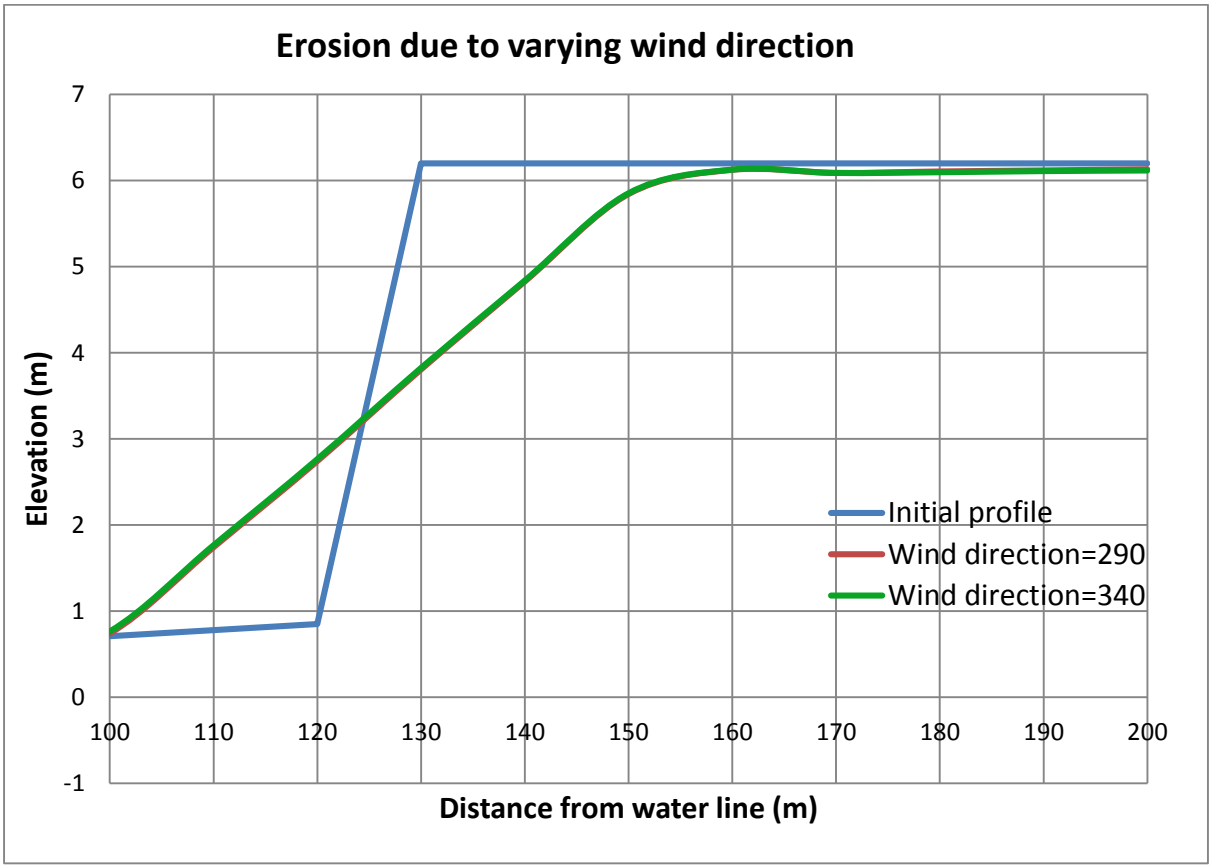

Figure 6.24: Cliff erosion due to varying wind direction

From Figure 6.23 no remarkable variation can be observed between two conditions. This can be explained by two points. Firstly, the dominating wave direction is around 290o and wind coming from this direction only plays a role to increase the wave energy. The wind from other directions have a component that only works in the same direction as wave does and their influence on the wave energy is not significant. Secondly, the bathymetry shows that the water depth for active wind field is comparatively shallow varying from 18m to 5m. Therefore the wind generated waves are not strong enough to dominate offshore waves. It has only very small effect on wave energy that causes erosion.

7 Conclusion and Recommendation

7.1 Summary

To sum up, a model to predict the coastal erosion mainly cliff erosion due to a storm event is prepared near Medynskiy area of Varandey, Russia using X-beach. The data from E. Guegan, 2013 is used to calibrate the model. It is validated using the cliff erosion data derived from 2010 and 2011. The model is found to simulate the erosion of this area convincingly.

The sensitivity analysis of wind speed, wind direction, critical avalanching slope above water and critical avalanching slope below water provide better insights to their impact on erosion of cliff. From the observation of the results, it can be concluded that wind speed and critical avalanching slope below water are important parameters for this model whereas wind direction and critical avalanching slope above water was not found to have a major impact on defining erosion.

The findings of the study are summarized here.

- X-beach can be used as a numerical modelling tool for estimation of coastal bluff erosion in the Arctic provided that the surrounding condition allows negligence of the thermal effects.
- The simulation of model is done with the data available. But there is scope for further improvement. This study mainly focuses to understand the hydrodynamic process involved in sediment transport.
- The wave energy and roller energy examined during the X-beach run are found to be practical considering the near-shore physical processes. The wave heights calculated from wave energy are found to decrease as the waves approach towards coast which represents the breaking of waves.
- The sensitivity analysis of wind stress establishes that wind parameters play very important role in simulation. The strong wind results in amplified cliff erosion by producing wind generated waves within the domain. For sensitivity analysis of wind direction, erosion analysis with single cross-shore profile is not found useful.
- The avalanching parameters are also very important as they influence the erosion mechanism by controlling slumping of beach material.
- From the sensitivity analysis, it is observed that increase of critical avalanching slope below water shows a decrease in cliff erosion.
- Changes in critical avalanching slope above water is not found to vary remarkablely through this study. But this is may be because of the specific cross-shore profile used in this case study. Further analysis with varying dune profile is necessary to reach a clear conclusion.
- A simulation is run with two dimensional bathymetry data to get an idea of the applicability of this tool for larger area. It is concluded that a 2D analysis can provide useful information to estimate coastal erosion.

- Simulation runs with two dimensional bathymetry data for two different wind directions are carried out. The result from analysis shows that wind direction does not have considerable effect on model as the offshore waves are predominant for causing erosion.

7.2 Limitations

The analysis and results provided here have some shortcomings. Time limitation and lack of enough data lead to these uncertainty.

To avoid long computation time by X-beach run, a 10m grid spacing along the cross-shore profile has been considered. A smaller grid spacing near the shore-face can produce results more precise and the changes in profile can be observed with better accuracy.

An exact beach profile along the shoreline could not be obtained because of lack of data. Therefore the tentative cross-profile selected cannot be expected to guarantee the representation of cross-profile everywhere along the coastline. There are variations in profiles as well as erosion rates in different areas. This cannot be modelled as the topography data for existing upper shore-face is not available.

Erosion data used for validation of the model actually describes the erosion rates over the year. As the objective of the current study is to model the coast for storm event only, erosion due to storm should be more appropriate for this case. Erosion deduced from field measurement of before-after cross-shore profile would be appropriate to use for the validation. It was not possible because of practical reasons.

7.3 Recommendation for further studies

Sediment properties for the cliff are considered to be same through top to bottom. But this is not the actual case as layers of different sediment class can easily be observed in Figure 5.3. The reliability of this model can be increased by introducing the individual properties for sediment classes from different layers.

In this study, both for wave modelling using SWAN and for cliff erosion analysis using X-beach a constant wind speed and direction is applied for ease of analysis. But this surely does not represent the existing scenario. The model can generate results more realistic if the varying wind speeds and directions in different grids within the domain could be taken into consideration separately.

The X-beach tool uses only avalanching process as erosion mechanism. There is scope for further improvement of this numerical modelling tool so that it can simulate the Arctic coast more accurately. The thermal factors and geotechnical instability of dune profile may be incorporated into the modules for better prediction of the dune erosion in the Arctic settings.

References

Afzal, M. (2012). Wave Propagation Over Rugged Topography Mehamn Harbour, Norway Using SWAN Model. Trondheim: NTNU.

Afzal, M., & Kulkarni, R. (2013).Development of Hydraulic Modeling Studies Template.NTNU.

Alegria-Arzaburu A.R., Williams J., Masselink G.,(2010) Application of X-beach to Model Storm Response on a Macrotidal Gravel Barrier. Proceedings of 32nd Conference on Coastal Engineering, Shanghai, China, 2010

Are, F., 1988. Thermal abrasion of sea coasts (part i) Polar Geography and Geology, 12(1).

Are, F.E., Grigoriev, M.N., Rachold, V. and Hubberten, H.-W., 2004. Opredeleniyeskorostiotstupaniyatermoerozionnykhberegovporazmeram (determination of retreat rates of thermoabrasionalcoasta from dimentions of thermo-terraces) KriosferaZemli (Earth's Cryosphere), VIII(3): 52-56.

Bagnold, R. A., 1966. An approach to the sediment transport problem from general physics.US Geol. Surv. Prof. Paper, 422, 231-291.

Battjes, J. A., & Janssen, J. P. F. M., 1978. Energy loss and set-up due to breaking of random waves. Coastal Engineering Proceedings, 1(16).

Belova, N.G. et al., 2009. Long-term coastal dynamics monitoring at the kharasavey area of yamal peninsula, kara sea, Geophysical Research Abstracts.

Bijker, E.W., 1967. Some considerations about scales for coastal models with movable bed. Delft Hydraulics Laboratory, Publication 50, Delft, The Netherlands.

BosboomJ.andStive M., 2013. Coastal Dynamics I. VSSD, Delft,The Netherlands.

Brown, J., O.J. Ferrians, J., Heginbottom, J.A. and Melnikov, E.S., 1997. Circum-Arctic map of permafrost and ground-ice conditions, Circum-Pacific Map Series CP-45.U.S. Geological Survey in Cooperation with the Circum-Pacific Council for Energy and Mineral Resources, Washington, DC.

Christensen, J.H. and Kuhry, P., 2000. High-resolution regional climate model validation and permafrost simulation for the east europeanrussianArctic. Journal of Geophysical Research, 105(D24): 29647-29658.

Coastlines of erosion and deposition. Retrieved June 15, 2015, from http:/ www.bbc.co.uk/education/guides/z3ndmp3/revision/3

Coastal Processes and Landforms. Retrieved June 22, 2015, from http://myweb.cwpost.liu.edu/vdivener/notes/coastal_geomorph.htm

Donelan, M. A., Hamilton, J., & Hui, W., 1985.Directional spectra of wind generated waves. Philosophical Transactions of the Royal Society of London. Series A, Mathematical and Physical Sciences, 315(1534), 509-562.

De Vriend H.J. (1991). Mathematical Modeling and Large-scale Coastal behaviour. J. Hydraulic Res.,29(6): 727-753.

Einstein, H. A., & Krone, R. B., 1962. Experiments to determine modes ofcohesive sediment transport in salt water. Journal of Geophysical Research, 67(4),1451-1461.

Eldeberky, Y., &Battjes, J. A., 1994.Nonlinear coupling in waves propagatingover a bar.Coastal Engineering Proceedings, 1(24).

Engelund, F. and Hansen, E., 1976. A Monograph on Sediment Transport inAlluvial Channels. Nordic Hydrology 7, pp. 293-306.

Engelund, F. and Hansen, E., 1976. A Monograph on Sediment Transport inAlluvial Channels. Nordic Hydrology 7, pp. 293-306.

ERA Interim, Daily. (n.d.). Retrieved June 5, 2015, from http://apps.ecmwf.int/datasets data/interim-full-daily/

Grigoriev, M.N., Razumov, S.O., Kunitzky, V.V. and Spektor, V.B., 2006. Dinamikaberegovvostochnykharkticheskikhmoreirossii: Osnovnyefaktory, zakonomernostiitendencii (dynamicsof the russian east Arctic sea coast: Major factors, regularities and tendencies),.KriosferaZemli (Earth's Cryosphere),, 10(4): 74-94.

Gubarkov, A.A., Khomutov, A.V. and Leibman, M.O., 2009. Contribution of lateral thermoerosion and thermodenudation to the coastal retreat at yugorsky peninsula, russia, EGU General Assembly 2009., Vienna, Austria, 19 – 24 April 2009.

Guegan, E., Sinitsyn, A., Kokin O., Vergun, A., Udalov, L., &Ogorodov, S. (2013). Investigations of Coastal Erosion Processes in Varandey Area, Barents Sea, SPE-166932. SPE Arctic and Extreme Environments Technical Conference and Exhibition.

Guegan, E., Sinitsyn, A., Nordal, S. Field investigations, remote sensing and modelling approach for Arctic coastal erosion (2014).XXV International Coastal Conference "Coastal Zone – Future Perspectives".

Gunther, F., Overduin, P.P., Sandakov, A.V., Grosse, G. and Grigoriev, M.N., 2013. Short- and long-term thermo-erosion of ice-rich permafrost coastsin the laptev sea region. Biogeosciences, 10: 4297–4318,.

Hasselmann, K., 1962. On the non-linear energy transfer in a gravity-wavespectrum. J. Fluid Mech, 12(481-500), 15.

Hasselmann, S., Hasselmann, K., Allender, J. H., & Barnett, T. P., 1985.Computations and Parameterizations of the Nonlinear Energy Transfer in aGravity-Wave Specturm. Part II: Parameterizations of the nonlinear energyTransfer for Application in wave models. Journal of Physical Oceanography,15(11), 1378-1391.

Holthuijsen, L. H., 2007. Waves in oceanic and coastal waters.CambridgeUniversity Press.

Holthuijsen, L.H, Booij, N. and Herbers, T.H.C., (1989) A Prediction Model forStationary, Short-crested Waves in Shallow Water with Ambient Currents,Coastal Engineering, 13, 23-54.

Hoque, M.A. and Pollard, W.H., 2009. Arctic coastal retreat through block failure. Canadian Geotechnical Journal, 46(10): 1103-1115.

Hurricane Impacts Due to Storm Surge, Wave, and Coastal Flooding.(n.d.). Retrieved June 15, 2015, from http:/ www.hurricanescience.org/society/impacts/stormsurge/

Janssen, P. A. E. M., Lionello, P., &Zambresky, L., 1989. On the interaction ofwind and waves.Philosophical Transactions of the Royal Society of London.Series A, Mathematical and Physical Sciences, 329(1604), 289-301.

Janssen, P. A., 1991. Quasi-linear theory of wind-wave generation applied towave forecasting. Journal of Physical Oceanography, 21(11), 1631-1642.

Kalinske, A. A., 1947. Movement of sediment as bed load in rivers. Transactions,American Geophysical Union, 28, 615-620.

Kobayashi, N., 1985. Formation of thermoerosional niches into frozen bluffs due to storm surges on the beaufort sea coast. Journal of Geophysical Research, 90(C6): 11983-11988.

Komen, G. J., Cavaleri, L., Donelan, M., Hasselmann, K., Hasselmann, S., &Janssen, P. A. E. M., 1996. Dynamics and modelling of ocean waves. CambridgeUniversity Press.

Kulkarni, R. (2013) Numerical Modelling of Coastal Erosion using MIKE21, MSc. Thesis, NTNU

Lantuit, H. et al., 2012. The Arctic coastal dynamics database: A new classification scheme and statistics on Arctic permafrost coastlines. Estuaries and Coasts, 35: 383-400.

Launder, B. E., & Spalding, D. B., 1974. The numerical computation of turbulentflows.Computer methods in applied mechanics and engineering, 3(2), 269-289.

Leont'yev, I. O., 2003. "Modeling Erosion of Sedimentary Coasts in the WesternRussian Arctic," Coastal Eng. 47, 413–429.

Light -- why does it bend/refract? Retrieved June 15, 2015, from https:/ www.physicsforums.com/threads/light-why-does-it-bend-refract.763828/

Longuet-Higgins, M. S., & Stewart, R. W., 1964, August. Radiation stresses inwater waves; a physical discussion, with applications. In Deep Sea Research andOceanographic Abstracts (Vol. 11, No. 4, pp. 529-562).Elsevier.

Mancheño, A. (2014). Numerical Model of Currents and Tides in an Inlet using MIKE 3. Trondheim: NTNU.

Meyer-Peter, E., & Müller, R., 1948, June. Formulas for bed-load transport. InProceedings of the 2nd Meeting of the International Association for HydraulicStructures Research (pp. 39-64). Delft: International Association of Hydraulic Research.

Miche, M., 1944.MouvementsOndulatories de la MerenProfondeurConstanteouDécroissante, Ann. PontsChauss., 25-28,131-164,270-292 and 369-406.

Nairn, R. B., Roelvink, J. D., & Southgate, H. N., 1990.Transition zone widthand implications for modelingsurfzone hydrodynamics.Coastal EngineeringProceedings, 1(22).

Nielsen, P., 1979. Some basic concepts of wave sediment transport, Series paper20 Institute of Hydrodynamic and Hydraulic Engineering, Technical University ofDenmark, 160 pp.

Nielsen, P. 2002. Shear stress and sediment transport calculations for swash zone modelling. *Coastal Engineering*, 45(1), 53-60.

Ogorodov, S.A., Kokin, O.V., Sinitsyn A.O. , Guegan E., Rodionov I.V. , Udalov L.E. , Kuznetsov D.E. , Likutov P.E. , Kondratieva S.T. (2013). Research on the Dynamics of the Coastal Area of the Barents and Kara Seas under Conditions of the Climate Change in the Arctic Region.N.NZubov State Oceanographic Institute, Moskow.

Ogorodov, S.A, Belova, N., Kuznetsov, D. and Noskov, A., 2011a. Using multi-temporal aerospace imagery for coastal dynamics investigations at kara sea. Earth from Space - the Most Effective Solutions, 10: 66-70.

Ogorodov, S.A., 2002. Application of wind-energetic method of popov-sovershaev for investigation of coastal dynamics in the Arctic, Ber.Polarforsch.Meeresrosch.

Ogorodov, S.A., 2004. Morpholitodynamics of coastal zone of varandey area in pechora sea under man-made impact. Geoecology, Engineering Geology, Hydrogeology, Geocryology, 3:1-6.

Ogorodov, S.A., 2005. Human impacts on coastal stability in the pechora sea. Geo-Mar Lett, 25: 190-195.

Ogorodov, S.A., 2008. Effects of changing climate and sea ice extent on pechora and kara seas coastal dynamics. The Ninth International Conference on Permafrost, Fairbanks, Alaska, US, p.^pp. 1317-1320.

Ogorodov, S.A., Unpublished results-a.Geoecological survey in coastal zone of barents sea in the area of varandey island, july 2003. Moscow State University.

Ogorodov, S.A., Unpublished results-b.Geomorhhological composition and morpholitodynamics of coast and coastal zone of pechora sea in varandey industrial area, 2000, MSU, Географическийфакультет МГУ им. М.В. Ломоносова, Научно-исследовательскаялабораториягеоэкологии Севера.

Ogorodov, S.A. etal., 2011b. Wave action as a forcing factor of coastal erosion in the western and eastern russianArctic. Proceedings of LOICZ Open Science Conference 2011 (OSC-2011), Yantai (China), p.^pp. 211.

Ogorodov, S.A., Kamalov, A.M., Lugovoy, N.N., Sedova, N.B. and Archipov, V.V., 2000. Technogenic factor in coast dynamics of the pechora sea, AQUATERRA, St. Petersburg, pp. 129-131.

Ogorodov, S.A. and Kokin, O.V., 2012. Geomorphological structure and dynamics of barrier islands in the barents sea. INQUA SEQS 2012 Meeting. At The Edge of the Sea: Sediments, Geomorphology, Tectonics and Stratigraphy in Quaternary Studies, SASSARI, Sardinia (Italy). September 26-27 2012, p.^pp. 74-75.

Phillips, O. M., 1981. Dispersion of short wavelets in the presence of a dominantlong wave.Journal of Fluid Mechanics, 107, 465-85.

Ris, R. C., Holthuijsen, L. H., &Booij, N., 1994. A spectral model for waves inthe near shore zone.Coastal Engineering Proceedings, 1(24).

Roelvink, D., &Reniers, A.(2012). *A guide to modeling coastal morphology*.

Roelvink, J. A., &Stive, M. J. F., 1989. Bargenerating cross-shore flowmechanisms on a beach. Journal of Geophysical Research: Oceans (1978–2012), 94(C4), 4785-4800.

Rooijen A.V., Reniers A., Vries J.T., Blenkinsopp C., McCall R. (2012). Modeling Swash Zone Sediment Transport at TrucVert Beach, France. 33rd International Conference on Coastal Engineering. Vol. 33 (2012).

Rottner, J., 1959. ‘‘A formula for bed-load transportation.’’Houille Blanche, 14(3), 285–307.

Ruessink, B. G., Walstra, D. J. R., & Southgate, H. N., 2003. Calibration andverification of a parametric wave model on barred beaches. Coastal Engineering,48(3), 139-149.

Schiereck, G., &Verhagen, H. (2012).*Introduction to bed, bank and shore protection* (2nd ed.). VSSD.

Shields, A., 1936. Application of Similarity Principles and Turbulence Research toBedload Movement, California Institute of Technology, Pasadena (translated fromGerman).

Shoaling and Refraction. Retrieved June 15, 2015, from http://magicseaweed.com/Shoaling-and-Refraction-Article/325/

Smagorinsky, J., 1963. General circulation experiments with the primitiveequations: i. The basic experiment*. Monthly weather review, 91(3), 99-164.

Southgate, H. N., & Nairn, R. B., 1993. Deterministic profile modelling ofnearshore processes. Part 1.Waves and currents.Coastal Engineering, 19(1), 27-56.

Swart D.H., (1976), Predictive equations regarding coastal transports. Proc 15thConf Coastal Engng, 2, pp. 1113–1132.

Tolman, H. L., 1994. Wind waves and moveable-bed bottom friction. Journal ofphysical oceanography, 24(5), 994-1009.

Trouw K., Zimmermann N., Mathys M., Delgado R., Roelvink D. (2012). Numerical Modeling of Hydrodynamics and Sediment Transport in the Surf Zone: A Sensitivity study with different types of Numerical Models. International Conference on Coastal Engineering (ICCE 2012), Santander, Spain, July 1-6 2012: book of papers. pp. [1-12]

Van Rijn, L. C., 1984. Sediment transport, part I: bed load transport.Journal ofhydraulic engineering, 110(10), 1431-1456.

Van Rijn, L. C., 1987. Mathematical modelling of morphological processes in thecase of suspended sediment transport (Doctoral dissertation, WaterloopkundigLab., Delft Hydraulics Comm-382).

Van Rijn, L. C., 1993. Principles of sediment transport in rivers, estuaries andcoastal seas (Vol. 1006). Amsterdam: Aqua publications.

Varandey Monthly Climate Average, Russia. Retrieved May 15, 2015, from http:/ www.worldweatheronline.com/Varandey-weather-averages/Nenets/RU.aspx

Vousdoukas M.I., Almeida L.P , and Ferreira Ó. (2011).Modelling storm-induced beach morphological change in a meso-tidal, reflective beach using XBeach. Journal of Coastal Research, SI 64 (Proceedings of the 11th International Coastal Symposium), 1916-1920. Szczecin, Poland, ISSN 0749-0208

Waves. Retrieved June 15, 2015, from http://www.geography.learnontheinternet.co.uk/topics/waves.html

Weber, N., 1991. Bottom friction for wind sea and swell in extreme depth-limitedsituations. Journal of physical oceanography, 21(1), 149-172.

Wilcox, D. C., 1994. Simulation of transition with a two-equation turbulencemodel.AIAA journal, 32(2), 247-255.

Wright L.D & Thom B.G.,(1977).Coastal Depositional Landforms: A morphodynamic approach. Progress in Physical Geography 1(3), pp. 412-459.

Young, I. R., & Van Vledder, G. P., 1993. A review of the central role ofnonlinear interactions in wind-wave evolution. Philosophical Transactions of theRoyal Society of London. Series A: Physical and Engineering Sciences,342(1666), 505-524.

Young, I. R., 1999. Wind generated ocean waves (Vol. 2). Elsevier Science.

Appendix- A

SWAN run

Sample code for SWAN run

```
$*************HEADING*************************************
$
PROJ 'bathy' 'SW05'
$
$ PURPOSE OF TEST: Test of the refraction formulation
$
$ --|-----------------------------------------------------------
|--
$   | This SWAN input file is part of the bench mark tests for     |
$   | SWAN.                                                        |
$ --|-----------------------------------------------------------
|--
$
$***********MODEL INPUT*************************************
$
SET  NAUTICAL
$
CGRID 18824 47791 0 190000 160000 543 457 SECTOR 200 330 100 0.05
0.25 40
$
INPGRID BOTTOM REGULAR 0 0 0 3019 3019 104 82.97
READINP BOTTOM -1 'bathy0500.bot' 4 0 FREE
$
WIND  21.8 284
$
BOU SHAPE JONswap 3.3 PEAK DSPR
BOUN SIDE W CCW CON PAR 10.4 14.9 287
$
OFF BREA
OFF WCAP
$
$************ OUTPUT REQUESTS ************************
$
BLOCK 'COMPGRID' nohead 'results.mat' XpYp Hs dir
$
TEST 1,0
$
POINTS 'output1' 198824 97791
POINTS 'output2' 203824 117791
POINTS 'output3' 194794 113458
POINTS 'output4' 194217 90458
TABLE 'output1' HEAD 'output.TBL' Distance DEP HS TM01 DIR DSPR
TABLE 'output2' HEAD 'output.TBL' Distance DEP HS TM01 DIR DSPR
TABLE 'output3' HEAD 'output.TBL' Distance DEP HS TM01 DIR DSPR
TABLE 'output4' HEAD 'output.TBL' Distance DEP HS TM01 DIR DSPR
$
COMPUT
STOP
$
```

Inputs

Table A.1 : Input parameters for SWAN analysis

Offshore Conditions						
sl.	Sig. wave height, Hs (m)	Peak period, Tp (sec.)	Peak direction, Theta p (°)	Mean direction, Theta m (°)	Wind speed at 10m elev., W10 (mps)	Wind direction at 10m elev., D10 (°)
1	5.2	9.2	257	239	21.1	239
2	10.4	13.5	272	261	24.9	254
3	12.1	14.9	272	269	24.8	265
4	11.6	14.9	272	277	23.8	278
5	10.4	14.9	287	284	21.8	284
6	9.1	13.5	287	290	20.8	287
7	7.9	12.3	287	295	19.6	292
8	6.8	12.3	302	300	17.6	297
9	5.6	11.2	302	305	15.8	304
10	4.4	11.2	317	309	13.4	309
11	3.6	10.2	317	311	13.2	311
12	3.1	9.2	317	312	12.2	311
13	2.7	8.4	317	312	12	312

Results

Table A.2 : Output parameters for Point 1 from SWAN analysis

Output 1			
sl.	Sig. wave height, Hs (m)	Peak period, Tp (sec.)	Mean direction, Theta m (°)
1	6.20	9.28	280.38
2	9.79	13.04	290.98
3	10.68	13.62	296.19
4	11.04	13.84	296.69
5	9.69	12.85	294.98
6	8.67	11.96	292.12
7	7.67	11.07	290.17
8	6.00	9.62	292.69
9	4.78	8.28	293.44
10	3.26	6.78	293.00
11	2.97	6.52	292.10
12	2.54	6.00	290.80
13	2.37	5.75	289.30

Table A.3 : Output parameters for Point 2 from SWAN analysis

Output 2			
sl.	Sig. wave height, Hs (m)	Peak period, Tp (sec.)	Mean direction, Theta m (°)
1	6.38	8.96	273.92
2	9.90	12.26	284.89
3	10.74	12.88	288.88
4	10.48	12.71	289.63
5	8.78	11.67	288.31
6	8.04	10.83	286.88
7	7.12	10.10	285.44
8	5.59	8.97	284.11
9	4.45	7.74	284.53
10	3.05	6.51	284.50
11	2.79	6.19	284.30
12	2.38	5.81	283.30
13	2.23	5.66	283.30

Table A.4 : Output parameters for Point 3 from SWAN analysis

Output 3			
sl.	Sig. wave height, Hs (m)	Peak period, Tp (sec.)	Mean direction, Theta m (°)
1	6.23	9.03	275.41
2	9.98	12.47	286.88
3	10.93	13.25	291.05
4	10.78	13.17	291.72
5	9.09	12.06	290.49
6	8.21	11.14	288.80
7	7.18	10.32	287.20
8	5.63	9.08	286.26
9	4.47	7.88	287.09
10	3.08	6.58	287.00
11	2.82	6.31	286.80
12	2.41	5.85	285.60
13	2.27	5.69	285.10

Table A.5 : Output parameters for Point 4 from SWAN analysis

Output 4			
sl.	Sig. wave height, Hs (m)	Peak period, Tp (sec.)	Mean direction, Theta m (°)
1	6.06	9.34	283.63
2	10.08	13.40	293.10
3	11.09	13.97	298.26
4	11.57	14.18	298.65
5	10.29	13.29	297.35
6	9.14	12.44	294.09
7	8.08	11.53	292.08
8	6.51	10.11	295.20
9	5.04	8.80	296.61
10	3.39	7.08	296.80
11	3.06	6.69	295.20
12	2.59	6.06	293.30
13	2.40	5.84	291.60

Result plots

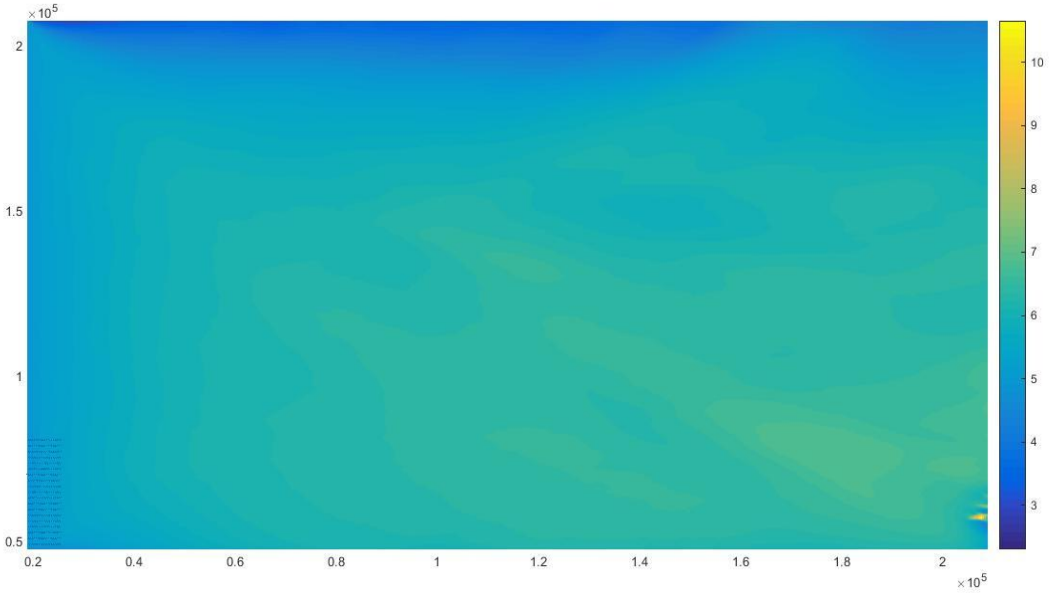

Figure A.1 : Colour grading plot of wave height from 0-3 hrs.

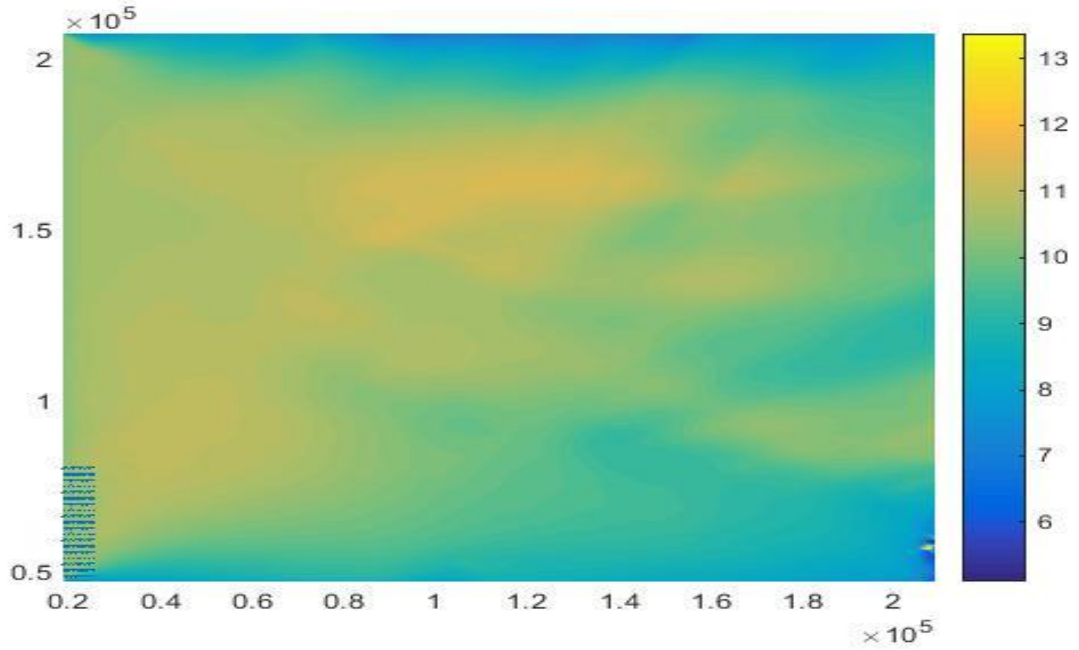

Figure A.2 : Colour grading plot of wave height from 3-6 hrs.

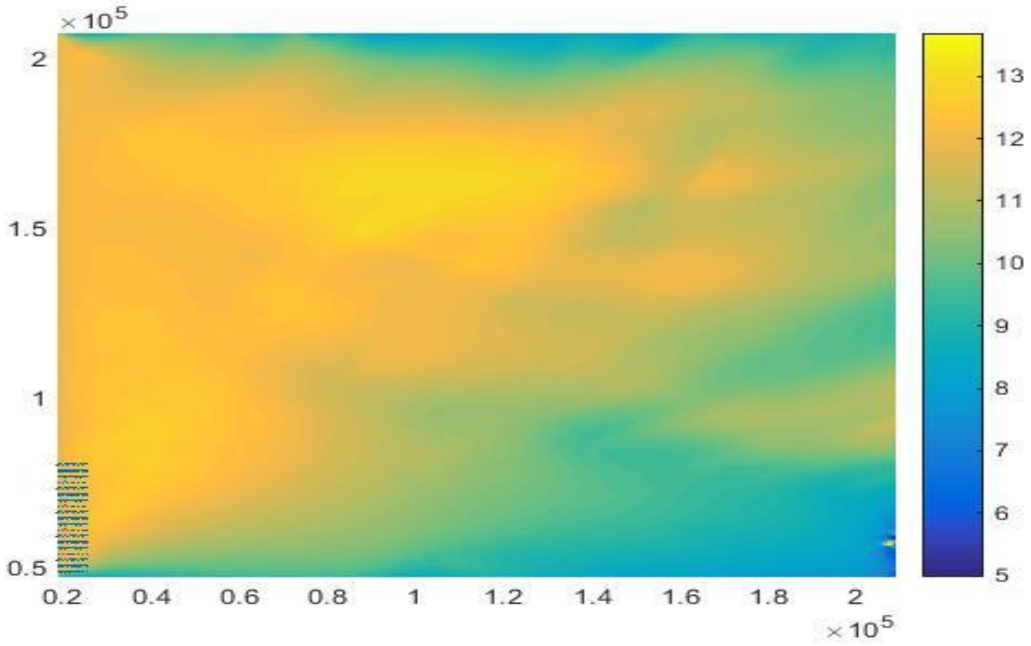

Figure A.3 : Colour grading plot of wave height from 6-9 hrs.

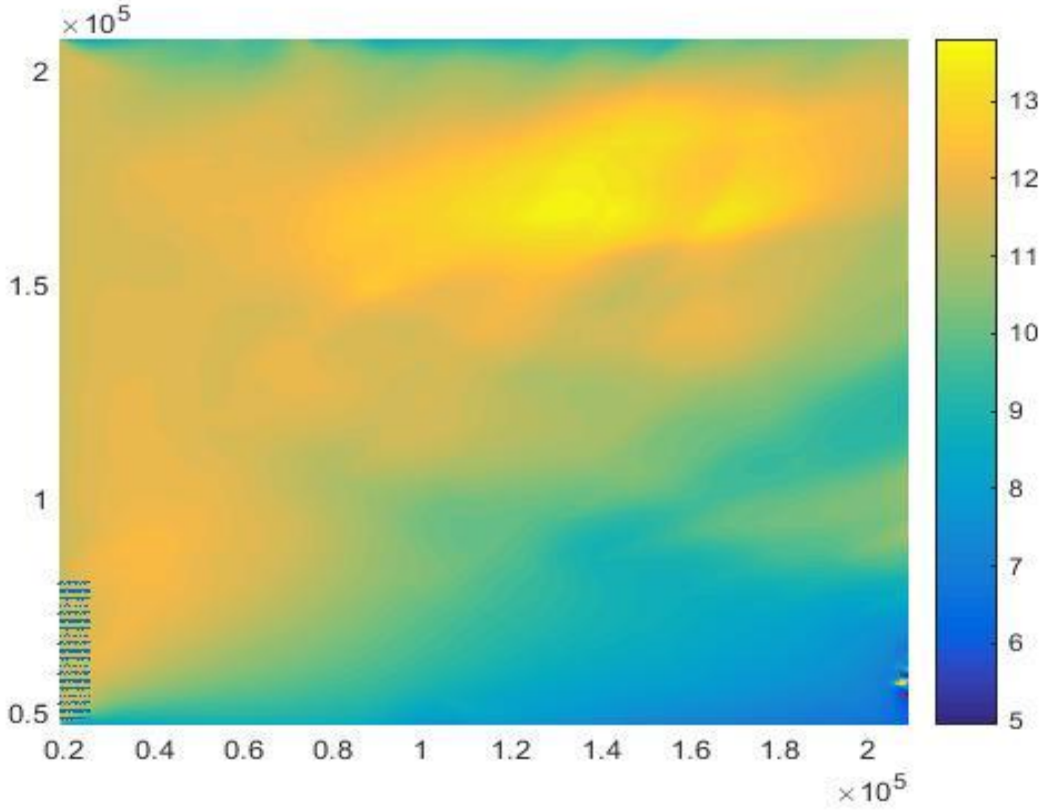

Figure A.4 : Colour grading plot of wave height from 9-12 hrs.

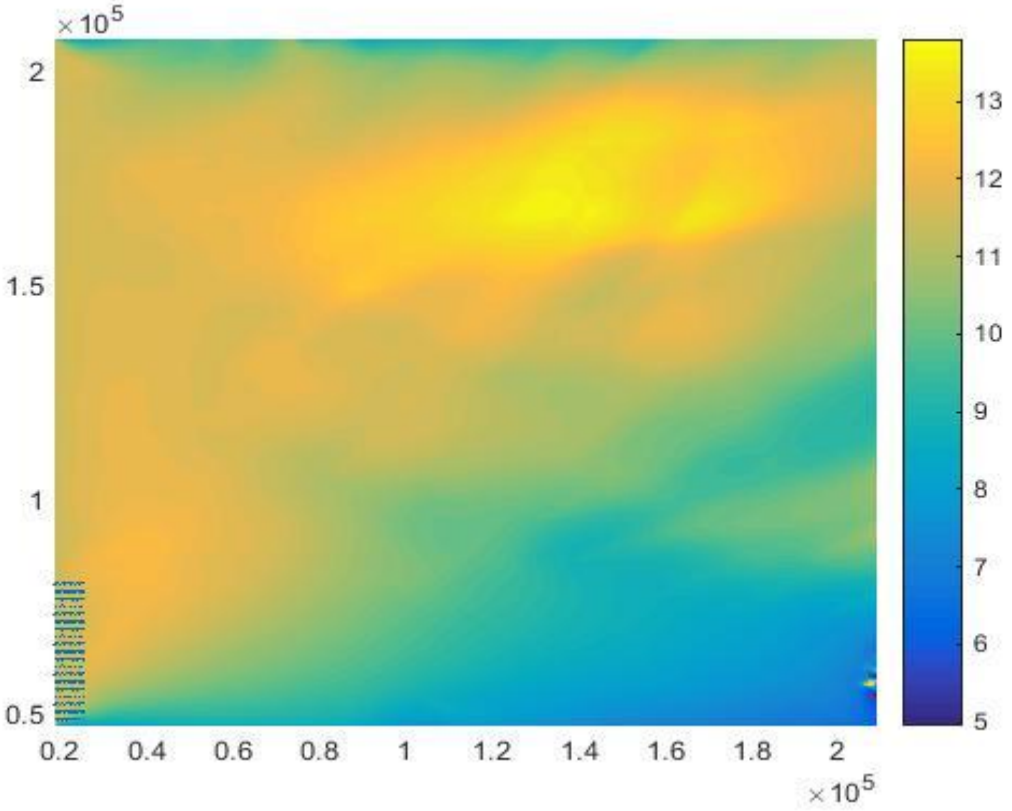

Figure A.5 : Colour grading plot of wave height from 12-15 hrs.

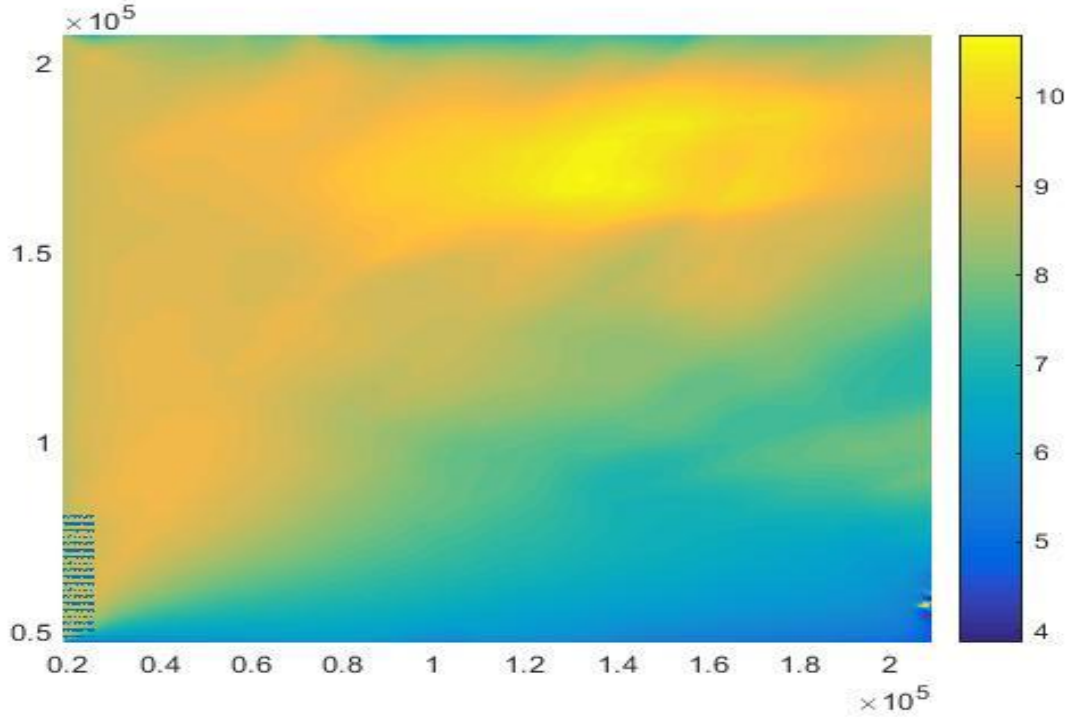

Figure A.6 : Colour grading plot of wave height from 15-18 hrs.

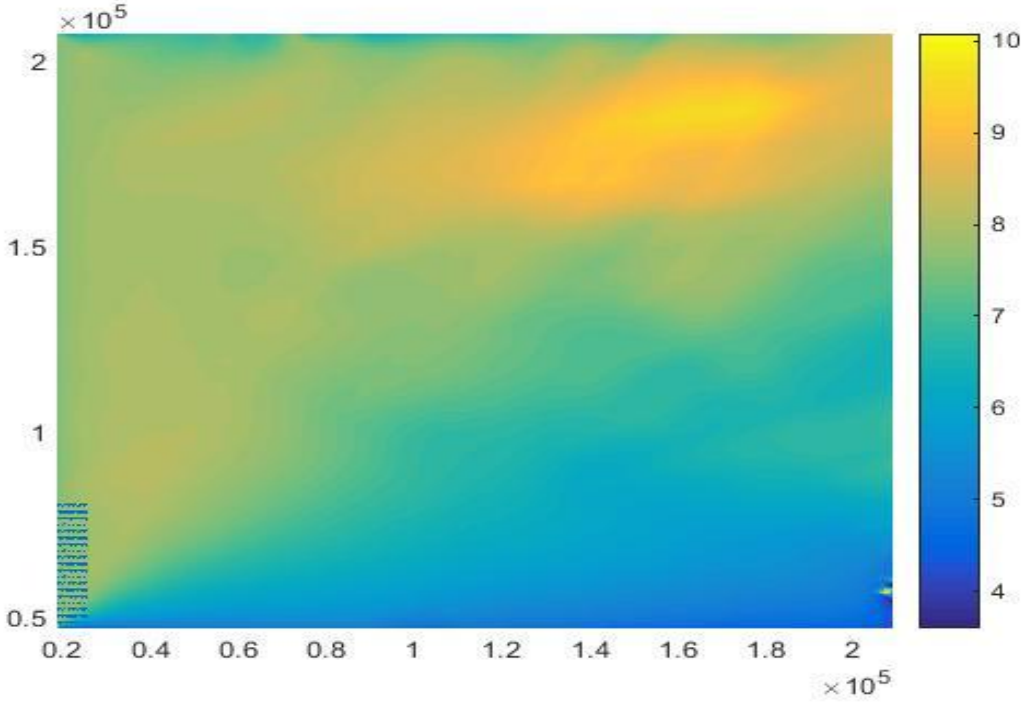

Figure A.7 : Colour grading plot of wave height from 18-21 hrs.

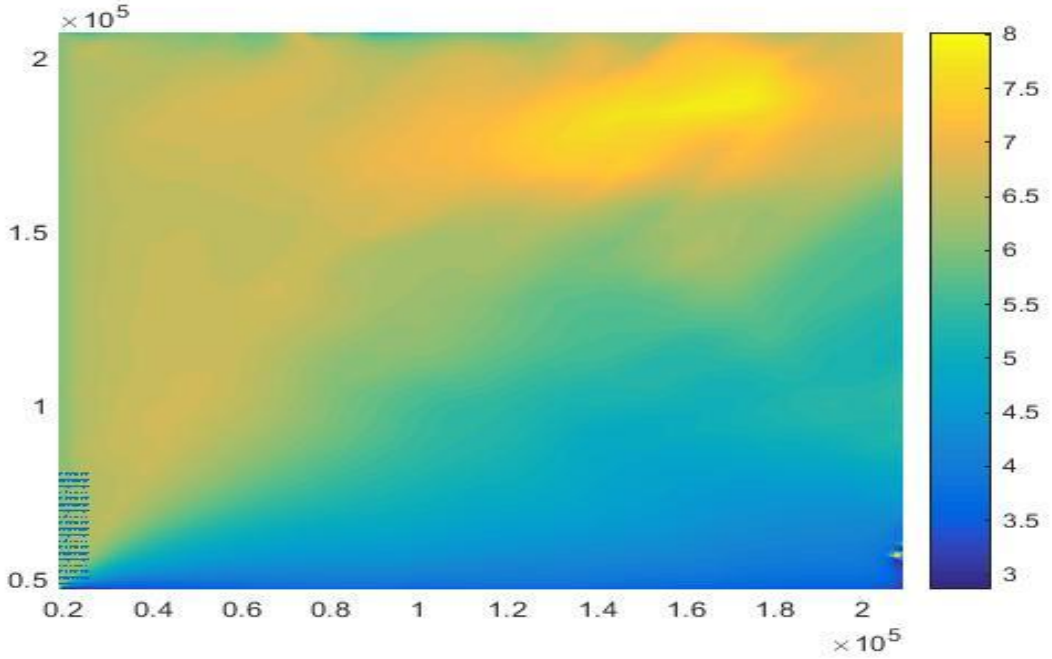

Figure A.8 : Colour grading plot of wave height from 21-24 hrs.

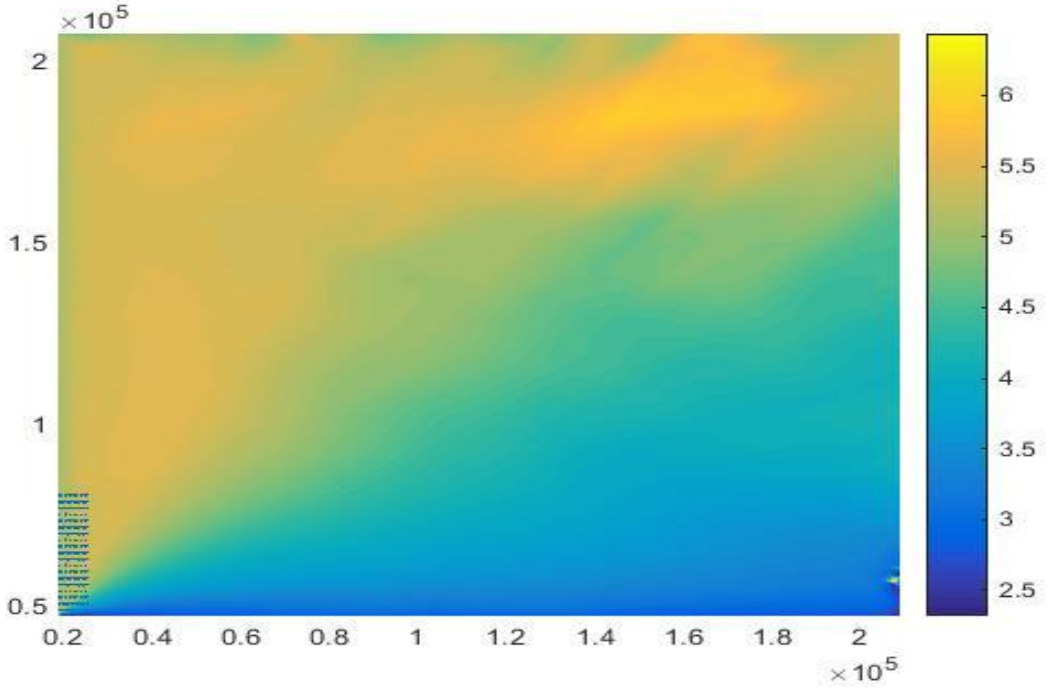

Figure A.9 : Colour grading plot of wave height from 24-27 hrs.

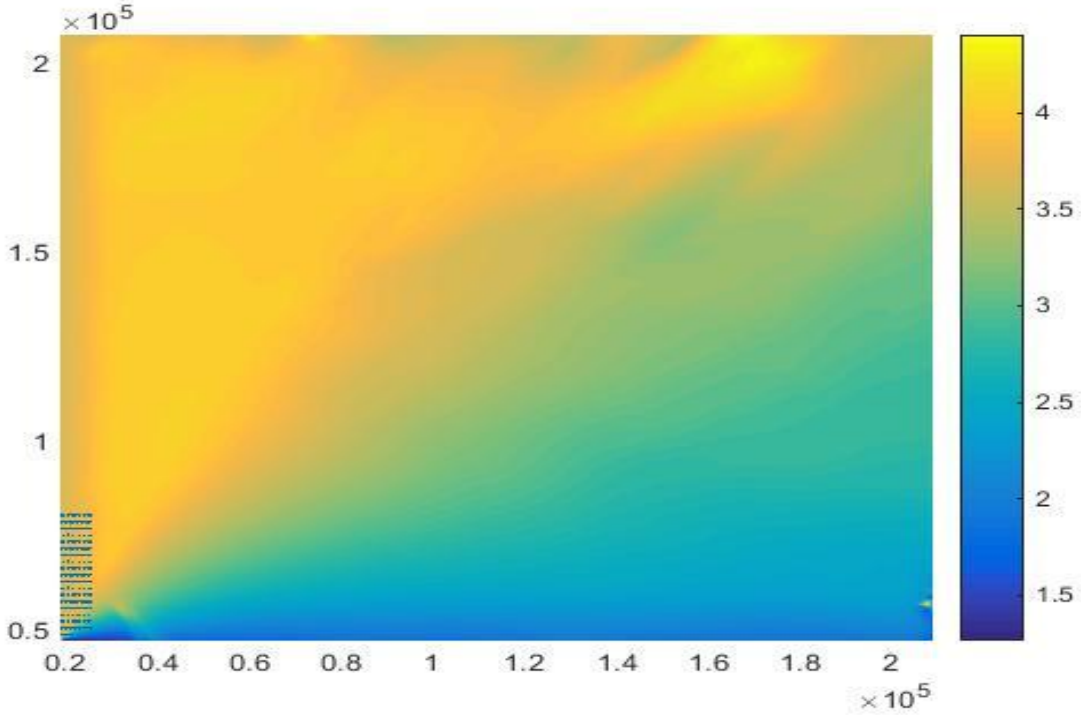

Figure A.10 : Colour grading plot of wave height from 27-30 hrs.

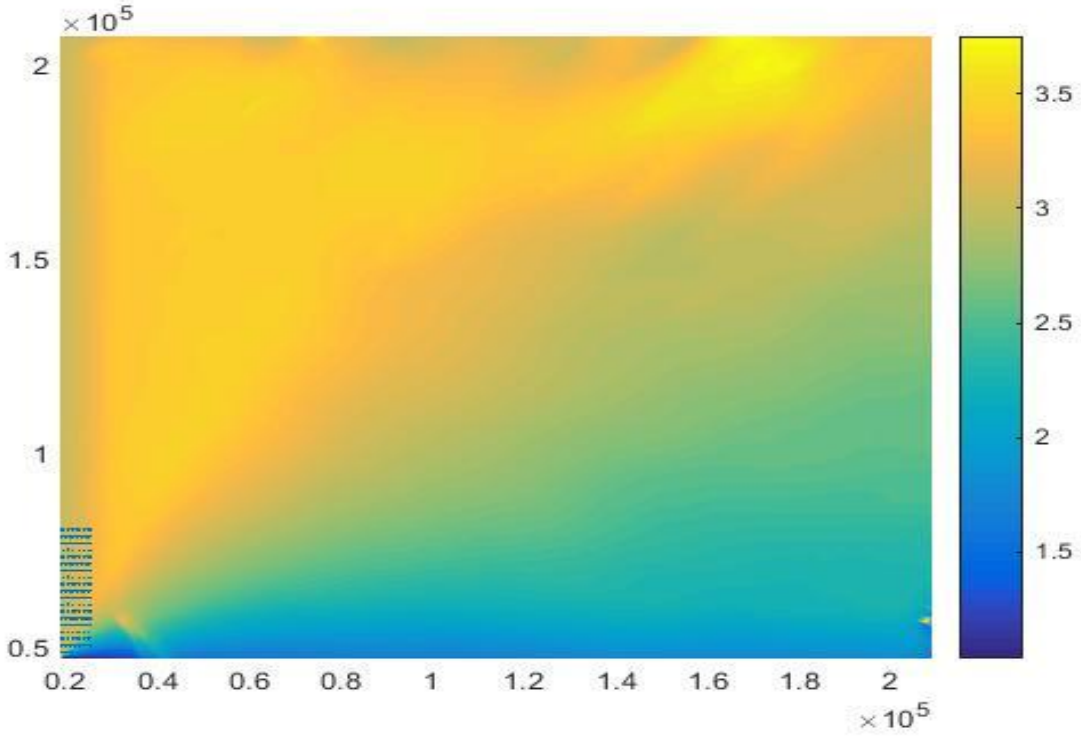

Figure A.11 : Colour grading plot of wave height from 30-33 hrs.

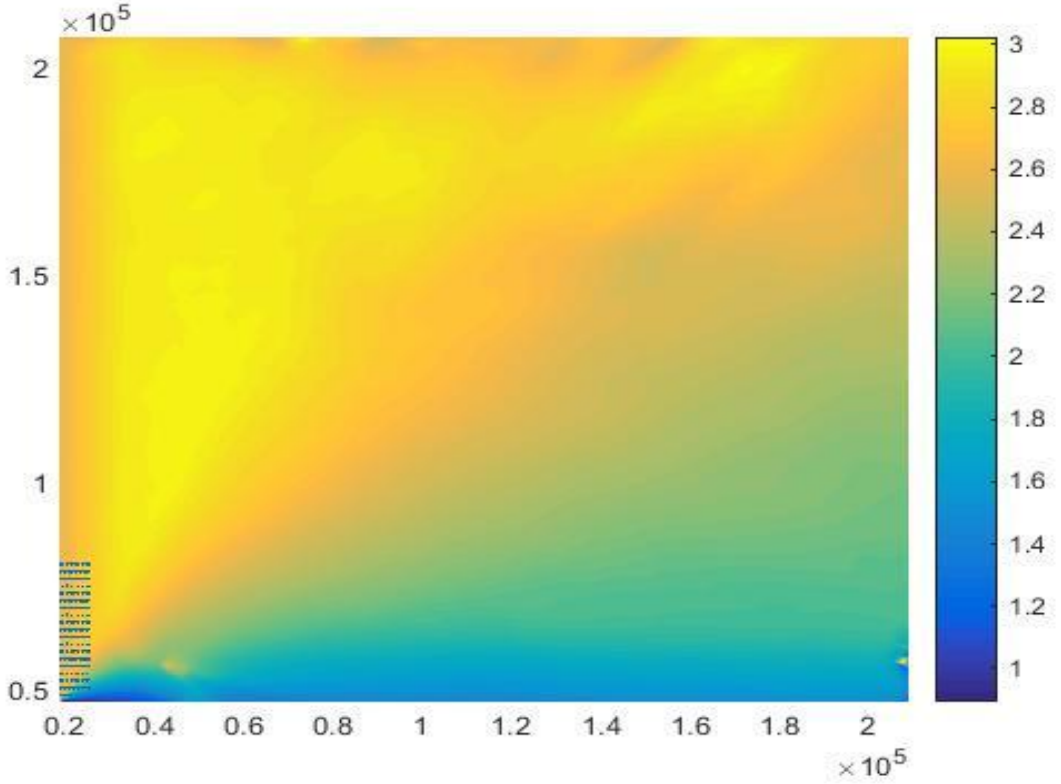

Figure A.12 : Colour grading plot of wave height from 33-36 hrs.

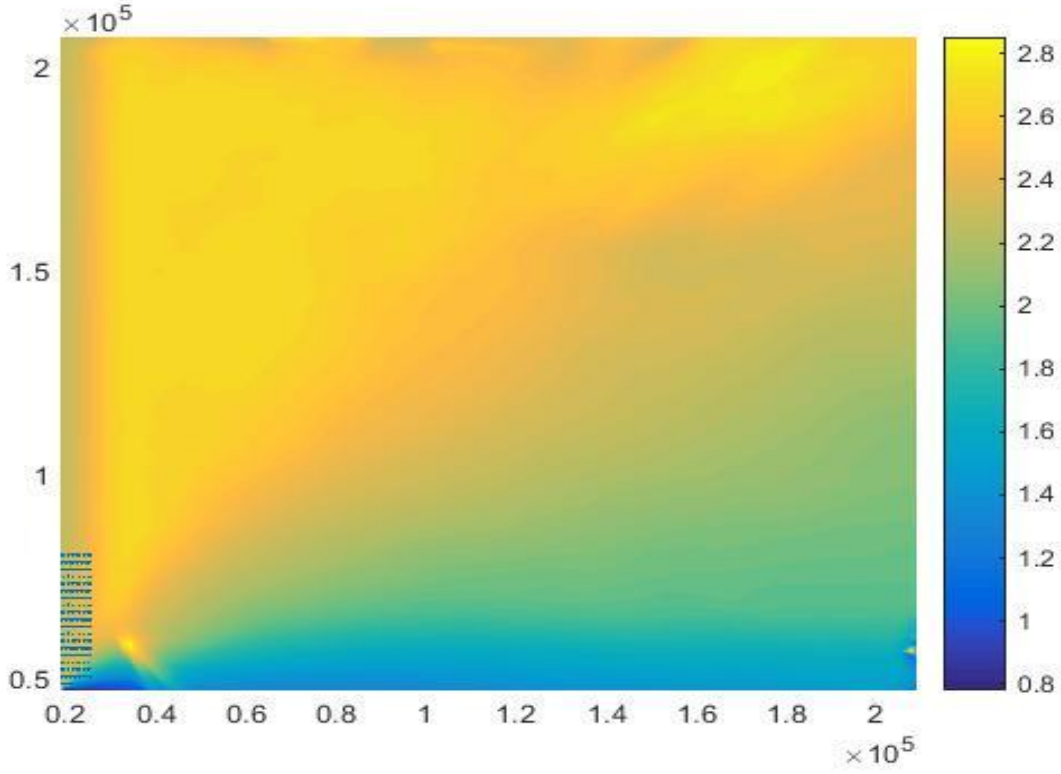

Figure A.13 : Colour grading plot of wave height from 36-39 hrs.

Appendix- B

X-beach run

Sample of Matlab code for X-beach run

```
% %   %%%%%% Loading bathymetry grid and bed level
x=load('x.grd');
y=load('y.grd');
z=load('z.grd');
surf (z,'EdgeColor','none','LineStyle','none','Facelighting','phong')

% %   %%%%%% Generating model
xbm = xb_generate_model('bathy', {'x', x, 'y', y, 'z', z,'optimize',
0,'posdwn',0,'world_coordinates',false},...
'waves', { 'Hm0', [6.06 10.08 11.08 11.57 10.29 9.14 8.08 6.51 5.04 3.39
3.06 2.59 2.40], 'Tp', [9.34 13.4 13.97 14.18 13.29 12.44 11.53 10.11 8.8
7.08 6.69 6.06 5.84], 'mainang', [283.6 293.1 298.3 298.7 297.3 294.1 292.1
295.2 296.6 296.8 295.2 293.3 291.6], 'duration', 10800 },...
'tide', {'front',[0.52 0.47 0.43 0.39 0.37 0.35 0.35 0.35 0.36 0.37 0.39
0.41 0.44 0.46 0.48 0.50 0.51 0.52 0.51 0.50 0.47 0.44 0.39 0.35 0.30 0.26
0.33 0.21 0.20 0.20 0.22 0.24 0.28 0.33 0.38 0.44 0.50 0.56 0.62 0.68 0.73
4.67 4.70 4.71 4.70 4.68 4.65 0.70 0.64 0.58 0.52 0.46 0.41 0.37 0.33 0.31
0.30 0.30 0.31 0.32 0.34 0.37 0.40 0.43 0.37 0.40 0.43 0.46 0.48 0.50 0.51
0.51 0.49 0.47 0.44 0.39 0.35 0.30 0.26],...
'back',[0], ...
'time', [0 1800 3600 5400 7200 9000 10800 12600 14400 16200 18000 19800
21600 23400 25200 27000 28800 30600 32400 34200 36000 37800 39600 41400
43200 45000 46800 48600 50400 52200 54000 55800 57600 59400 61200 63000
64800 66600 68400 70200 72000 73800 75600 77400 79200 81000 82800 84600
86400 88200 90000 91800 93600 95400 97200 99000 100800 102600 104400 106200
108000 109800 111600 113400 115200 117000 118800 120600 122400 124200
126000 127800 129600 131400 133200 135000 136800 138600 140400]},...
'wavegrid', { 'nbins', 5, },...
'settings', {'thetanaut',0,'thetamin', -70, 'thetamax',30,'dtheta',10,...
'alfa',abs(xb_grid_rotation(y, x,
z)),'yori',min(min(y)),'xori',max(max(x)),'cfl',0.9,'tstop',140399,'tint',9
00,...
'tideloc',1,'paulrevere',0,'morfac',3, ...
'windv',18,'windth',290,...
'C',65,'eps',0.01,'hmin',0.20,...
'rhos', 1300,'por', 0.30 ,'D50', 0.000007, 'D90', 0.000011, 'wetslp', 0.1,
'dryslp',1,...
'scheme',2,'waveform',2, 'form', 2,...
'outputformat','netcdf'},...
'write',true,...
'path', 'C:\ Path_to_model\')

% %   %%%%%% View generated model
xb_view(xbm);
%
% %   %%%%%% Running Xbeach
path_model = 'C:\Path_to_model\';
run_xb = 'call "C:\Users\computername\Desktop\Xbeach\2014-02-
07_XBeach_1.21.3657_Groundhog_Day_x64_netcdf_parallel-MPI\xbeach.exe"';

cd(path_model)
system(run_xb)
```